To the Graduate Council:

I am submitting herewith a dissertation written by Hajime Sakamoto entitled "Analysis of Conopulse Radar Systems." I recommend that it be accepted in partial fulfillment of the requirements for the degree of Doctor of Philosophy, with a major in Electrical Engineering.

Peyton Z. Peebles, Jr.
Peyton Z. Peebles, Jr., Major Professor

We have read this dissertation
and recommend its acceptance:

Marshall Pace

Hubert D. Griffiths

Randall E. Cline

J. Dunn

Accepted for the Council:

Hilton A. Smith
Vice Chancellor
Graduate Studies and Research

TK6553
.T56
.S252
cop.2

ANALYSIS OF CONOPULSE RADAR SYSTEMS

A Dissertation

Presented for the

Doctor of Philosophy

Degree

The University of Tennessee

Hajime Sakamoto

December 1975

1269171

ACKNOWLEDGMENTS

The author wishes to express his appreciation to Dr. Peyton Z. Peebles, Jr., for his systematic guidance, informative counseling and kind supervision of this work and his course work.

Foreign students usually have various kinds of difficulties living away from home. The author has received kind help on such difficulties from Mr. and Mrs. John D. Vick and Mr. and Mrs. Jules W. Bernard. The author is convinced that he would not have finished all his work without their help. The author would like to express his thanks for their kind help.

The author has also received much help from Mr. and Mrs. O. G. Dunbar, Mr. and Mrs. W. L. Brown, Mr. and Mrs. W. L. Breazeale, Dr. and Mrs. D. W. Roberds. Their assistance is appreciated by the author.

The author would like to thank Dr. E. C. Huebschmann who was his advisor at the University of Tennessee Space Institute for his counseling.

The author is indebted to professors B. H. Goethert, R. L. Young, and J. M. Googe. The author wishes to express his appreciation to them.

Thanks go to Mr. W. H. Nelson, Mr. V. A. Thomason, Mr. J. P. Baker, Mr. S. T. Alexander, and Dr. R. W. Rice for correcting the manuscript.

Finally, the author wants to thank his supervisors at the Institute of Technical Research and Development, Japan Defense Agency.

They granted an educational leave of absence and provided partial support to the author, enabling him to complete his program of graduate studies.

ABSTRACT

The purpose of this investigation was to analyze the conopulse tracking radar system which is a hybrid of monopulse and conical scan tracking radar systems. Two methods, the monopulse-conical scan method and the conical scan-monopulse method, were developed to extract the angle-error signals in this system.

The extraction of the angle-error signals for small pattern squint and target angle was first described. The two different approaches were applied to the analyses under this condition. Since the angle-error signals depended on the antenna patterns used, they were expanded into the Maclaurin's series. It was called the Maclaurin series method. Each pattern was expanded into the suitable series for the practical pattern representation as alternate approach. These series were used for the extraction of the angle-error signals. These two approaches were applied to the Bessel and Gaussian function antenna pattern representations and the same results were obtained.

The angle-error signals for comparatively large pattern squint and target angles were next derived by means of the Maclaurin's series method. The time dependent error signal in the monopulse-conical scan method and the sum $\Sigma(t)$ and difference $\Delta(t)$ signals in the conical scan-monopulse method can be expanded into the Fourier series with respect to the antenna rotation frequency for the particular antenna representations. Their first coefficients were used for the extraction of the angle-error signals. It was called the Fourier series method. Those two approaches were also applied to the Bessel and Gaussian

function pattern representations. The results were compared. Especially, in case of the Bessel function antenna pattern representation, the results were well matched over the target angle expected.

In the above discussion, the carrier component was not taken into account. The practical designs of the monopulse-conical scan method and the conical scan-monopulse method were carried out in considering the carrier component.

A noise-free assumption was made throughout the above analyses. However, the noise caused an inaccurate determination in the system. The accuracy for the signal just after the two antennas which is the theoretical limit was analyzed and the accuracies in the real systems were obtained. The closed form of the Cramer-Rao lower bounds was developed to obtain the theoretical limit and the maximum-likelihood method was applied to the analyses of the accuracies in the real systems. Then, these results of the accuracies were compared and how the accuracies in the real systems approach to the theoretical limit was discussed.

TABLE OF CONTENTS

CHAPTER		PAGE
I.	INTRODUCTION	1
	Conical Scan Tracking	1
	Monopulse Tracking	3
	Conopulse Tracking	5
II.	ERROR SIGNAL EXTRACTION WITHOUT NOISE	10
	Small Target and Pattern Squint Angles Using Arbitrary Antenna Pattern	10
	Monopulse conical scan method	17
	Conical scan-monopulse method	20
	Special cases of Bessel and Gaussian patterns	29
	Alternate Analysis of Bessel Pattern	33
	Monopulse-conical scan method	36
	Conical scan-monopulse method	37
	Alternate Analysis of Gaussian Pattern	39
	Monopulse-conical scan method	41
	Conical scan-monopulse method	43
	Comparison of Small Angle Results	45
	General Analysis for Large Target and Squint Angles Using Arbitrary Pattern	45
	Monopulse-conical scan method	49
	Conical scan-monopulse method for active target	54
	Conical scan-monopulse method for passive target	62
	Numerical Results for Large Pattern Squint and Target Angles	69
	Monopulse-conical scan method	73
	Conical scan-monopulse method for active target	78
	Conical scan-monopulse method for passive target	78
	Comparison of numerical results from two methods	85
III.	PRACTICAL DESIGN OF CONOPULSE SYSTEM	95
	Monopulse-Conical Scan Method	95
	Hybrid junction stage	95
	RF amplifier stage and mixer stage	98
	IF amplifier stage with IAGC	99
	Phase-sensitive detector	100
	Conical Scan-Monopulse Method	102
	IF amplifier stage with AGC	103
	Second mixer stage	104
	Multiplier stage and base band amplifier stage	104
IV.	NOISE IN CONOPULSE SYSTEM	106
	Theoretical Lower Limit of Accuracy	107
	True Accuracy of Real System	121

CHAPTER PAGE

Monopulse-conical scan method 124
Conical scan-monopulse method 131
Comparison of Accuracies 140

V. DISCUSSION, CONCLUSION, AND POSSIBLE FUTURE WORK 142
Discussion and Conclusion 142
Possible Future Work 143

BIBLIOGRAPHY 146

APPENDICES 149
Appendix A 150
Appendix B 152
Appendix C 154
Appendix D 156
Appendix E 161
Appendix F 164
Appendix G 167
Appendix H 172
Appendix I 175
Appendix J 182
Appendix K 184

VITA 188

LIST OF FIGURES

FIGURE		PAGE
1.1.	Antenna Beam and Received Pulse Train of Conical Scan . .	2
1.2.	Monopulse Antenna Beams for One Angular Coordinate	4
1.3.	Scanning of Two Antenna Beams in Conopulse Radar System .	6
1.4.	Theoretical Block Diagram of Monopulse-Conical Scan Method	8
1.5.	Theoretical Block Diagram of Conical Scan-Monopulse Method	9
2.1.	Geometrical Relation of Two Antenna Beams and Target . . .	13
2.2.	Relations of Wave Forms and Spectra in Conical Scan-Monopulse Method	25
2.3.	Coherent Demodulation for Δ Signal and Low Pass Filtering for Σ Signal	28
2.4.	Spectra of $\Sigma(t)$ and $\Delta(t)$ in Terms of $K'(\omega)$ in Case of Active Target	59
2.5.	Spectra of $\Sigma(t)$ and $\Delta(t)$ in terms of $S(\omega)$ in Case of Passive Target	66
2.6.	Wave Shapes of $\Delta(t)$, $\Sigma(t)$, and $e(t)$	70
2.7.	Error-Signal Voltage of Monopulse-Conical Scan Method (Bessel Function Antenna Pattern) by Maclaurin Series Method	74
2.8.	Error-Signal Voltage of Monopulse-Conical Scan Method (Gaussian Function Antenna Pattern) by Maclaurin Series Method	75
2.9.	Error-Signal Voltage of Monopulse-Conical Scan Method (Bessel Function Antenna Pattern) by Fourier Series Method	76
2.10.	Error-Signal Voltage of Monopulse-Conical Scan Method (Gaussian Function Antenna Pattern) by Fourier Series Method	77

FIGURE PAGE

2.11. Error-Signal Voltage of Conical Scan-Monopulse Method (Bessel Function Antenna Pattern) for Active Target by Maclaurin Series Method 79

2.12. Error-Signal Voltage of Conical Scan-Monopulse Method (Gaussian Function Antenna Pattern) for Active Target by Maclaurin Series Method 80

2.13. Error-Signal Voltage of Conical Scan-Monopulse Method (Bessel Function Antenna Pattern) for Active Target by Fourier Series Method 81

2.14. Error-Signal Voltage of Conical Scan-Monopulse Method (Gaussian Function Antenna Pattern) for Active Target by Fourier Series Method 82

2.15. Error-Signal Voltage of Conical Scan-Monopulse Method (Bessel Function Antenna Pattern) for Passive Target by Maclaurin Series Method 83

2.16. Error-Signal Voltage of Conical Scan-Monopulse Method (Gaussian Function Antenna Pattern) for Passive Target by Maclaurin Series Method 84

2.17. Error-Signal Voltage of Conical Scan-Monopulse Method (Bessel Function Antenna Pattern) for Passive Target by Fourier Series Method 86

2.18. Error-Signal Voltage of Conical Scan-Monopulse Method (Gaussian Function Antenna Pattern) for Passive Target by Fourier Series Method 87

2.19. Comparison of Error-Signal Voltages for Monopulse-Conical Scan Method (Bessel Function Antenna Pattern) from Two Error Signal Extraction Methods at the Squint Angle $\theta_q/\theta_B = 0.1$ 89

2.20. Comparison of Error-Signal Voltages for Monopulse-Conical Scan Method (Bessel Function Antenna Pattern) from Two Error Signal Extraction Methods at the Squint Angle $\theta_q/\theta_B = 0.2$ 90

2.21. Comparison of Error-Signal Voltages for Monopulse-Conical Scan Method (Bessel Function Antenna Pattern) from Two Error Signal Extraction Methods at the Squint Angle $\theta_q/\theta_B = 0.3$ 91

FIGURE PAGE

2.22. Comparison of Error-Signal Voltages for Monopulse-Conical Scan Method (Bessel Function Antenna Pattern) from Two Error Signal Methods at the Squint Angle $\theta_q/\theta_B = 0.4$ 92

2.23. Comparison of Error-Signal Voltages for Monopulse-Conical Scan Method (Bessel Function Antenna Pattern) from Two Error Signal Extraction Methods at the Squint Angle $\theta_q/\theta_B = 0.5$ 93

2.24. Comparison of Error-Signal Voltages for Conical Scan-Monopulse Method (Bessel Function Antenna Pattern: Passive Target) from Two Error Signal Extraction Methods 94

3.1. Block Diagram of Monopulse-Conical Scan Method 96

3.2. Block Diagram of Conical Scan-Monopulse Method 103

4.1. Accuracy of Raw Data 108

4.2. Signal Processor at Early Stages 110

4.3. Relation of Target Angles and Their Axes on Target Plane 113

4.4. Theoretical Model of Monopulse-Conical Scan Method 125

4.5. Relation of Pulse Width 128

4.6. Theoretical Model of Conical Scan-Monopulse Method 132

4.7. Relation of Noises $n_D(t)G_k(t)$ and $n_D'(t)$ 135

4.8. Relation of Pulse Shape $F_k(t)$ and its First Mean Value . . . 136

K-1. Output Pulse of Matched Filter for Rectangular Pulse 186

CHAPTER I

INTRODUCTION

A tracking radar system continuously measures the relative position of a target in range, azimuth angle, and elevation angle. A high degree of precision and an accurate prediction of the future position are often required. A large variety of methods for tracking radar systems are available now. They may be classified, however, as Sequential Lobing and Simultaneous Lobing. The most established methods are Conical Scan and Monopulse in both sequential lobing and simultaneous lobing categories, respectively.

I. CONICAL SCAN TRACKING

The conical scan method is one of the earliest forms of the tracking radar system (31, pp. 21-5-21-10; 32, pp. 164-175). In the conical scan system one antenna beam, offset from the boresight axis, is rotated about the axis as shown in Figure 1.1(A). When the target is not on the boresight axis, the echo signal will be modulated at a frequency equal to the rotation frequency of the beam as shown in Figure 1.1(B). When the target is just on the boresight axis, the line of sight to the target and the boresight coincide, and the conical scan modulation is zero. Thus, the radar video output contains the angle-tracking-error information in the envelope of the pulses. The percentage of modulation is proportional to the target angle between the boresight axis and target axis as shown in Figure 1.1, and the phase shift of

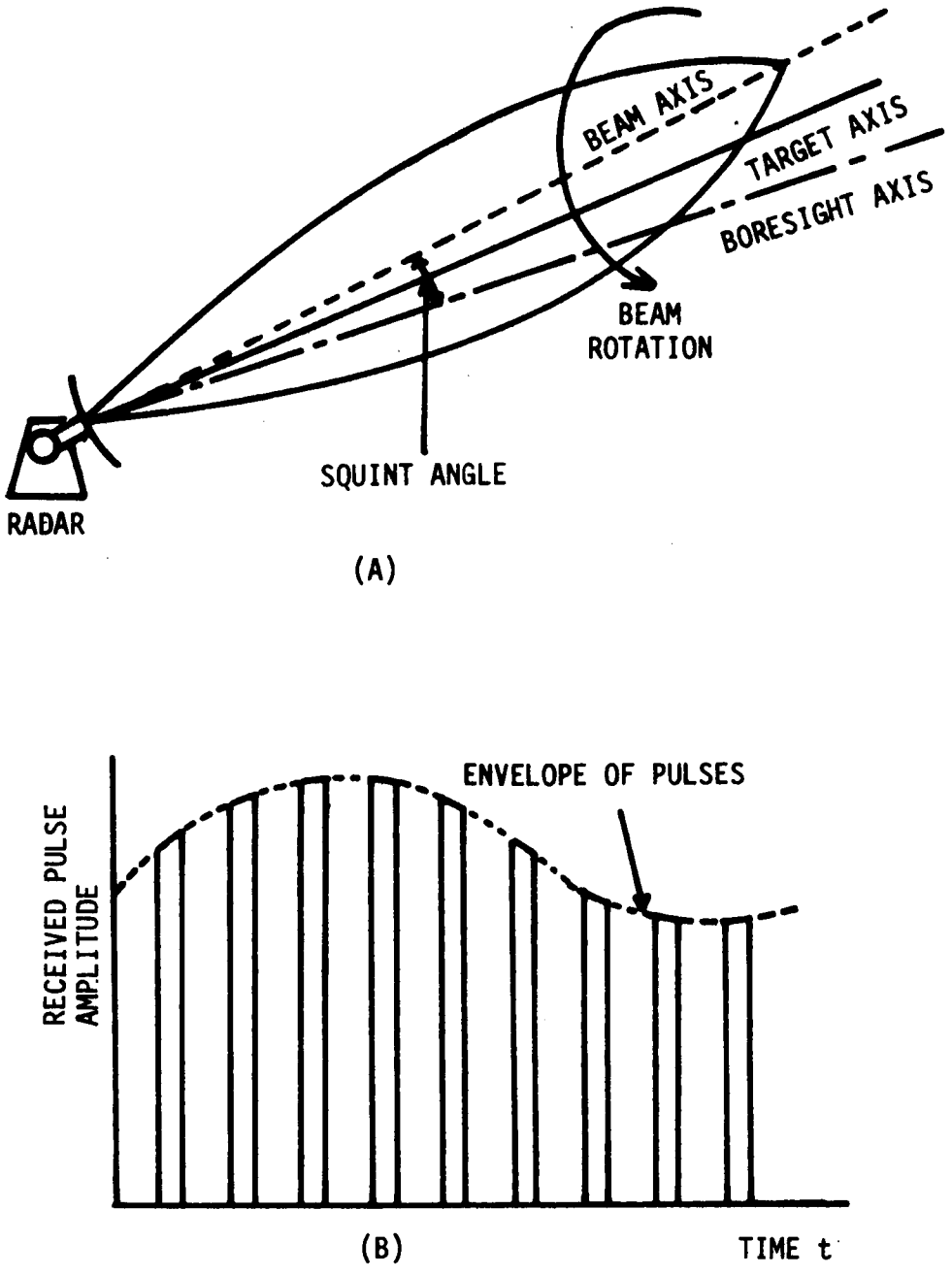


Figure 1.1. Antenna beam and received pulse train of conical scan. (A) Antenna beam of conical scan; (B) Pulse train with conical scan modulation.

the envelope signal compared with the antenna rotation signal is determined by the direction of target from an arbitrary reference axis. The phase comparison with the antenna rotation signal and the 90 degrees phase shifted signal provide the azimuth-error and elevation-error signals, respectively.

The merit of conical scan is simplicity. It requires only one antenna beam and one receiver to develop full two-dimensional target angle data. The main disadvantage is sensitivity for fluctuations in target echo strength on a pulse to pulse basis. If the fluctuation is random, the signal to noise ratio will be degraded and it can cause false indication of tracking error. The undesired fluctuations which cause most difficulty occur at nearly the same frequency as the scanning rate, and the effect is a slowly varying bias error.

II. MONOPULSE TRACKING

There are two main kinds of monopulse tracking radar systems: Amplitude-comparison monopulse, and Phase-comparison monopulse (27; 31, pp. 21-11-21-13; 32, pp. 175-178). The amplitude-comparison monopulse, however, will be described as a monopulse tracking radar system in this section because the application of phase-comparison monopulse is limited and it will not be applied to our Conopulse tracking radar system.

Monopulse employs two overlapping antenna beams for one angular coordinate as shown in Figure 1.2 and the overlapping point is on the boresight axis (10; 32; 23). When the target is not on the boresight axis, the difference of signals from the two antenna beams has a value since output signals from each antenna beam are different.

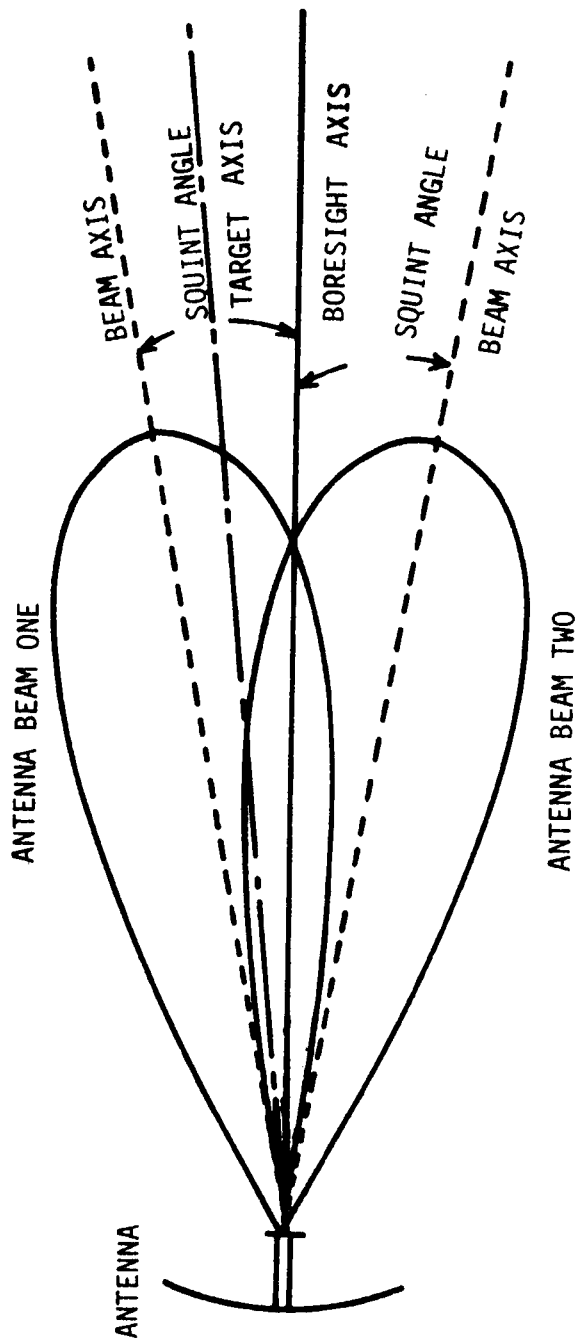


Figure 1.2. Monopulse antenna beams for one angular coordinate.

On the other hand, if the target is on the boresight axis, the difference is zero since output signals from each antenna beam are the same. The sum of the signals from the two antenna beams provides the range measurement and is also used to cancel out the effect of echo fluctuation on a pulse to pulse basis. Both the sum and difference signal may have the same amount of fluctuation from the echo on each pulse. It may be cancelled by the comparison taking a ratio of amplitudes of two sum and difference signals on each received pulse.

Thus, the monopulse tracking radar system does not have the disadvantage of sensitivity for amplitude fluctuation common to conical scan.

The principle of monopulse for one angular coordinate is described above. At least three or usually four antenna beams and three receivers have to be used to get full two-dimensional target angle data. Therefore, it could be said that the disadvantage of monopulse is complexity.

III. CONOPULSE TRACKING

A hybrid system, here called Conopulse, has been proposed to obtain the simplicity of conical scan with the independence of echo fluctuation of monopulse. In the conopulse system two antenna beams are rotated about the boresight axis as shown in Figure 1.3. At any instant in time the system would form sum Σ and difference Δ outputs by hybrid circuitry just as in an ordinary one-dimensional monopulse system. Since the conopulse is the combination of conical scan with a monopulse system, two variations of signal processing would be considered. The first variation has the signal processing of monopulse

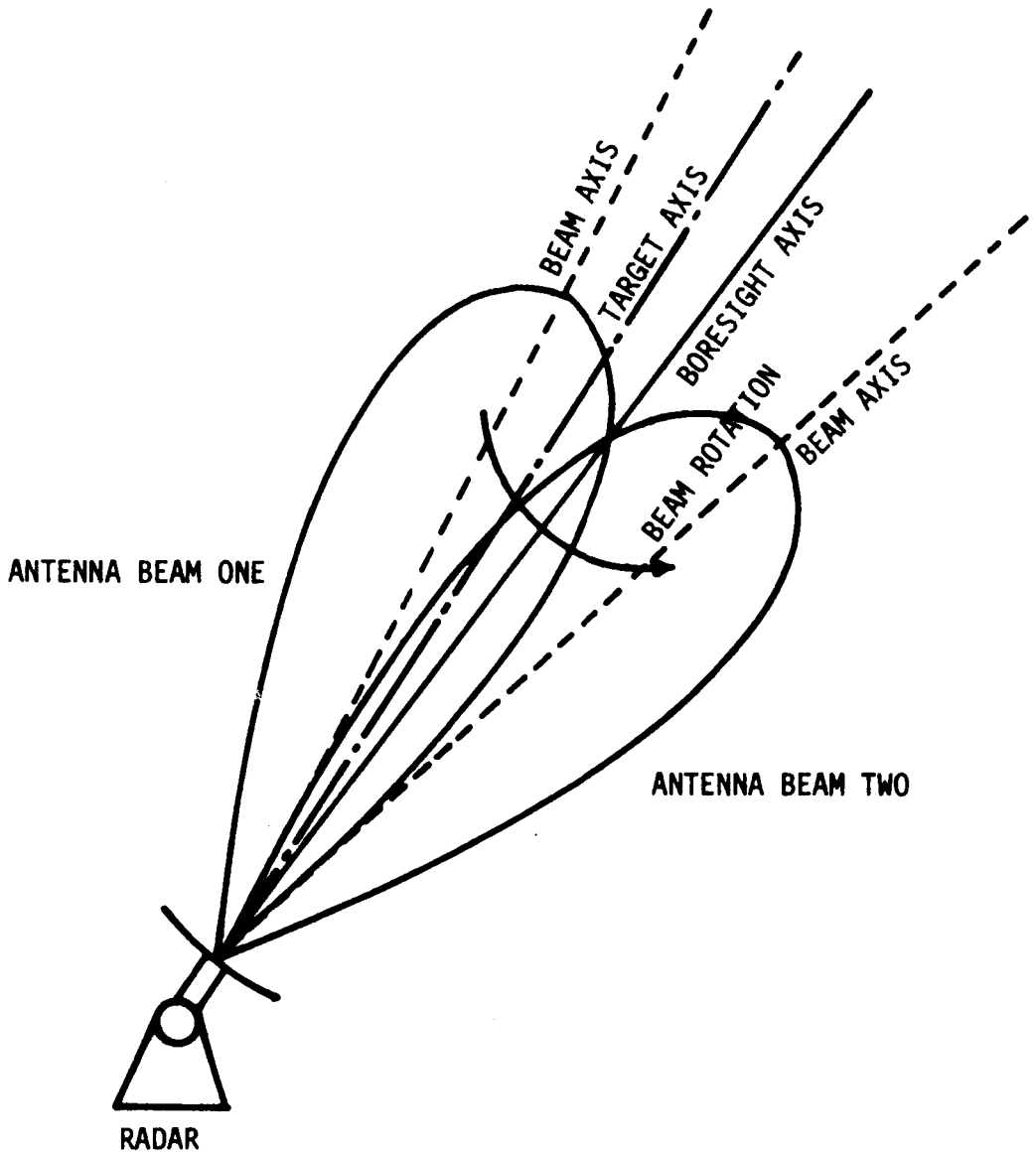


Figure 1.3. Scanning of two antenna beams in conopulse radar system.

and then one of conical scan called Monopulse-conical scan method, and the second variation has the signal processing of conical scan and then one of monopulse called Conical scan-monopulse method.

In the monopulse-conical scan method the signal processor would form the ratio Δ/Σ as in monopulse to develop a signal e(t) which would be independent of echo fluctuation. Since e(t) is time dependent because the two antenna beams rotate in space, the signal processing the same as conical scan would extract two-dimensional target angular components. The theoretical block diagram of this system is shown in Figure 1.4.

In the conical scan-monopulse method the two-dimensional angular data would be first extracted from the difference Δ signal by the processor similar to conical scan. Since they are not independent of echo fluctuation, the next signal processor would also cancel out echo fluctuation by forming the ratio with the fundamental frequency component of Σ since they would have the same amount of echo fluctuation. The theoretical block diagram is shown in Figure 1.5.

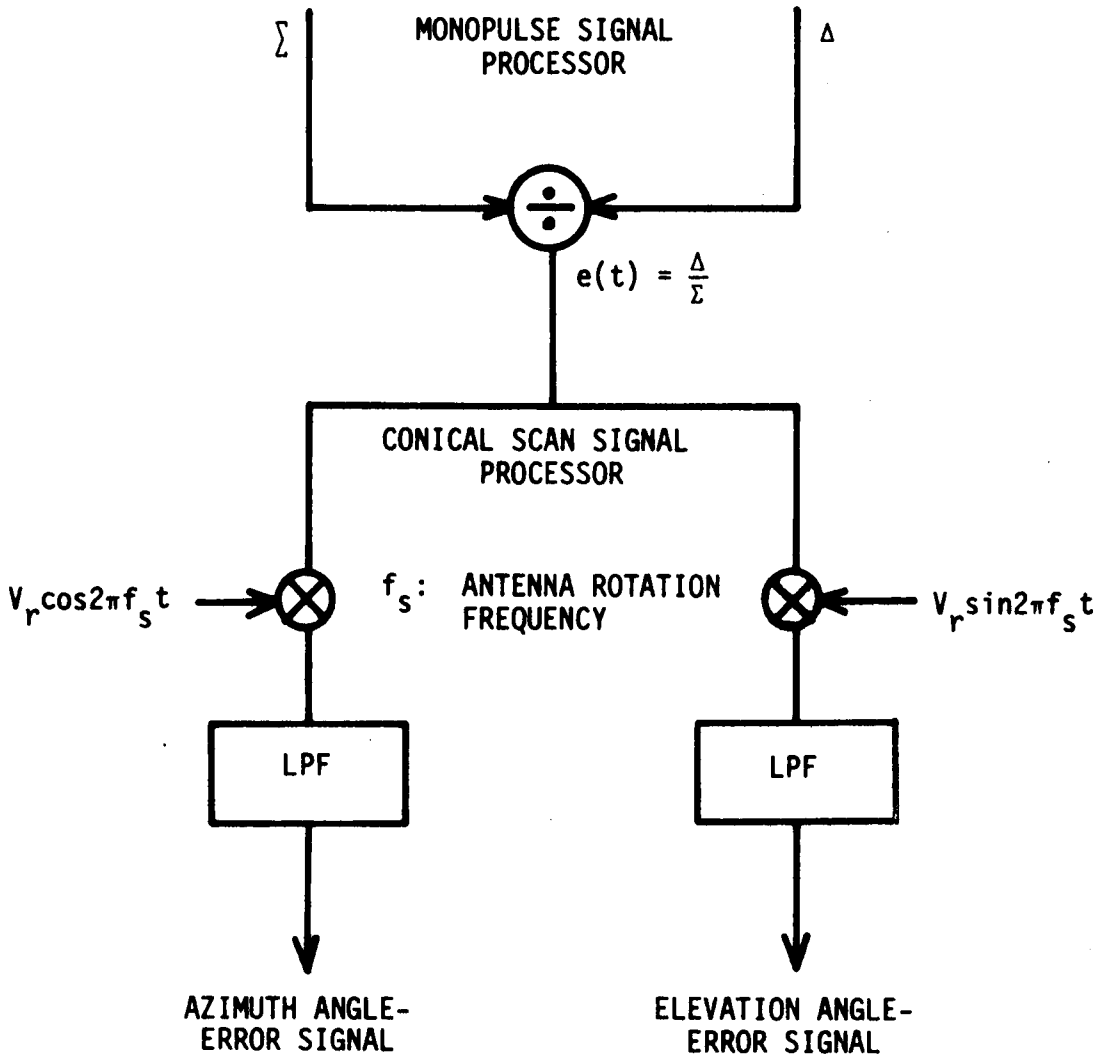


Figure 1.4. Theoretical block diagram of monopulse-conical scan method.

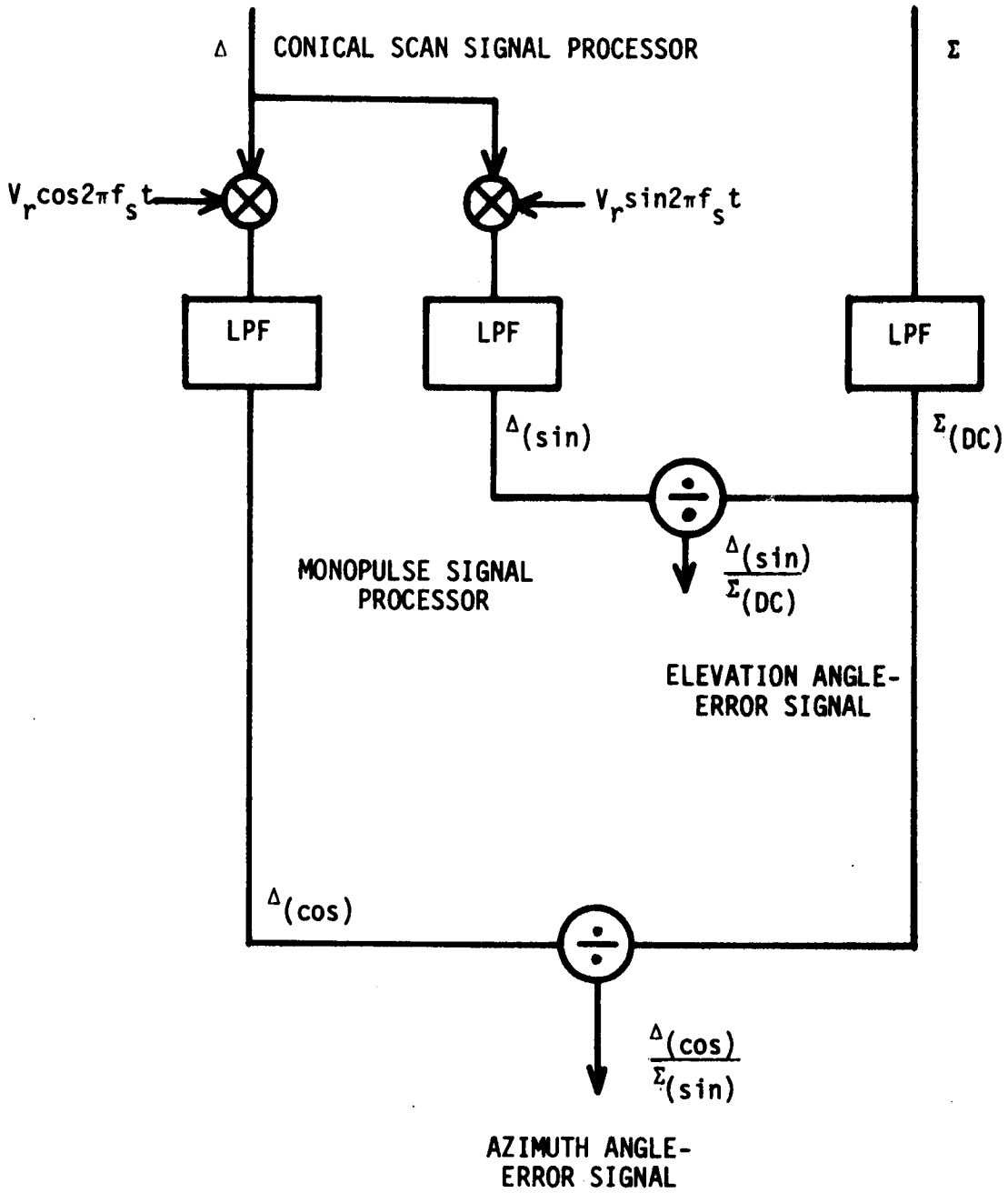


Figure 1.5. Theoretical block diagram of conical scan-monopulse method.

CHAPTER II

ERROR SIGNAL EXTRACTION WITHOUT NOISE

We will discuss the extraction of error-signals in this system. We assume a noise-free situation throughout this chapter.

The error-signal for small target and pattern squint angles will be first obtained as simpler case. The solution for the error-signal is expected to be linear for the parameters. There are the two approaches considered. They correspond to an arbitrary antenna pattern and to a particular pattern. The results from the two approaches may be compared and we will confirm that they give the same results.

The error-signals for large target and pattern squint angles will be next solved for an arbitrary antenna pattern. The numerical computation method will be applied to particular antenna pattern cases. Then, the results will be compared as same as in the small target and pattern squint angles case.

I. SMALL TARGET AND PATTERN SQUINT ANGLES USING ARBITRARY ANTENNA PATTERN

The conopulse tracking radar system has two antenna beams rotating about the boresight axis as described in Chapter I. The video output signals from those antenna beams may be represented by the expressions (32, p. 172)

$$V_1(t) = K' \, G_1(t) \, F_k(t), \qquad (2.1)$$

and

$$V_2(t) = K' G_2(t) F_k(t), \tag{2.2}$$

where $V_1(t)$ and $V_2(t)$ are video output signals from two antenna beams, K' is determined by parameters of the radar equation, $G_1(t)$ and $G_2(t)$ are modulation due to rotation of each antenna beam, and $F_k(t)$ is the pulse train signal transmitted.

The term K' in Eqs. (2.1) and (2.2) may be independent of the rotation of the transmitter antenna since it is related to the sum of the two antenna beams and the squint angle is now very small.

First the expressions for the antenna modulation factors $G_1(t)$ and $G_2(t)$ will be derived. It will be assumed that an arbitrary antenna pattern has such characteristics that

1) antenna pattern $G(x)$ is rotationally symmetric about the axis of maximum point,
2) $G(x)$ processes all derivatives with respect to x on $(-\infty, \infty)$,
3) $G(x)$ has a maximum value at $x = 0$,
4) $G(x)$ is an even function for the variable x, and
5) $G(x)$ converges to zero as $x \to \pm \infty$.

The arbitrary antenna pattern $G(x)$ satisfying the above conditions may be written in the Maclaurin's series expansion (11, p. 444) as

$$G(x) = \sum_{n=0}^{\infty} \frac{x^{2n}}{(2n)!} G^{(2n)}(0). \tag{2.3}$$

Antenna pattern is usually as a function of angle off beam axis θ. Therefore, x may be also a function of θ as

$$x = f(\theta). \tag{2.4}$$

Denoting $G[f(\theta)]$ as $G(\theta)$ and substituting Eq. (2.4) into Eq. (2.3), we have

$$G(\theta) = \sum_{n=0}^{\infty} \frac{c_{2n}}{(2n)!}[f\theta] \tag{2.5}$$

where

$$c_{2n} = G^{(2n)}(0). \tag{2.6}$$

Referring to Figure 2.1(A) (32, p. 172), the angles θ_q and θ_q' are squint angles of antenna beam one and two, respectively, and the angle θ_T is the angle between the boresight axis and the target axis; the angles ϕ and ϕ' are the rotation angles of the antenna beams one and two as measured from some arbitrary reference; the angle ϕ_o is the angle defined by the target and the reference axis; and the angles θ and θ' are angles between each antenna beam axis and the target axis.

The angles θ, θ', θ_q, θ_q', and θ_T may also be defined by the lengths of arc $R\theta$, $R\theta'$, $R\theta_q$, $R\theta_q'$, and $R\theta_T$ on a sphere of radius R as shown in Figure 2.1(B).

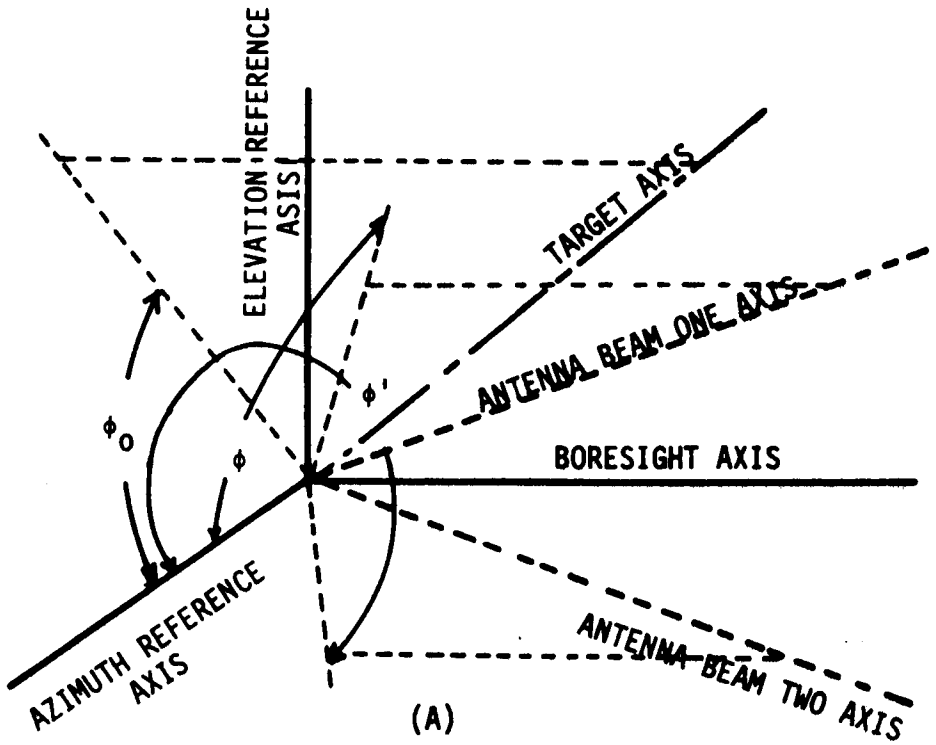
Since the distance $R\theta$, $R\theta'$, $R\theta_q$, $R\theta_q'$, and $R\theta_T$ are small, they may be related by the law of cosines to the angles $\phi-\phi_o$ and $\phi'-\phi_o$.

$$(R\theta)^2 = (R\theta_q)^2 + (R\theta_T)^2 - 2R^2\theta_q\theta_T \cos(\phi-\phi_o), \tag{2.7}$$

and

$$(R\theta')^2 = (R\theta_q')^2 + (R\theta_T)^2 - 2a^2\theta_q\theta_T \cos(\phi'-\phi_o), \tag{2.8}$$

Substituting the relations of $\theta_q = \theta_q'$ and $\phi=\phi + \pi$ due to symmetric location of two antenna beams into Eq. (2.8) and dividing both sides of Eqs. (2.7) and (2.8) by R^2, we have



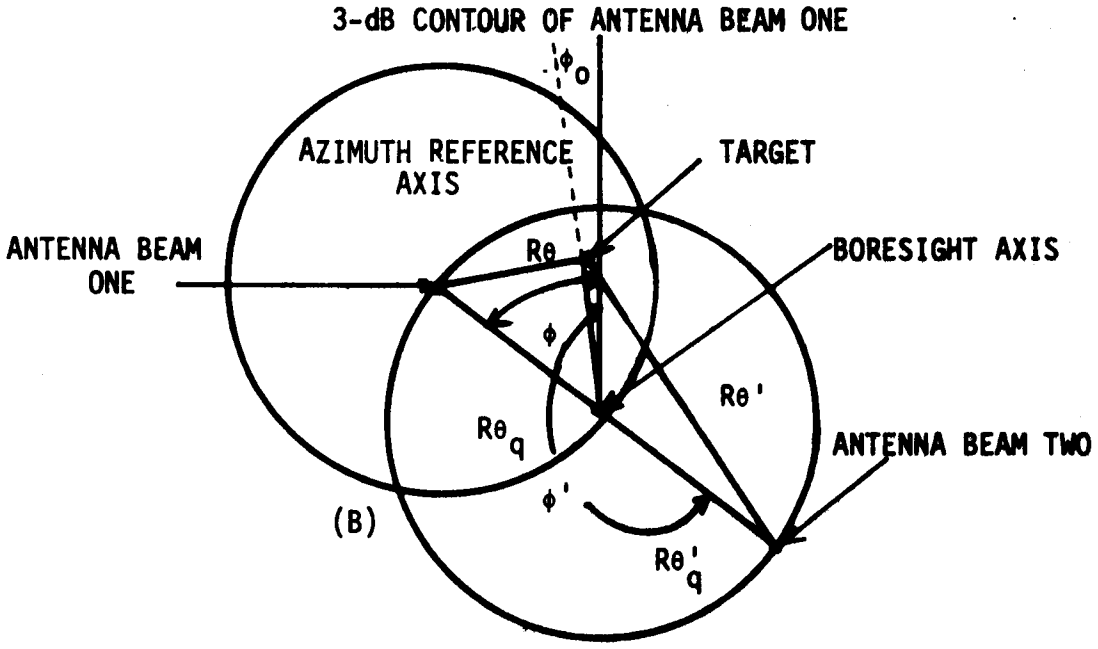


Figure 2.1. Geometrical relation of two antenna beams and target. (A) Geometry and symbols for derivation of conopulse error signal; (B) Head-on view of conopulse antenna beams.

$$\theta^2 = \theta_q^2 + \theta_T^2 - 2\theta_q\theta_T \cos(\phi-\phi_o), \tag{2.9}$$

and

$$\theta'^2 = \theta_q^2 + \theta_T^2 + 2\theta_q\theta_T \cos(\phi-\phi_o). \tag{2.10}$$

Since two antenna beams are rotating in an arbitrary angular speed ω_s and frequency of rotation f_s, ϕ is defined by

$$\phi = \omega_s t = 2\pi f_s t . \tag{2.11}$$

The angles θ and θ' express angles off each antenna beam axis and they are functions of time. Thus, $G_1(t)$ and $G_2(t)$ are written as

$$G_1(t) = G_1(\theta) = G(\theta) = \sum_{n=0}^{\infty} \frac{c_{2n}}{(2n)!} [f(\theta)]^{2n}, \tag{2.12}$$

and

$$G_2(t) = G_2(\theta') = G(\theta') = \sum_{n=0}^{\infty} \frac{c_{2n}}{(2n)!} [f(\theta')]^{2n}. \tag{2.13}$$

Since x must have the same sign as θ, x is an odd function of θ. Therefore x can be also expanded in the Maclaurin's series having only odd terms as

$$x = f(\theta) = \sum_{m=0}^{\infty} \frac{d_{2m+1}}{(2m+1)!} \left(\frac{\theta}{\theta_B}\right)^{2m+1}, \tag{2.14}$$

where

$$d_{2m+1} = f^{(2m+1)}(\theta)\ \theta_B^{2m+1}, \tag{2.15}$$

and θ_B is antenna beamwidth measured between 3dB points of the antenna pattern.

Upon using Eqs. (2.12), (2.13), and (2.14), we have

$$G_1(\theta) = \sum_{n=0}^{\infty} \frac{c_{2n}}{(2n)!} \left[\sum_{m=0}^{\infty} \frac{d_{2m+1}}{(2m+1)!} \left(\frac{\theta}{\theta_B} \right)^{2m+1} \right]^{2n}, \tag{2.16}$$

and

$$G_2(\theta') = \sum_{n=0}^{\infty} \frac{c_{2n}}{(2n)!} \left[\sum_{m=0}^{\infty} \frac{d_{2m+1}}{(2m+1)!} \left(\frac{\theta'}{\theta_B} \right)^{2m+1} \right]^{2n}. \tag{2.17}$$

Since the target angle θ_T and the squint angle θ_q are now small, it can be assumed that

$$\frac{\theta}{\theta_B} \text{ and } \frac{\theta'}{\theta_B} << 1 \tag{2.18}$$

Thus, the terms inside of the brackets in Eqs. (2.16) and (2.17) may be approximated as

$$\sum_{m=0}^{\infty} \frac{d_{2m+1}}{(2m+1)!} \left(\frac{\theta}{\theta_B} \right)^{2m+1} \simeq d_1 \left(\frac{\theta}{\theta_B} \right), \tag{2.19}$$

and

$$\sum_{m=0}^{\infty} \frac{d_{2m+1}}{(2m+1)!} \left(\frac{\theta'}{\theta_B} \right)^{2m+1} \simeq d_1 \left(\frac{\theta'}{\theta_B} \right). \tag{2.20}$$

Substituting Eqs. (2.19) and (2.20) into Eqs. (2.16) and (2.17), respectively, we have

$$G_1(\theta) = \sum_{n=0}^{\infty} \frac{c_{2n} d_1^{2n}}{(2n)!} \left(\frac{\theta}{\theta_B} \right)^{2n}, \tag{2.21}$$

and

$$G_2(\theta') = \sum_{n=0}^{\infty} \frac{c_{2n} d_1^{2n}}{(2n)!} \left(\frac{\theta'}{\theta_B} \right)^{2n}. \tag{2.22}$$

By the binomial theorem, we have such relations as, from Eqs. (2.9) and (2.10),

$$\left(\frac{\theta}{\theta_B}\right)^{2n} = \sum_{n=1}^{n}(-1)^r \binom{n}{r}\left[\left(\frac{\theta_q}{\theta_B}\right)^2 + \left(\frac{\theta_T}{B}\right)^2\right]^{n-r}\left[\frac{2\theta_q\theta_T}{\theta_B^2}\cos(\phi-\phi_o)\right]^r , \qquad (2.23)$$

and

$$\left(\frac{\theta'}{\theta_B}\right)^{2n} = \sum_{r=1}^{n}\binom{n}{r}\left[\left(\frac{\theta_q}{\theta_B}\right)^2 + \left(\frac{\theta_T}{\theta_B}\right)^2\right]^{n-r}\left[\frac{2\theta_q\theta_T}{\theta_B^2}\cos(\phi-\phi_o)\right]^r . \qquad (2.24)$$

Substituting Eqs. (2.23) and (2.24) into Eqs. (2.21) and (2.22), respectively, we have

$$G_1(\theta) = \sum_{n=0}^{\infty}\frac{c_{2n}d_1}{(2n)!}\sum_{r=1}^{n}(-1)^r\binom{n}{r}\left[\left(\frac{\theta_q}{\theta_B}\right)^2 + \left(\frac{\theta_T}{\theta_B}\right)^2\right]^{n-r}\left[\frac{2\theta_q\theta_B}{\theta_B^2}\cos(\phi-\phi_o)\right]^r , \qquad (2.25)$$

and

$$G_2(\theta) = \sum_{n=0}^{\infty}\frac{c_{2n}d_1^{2n}}{(2n)!}\sum_{r=0}^{n}\binom{n}{r}\left[\left(\frac{\theta_q}{\theta_B}\right)^2 + \left(\frac{\theta_T}{\theta_B}\right)^2\right]^{n-r}\left[\frac{2\theta_q\theta_T}{\theta_B^2}\cos(\phi-\phi_o)\right]^r . \qquad (2.26)$$

Rearranging Eqs. (2.25) and (2.26) in order of r gives

$$G_1(\theta) = \sum_{r=0}^{\infty}(-1)^r\left\{\sum_{n=r}^{\infty}\frac{c_{2n}d_1^{2n}}{(2n)!}\binom{n}{r}\left[\left(\frac{\theta_q}{\theta_B}\right)^2 + \left(\frac{\theta_T}{\theta_B}\right)^2\right]^{n-r}\left[\frac{2\theta_q\theta_T}{\theta_B^2}\cos(\phi-\phi_o)\right]^n\right\} , \qquad (2.27)$$

and

$$G_2(\theta) = \sum_{r=0}^{\infty}\left\{\sum_{n=r}^{\infty}\frac{c_{2n}d_1^{2n}}{(2n)!}\binom{n}{r}\left[\left(\frac{\theta_q}{\theta_B}\right)^2 + \left(\frac{\theta_T}{\theta_B}\right)^2\right]^{n-r}\left[\frac{2\theta_q\theta_T}{\theta_B^2}\cos(\phi-\phi_o)\right]^r\right\} . \qquad (2.28)$$

Hence the video signals for the sum Σ and the difference Δ are

$$\Sigma = V_1(t) + V_2(t) = K'F_k(t)[G_1(t) + G_2(t)]$$

$$= K'F_k(t) \sum_{r=0}^{\infty} [1 + (-1)^r]$$

$$x\left\{\sum_{n=r}^{\infty} \frac{c_{2n}d_1^{2n}}{(2n)!}\binom{n}{r}\left[\left(\frac{\theta_q}{\theta_B}\right)^2 + \left(\frac{\theta_T}{\theta_B}\right)^2\right]^{n-r}\right\}\left[\frac{2\theta_q\theta_T}{\theta_B^2}\cos(\phi-\phi_o)\right]^r, \quad (2.29)$$

and

$$\Delta = V_1(t) - V_2(t) = -K'F_k(t)[G_1(t) - G_2(t)]$$

$$= -K'F_k(t) \sum_{r=0}^{\infty} [1 - (-1)^r]$$

$$x\left\{\sum_{n=r}^{\infty} \frac{c_{2n}d_1^{2n}}{(2n)!}\binom{n}{r}\left[\left(\frac{\theta_q}{\theta_B}\right)^2 + \left(\frac{\theta_T}{\theta_B}\right)^2\right]^{n-r}\right\}\left[\frac{2\theta_q\theta_T}{\theta_B^2}\cos(\phi-\phi_o)\right]^r. \quad (2.30)$$

1. Monopulse-Conical Scan Method

As described in Chapter I, this method has the first signal processor to form the ratio Δ/Σ shown in Figure 1.4, p. 8. Since Δ and Σ have the common term $K'F_k(t)$, the error signal derived by the ratio Δ/Σ is written as

$$e(t) = \frac{\Delta}{\Sigma} = \frac{G_1(t) - G_2(t)}{G_1(t) + G_2(t)}. \quad (2.31)$$

It can be assumed that in Eqs. (2.29) and (2.30),

$$\text{the term } \left(\frac{\theta_q}{\theta_B}\right)^3 \text{ or higher order terms} \simeq 0, \tag{2.32}$$

$$\text{the term } \left(\frac{\theta_T}{\theta_B}\right)^3 \text{ or higher order terms} \simeq 0, \tag{2.33}$$

$$\text{the term } \left(\frac{2\theta_q\theta_T}{\theta_B^2}\right)^2 \text{ or higher order terms} \simeq 0, \tag{2.34}$$

$$\text{and the third order of the term of the product of } \theta_T/\theta_B, \text{ and } 2\theta_q\theta_T/\theta_B^2 \text{ or higher order terms} \simeq 0, \tag{2.35}$$

where these terms include their coefficients, since the target angle θ_T and the squint angle θ_q are now small so that

$$\left(\frac{\theta_q}{\theta_B}\right)^2 << 1, \left(\frac{\theta_T}{\theta_B}\right)^2 << 1, \text{ and } \frac{2\theta_q\theta_T}{\theta_B^2} << 1, \tag{2.36}$$

and the coefficient of each term $\frac{c_{2n}d_1^{2n}}{(2n)!}\binom{n}{r}$ is not so large for any n and r because G(x) converges to zero as $x \to \pm\infty$.

Upon applying the conditions of Eq. (2.32) through Eq. (2.35) on Eqs. (2.29) and (2.30), the sum and difference of $G_1(t)$ and $G_2(t)$ may be approximated as

$$G_1(t) + G_2(t) \simeq 2\left\{C_o + \frac{c_2d_1^2}{2!}\left[\left(\frac{\theta_q}{\theta_B}\right)^2 + \left(\frac{\theta_T}{\theta_B}\right)^2\right]\right\}, \tag{2.37}$$

$$G_1(t) - G_2(t) \simeq -(2c_2d_1^2)\frac{\theta_q\theta_T}{\theta_B^2}\cos(2\pi f_s t - \phi_o). \tag{2.38}$$

Substituting Eqs. (2.37) and (2.38) into Eq. (2.31), the time dependent error-signal e(t) becomes

$$e(t) = \frac{-\frac{c_2 d_1^2}{c_o}\frac{\theta_q \theta_T}{\theta_B^2}\cos(2\pi f_s t - \phi_o)}{1 + \frac{c_2 d_1^2}{2! c_o}\left[\left(\frac{\theta_q}{\theta_B}\right)^2 + \left(\frac{\theta_T}{\theta_B}\right)^2\right]}. \tag{2.39}$$

By using the relation

$$\frac{1}{1+x} = 1 - x^2 + x^3 - \ldots, \text{ if } |x| < 1, \tag{2.40}$$

and assuming

$$\left|\frac{c_2 d_1^2}{2! c_o}\left[\left(\frac{\theta_q}{\theta_B}\right)^2 + \left(\frac{\theta_T}{\theta_B}\right)^2\right]\right| < 1,$$

the error-signal e(t) may be written as

$$e(t) \simeq -\frac{c_2 d_1^2}{c_o}\frac{\theta_q \theta_T}{\theta_B^2}\cos(2\pi f_s t - \phi_o). \tag{2.41}$$

The time dependent error signal represented by Eq. (2.41) is fed into the signal processors consisting of a product device and a low pass filter (LPF) as shown in Figure 1.4, p. 8. In these signal processors the horizontal and vertical projection of the target angle θ_T are extracted and they are called azimuth angle-error signal and elevation angle-error signal, respectively. One of the product devices (for example, the azimuth channel) is supplied with a reference

signal $V_r \cos 2\pi f_s t$, while the other is supplied with $V_r \sin 2\pi f_s t$, where V_r is the amplitude of the reference signal.

Multiplying Eq. (2.41) by the reference signals, respectively, and picking only their d-c components by the low pass filters, the azimuth angle-error signal and the elevation angle-error signal become

$$\text{Azimuth angle-error signal} = -\frac{V_r}{2}\frac{c_2 d_1^2}{c_o}\frac{\theta_q \theta_T}{\theta_B^2}\cos\phi_o, \tag{2.42}$$

and

$$\text{Elevation angle-error signal} = -\frac{V_r}{2}\frac{c_2 d_1^2}{c_o}\frac{\theta_q \theta_T}{\theta_B^2}\sin\phi_o. \tag{2.43}$$

They are voltages proportional to the target angle θ_T for constant ϕ_o. Therefore, the radar is able to point to the target when both angle-error signals are zero.

2. Conical Scan-Monopulse Method

The two-dimensional angular data corresponding to the azimuth angle and elevation angle-error signals are first extracted from the difference Δ signal by the signal processors consisting of a product device and a LPF similar to the angular-error detector of conical scan tracking radar. Also the fundamental frequency component of the sum Σ signal is picked up by LPF. Those three signals have the same echo fluctuation component. By forming the ratio of them, the echo fluctuation component in the two-dimensional data is cancelled out as described in Chapter I.

Under the condition of small pattern squint angle and target, the sum $\Sigma(t)$ signal and the difference $\Delta(t)$ signal are written as, from Eqs. (2.29), (2.30), (2.37), and (2.38),

$$\Sigma(t) \simeq 2K'(t)F_k(t) \left\{ c_o + \frac{c_2 d_1^2}{2!} \left[\left(\frac{\theta_q}{\theta_B} \right)^2 + \left(\frac{\theta_T}{\theta_B} \right)^2 \right] \right\}, \tag{2.44}$$

and

$$\Delta(t) \simeq -2K'(t)F_k(t)\, c_2 d_1^2 \frac{\theta_q \theta_T}{\theta_B^2} \cos(2\pi f_s t - \phi_o). \tag{2.45}$$

Here, K' is expressed as a function of time $K'(t)$.

For the sake of convenience, letting

$$\left.\begin{aligned} f_1(t) &= K'(t) \cos(\omega_s t - \phi_o), \\ D_o &= 2 \left\{ c_o + \frac{c_2 d_1^2}{2!} \left[\left(\frac{\theta_q}{\theta_B} \right)^2 + \left(\frac{\theta_T}{\theta_B} \right)^2 \right] \right\}, \\ D_1 &= -2\, c_2 d_1^2 \frac{\theta_q \theta_T}{\theta_B^2}, \end{aligned}\right\} \tag{2.46}$$

and

$$\omega_s = 2\pi f_s,$$

Eqs. (2.44) and (2.45) are simplified as

$$\Sigma(t) = D_o\, K'(t) F_k(t), \tag{2.47}$$

and

$$\Delta(t) = D_1 f_1(t) F_k(t). \tag{2.48}$$

Now, it can be seen that $f_1(t)$ is the same form as Amplitude Modulation (AM) (24), since $K'(t)$ has the d-c component, and it could be also assumed that $K'(t)$ is bandlimited between $-\omega_{max}$ and ω_{max}, where ω_{max} is the maximum frequency.

In order to avoid aliasing, ω_s has to be chosen such that

$$\omega_s > 2\omega_{max}. \tag{2.49}$$

Taking the Fourier transform of $f_1(t)$ gives

$$F_1(\omega) = \mathcal{F}[f_1(t)]$$

$$= \frac{e^{-j\phi_o}}{2} K'(\omega-\omega_s) + \frac{e^{j\phi_o}}{2} K'(\omega+\omega_s), \tag{2.50}$$

where

$$K'(\omega) = \mathcal{F}[K'(t)]. \tag{2.51}$$

Similarly, the Fourier transforms of $\Sigma(t)$ and $\Delta(t)$ may become

$$\Sigma(\omega) = \mathcal{F}[\Sigma(t)] = \frac{D_o}{2\pi} K'(\omega) * F_k(\omega), \tag{2.52}$$

and

$$\Delta(\omega) = \mathcal{F}[\Delta(t)] = \frac{D_1}{2\pi} F_1(\omega) * F_k(\omega), \tag{2.53}$$

where the asterisk expresses convolution integral and

$$F_k(\omega) = \mathcal{F}[F_k(t)]. \tag{2.54}$$

$F_k(t)$ is a pulse train of an arbitrary wave shape so that

$$F_k(t) = \sum_{n=-\infty}^{\infty} p(t-nT_p), \tag{2.55}$$

where $p(t)$ expresses an arbitrary wave shape and T_p is the pulse interval.

$F_k(t)$ can be expanded into its complex Fourier series having coefficient C_n as

$$F_k(t) = \sum_{n=-\infty}^{\infty} C_n e^{jn\omega_p t}, \tag{2.56}$$

where

$$\omega_p = \frac{2\pi}{T_p}. \tag{2.57}$$

Taking the Fourier transform on Eq. (2.56) gives

$$F_k(\omega) = \mathcal{F}[F_k(t)] = 2\pi \sum_{n=-\infty}^{\infty} C_n \delta(\omega-n\omega_p). \tag{2.58}$$

Here, we assumed that ω_p is constant, i.e., the received pulse interval T_p is constant. The received pulse interval from a moving target may not be constant but the changing of the pulse interval would be very slow. Thus, it could be assumed that the spectrum of $F_k(t)$ would be expressed by Eq. (2.58) and it would be a function of ω_p.

It may be usually satisfied that

$$\omega_p >> \omega_s, \tag{2.59}$$

to avoid aliasing.

Substituting Eq. (2.58) into Eqs. (2.52) and (2.53), we have

$$\Sigma(\omega) = \frac{D_0}{2\pi}\int_{-\infty}^{\infty} K'(Y)F_k(\omega-Y)dY$$

$$= D_0\int_{-\infty}^{\infty} K'(Y) \sum_{n=-\infty}^{\infty} C_n \delta(\omega-Y-n\omega_p)dY$$

$$= D_0 \sum_{n=-\infty}^{\infty} C_n K'(\omega-n\omega_p), \tag{2.60}$$

and

$$\Delta(\omega) = \frac{D_1}{2\pi}\int_{-\infty}^{\infty} F_1(Y)F_k(\omega-Y)dY$$

$$= D_1 \sum_{n=-\infty}^{\infty} C_n F_1(\omega-n\omega_p). \tag{2.61}$$

Substituting Eq. (2.50) into Eq. (2.61), $\Delta(\omega)$ in terms of $K'(\omega)$ becomes

$$\Delta(\omega) = D_1 \sum_{n=-\infty}^{\infty} C_n \left\{\frac{e^{-j\phi_0}}{2} K'(\omega-n\omega_p-\omega_s) + \frac{e^{j\phi_0}}{2} K'(\omega-n\omega_p+\omega_s)\right\}. \tag{2.62}$$

The relations of those wave forms and spectra are shown in Figure 2.2.

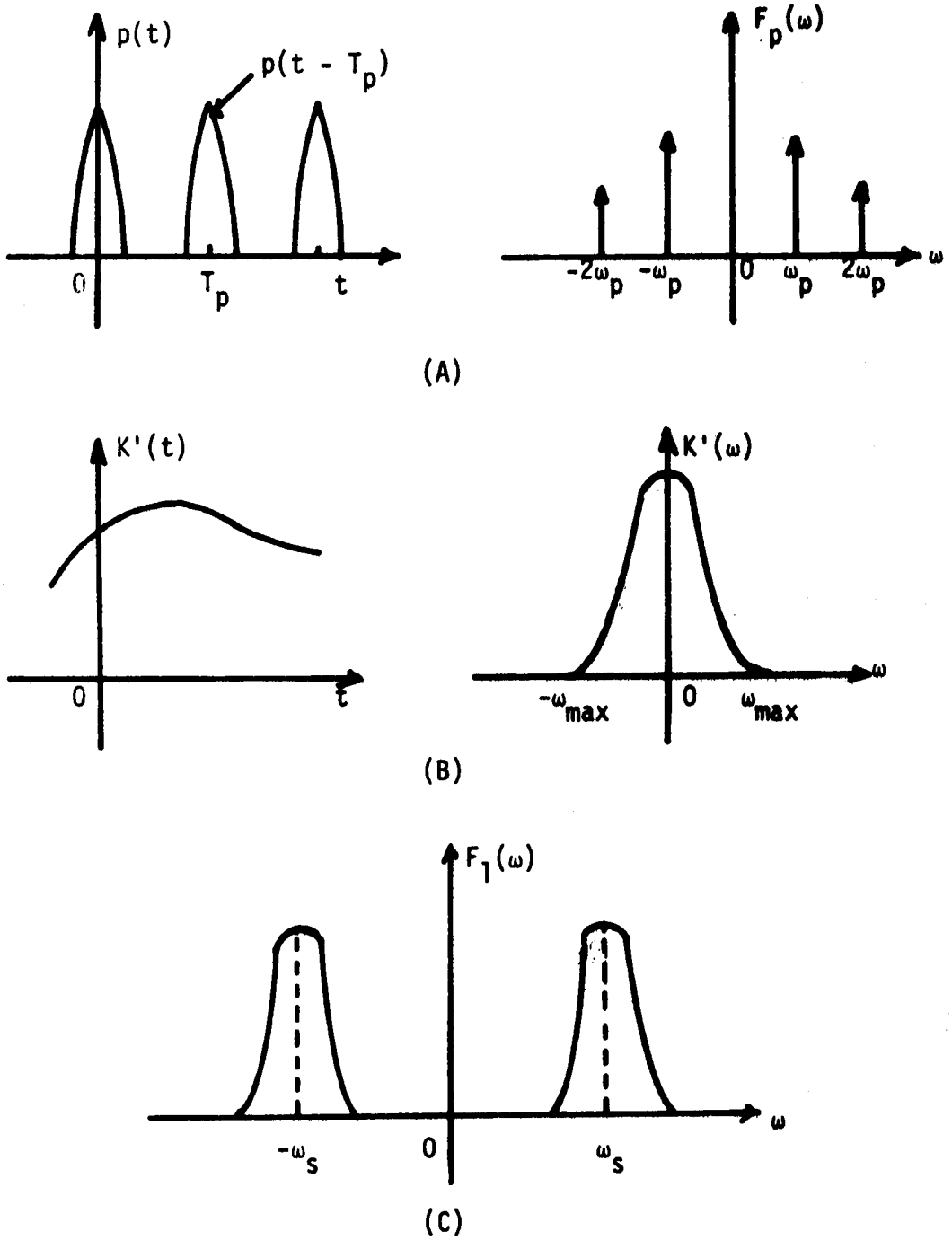


Figure 2.2. Relations of wave forms and spectra in conical scan-monopulse method. (A) Pulse train and its spectrum; (B) K'(t) and its spectrum; (C) Spectrum of $F_1(\omega)$; (D) Spectra of $\Delta(\omega)$ and $\Sigma(\omega)$.

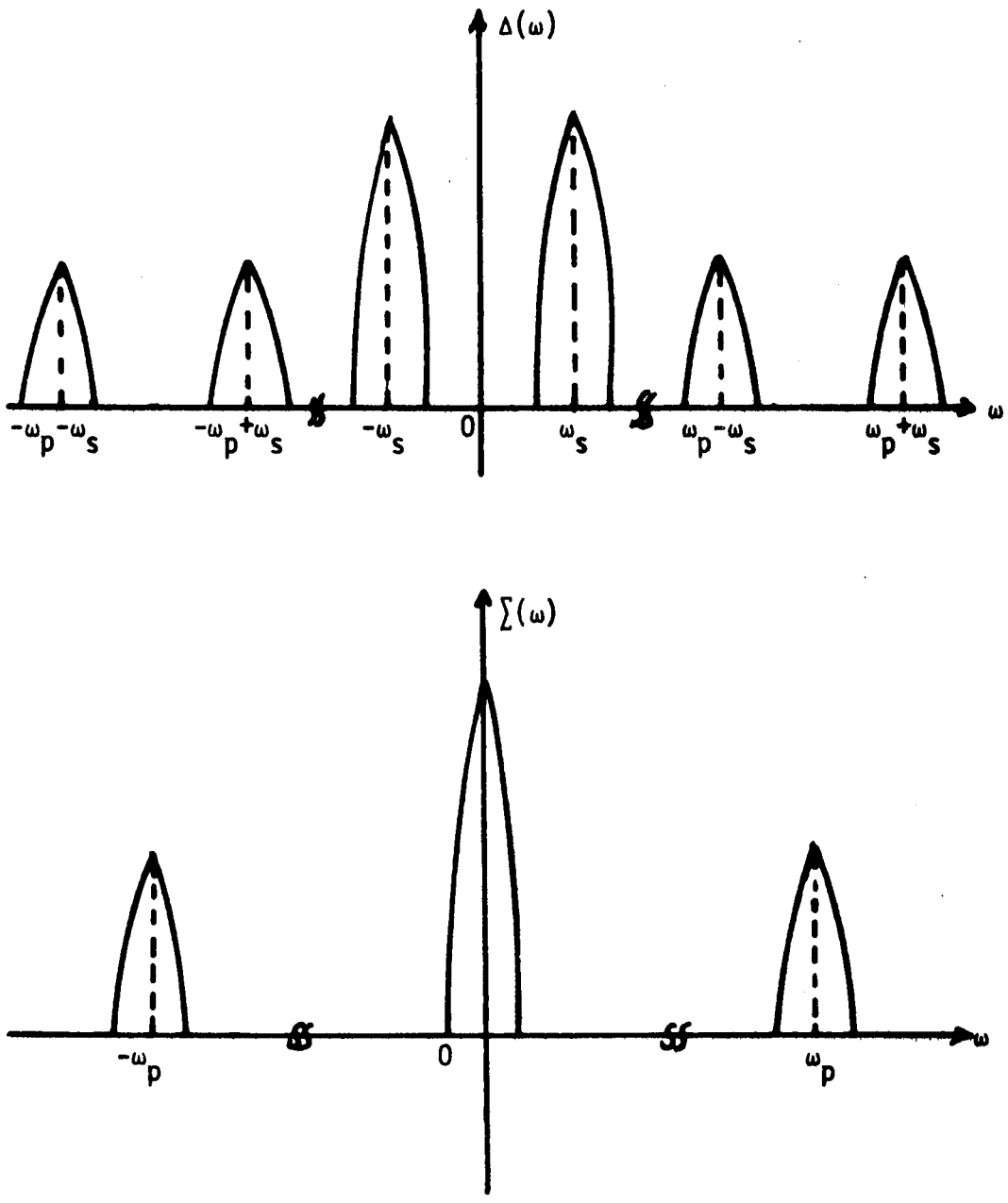


Figure 2.2 (Continued)

We consider the coherent demodulation of Δ signal with respect to $\cos\omega_s t$ and $\sin\omega_s t$ to detect the lowest frequency component and the low pass filtering for the Σ signal to pass only the fundamental frequency component as shown in Figure 2.2. The block diagrams are shown in Figure 2.3.

Following the block diagram of Figure 2.3 and denoting the output signal of the LPF as $\Delta_{d(\cos)}(\omega)$ for the reference signal $V_r \cos\omega_s t$ and $\Delta_{d(\sin)}(\omega)$ for the reference signal $V_r \sin\omega_s t$, they may be easily obtained as[†]

$$\Delta_{d(\cos)}(\omega) = \frac{V_r}{2} D_1 C_o K'(\omega)\cos\phi_o, \tag{2.63}$$

and

$$\Delta_{d(\sin)}(\omega) = \frac{V_r}{2} D_1 C_o K'(\omega)\sin\phi_o. \tag{2.64}$$

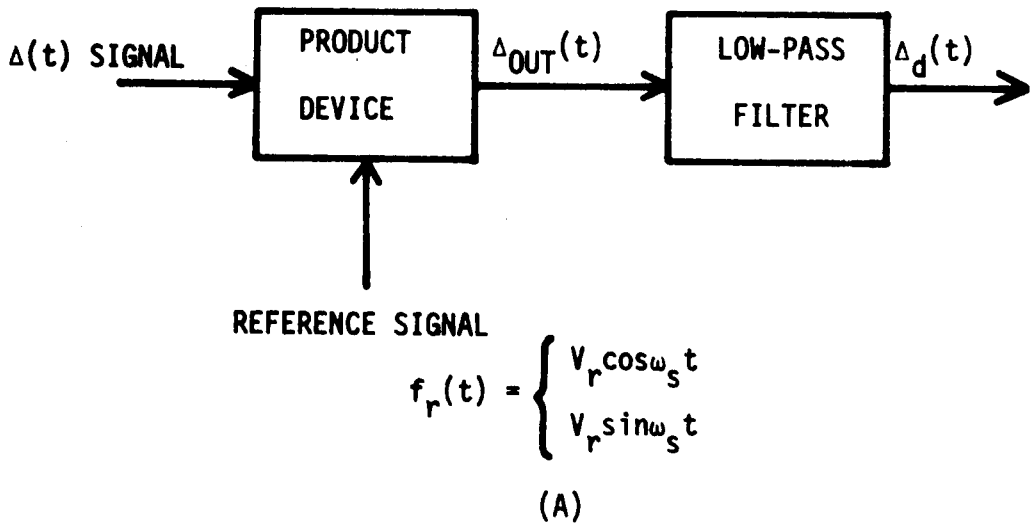
The output signal of the LPF on the Σ channel may be

$$\Sigma_d(\omega) = D_o C_o K'(\omega). \tag{2.65}$$

Since the $\Delta_{d(\cos)}(\omega)$ and $\Delta_{d(\sin)}(\omega)$ are divided by the $\Sigma_d(\omega)$ in time domain to get the azimuth and elevation angle-error signals, as in Figure 1.5, p. 9, they are expressed as

$$\text{Azimuth angle-error signal} = \frac{V_r}{2}\frac{D_1}{D_o}\cos\phi_o, \tag{2.66}$$

[†]Appendix A.



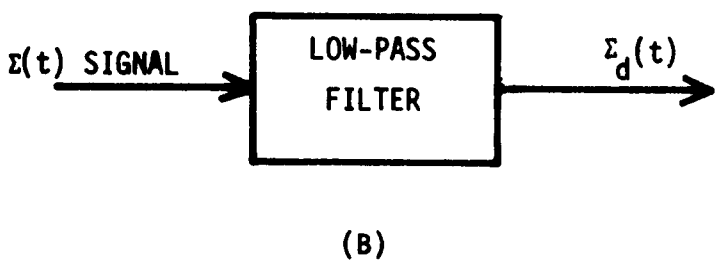


Figure 2.3. Coherent demodulation for Δ signal and low pass filtering for Σ signal. (A) Coherent demodulation; (B) Low pass filtering.

$$\text{Elevation angle-error signal} = \frac{V_r}{2}\frac{D_1}{D_0}\sin\phi_0, \tag{2.67}$$

From Eq. (2.46), the term D_1/D_0 becomes

$$\frac{D_1}{D_0} = \frac{-2c_0 d_1^2 \frac{\theta_q\theta_T}{\theta_B^2}}{2\left\{c_0 + \frac{c_2 d_1^2}{2!}\left[\left(\frac{\theta_q}{\theta_B}\right)^2 + \left(\frac{\theta_T}{\theta_B}\right)^2\right]\right\}}$$

$$\simeq -\frac{c_2 d_1^2}{c_0}\frac{\theta_q\theta_T}{\theta_B^2}\ . \tag{2.68}$$

Thus, the angle-error signals finally become

$$\text{Azimuth angle-error signal} = -\frac{V_r}{2}\frac{c_2 d_1^2}{c_0}\left(\frac{\theta_q\theta_T}{\theta_B^2}\right)\cos\phi_0, \tag{2.69}$$

and

$$\text{Elevation angle-error signal} = -\frac{V_r}{2}\frac{c_2 d_1^2}{c_0}\left(\frac{\theta_q\theta_T}{\theta_B^2}\right)\sin\phi_0. \tag{2.70}$$

They are the same as the results for the monopulse-conical scan method.

3. Special Cases of Bessel and Gaussian Patterns

In the previous sections, we have obtained the azimuth angle-error and elevation angle-error signals for an arbitrary antenna pattern in both the monopulse-conical scan and conical scan-monopulse

methods. The error signals for antenna patterns expressed by the Bessel function and the Gaussian function will be discussed as the particular cases in this section.

Bessel pattern. The antenna pattern for a circular aperture with uniform distribution may be defined by (30, pp. 192-199; 32, p. 269)

$$G(x) = 2\pi r_o^2 \frac{J_1(x)}{x}, \tag{2.71}$$

and

$$x = \frac{2\pi r_o}{\lambda} \sin\theta = \frac{\pi D}{\lambda} \sin\theta, \tag{2.72}$$

where

r_o = radius of aperture,

D = diameter of aperture,

λ = wave-length of signal,

and

$J_1(x)$ = first-order Bessel function.

The following relationship may be derived from expressions for Bessel functions (41, p. 355):

$$\frac{J_1(x)}{x} = \sum_{r=0}^{\infty} \frac{(-1)^r x^{2r}}{2^{2r+1} r!(r+1)!}. \tag{2.73}$$

Upon using Eqs. (2.6), (2.15), (2.71), and (2.73), the coefficients c_0, c_2, and d_1 in the error signal equations are given as follows

$$c_0 = G(0) = 2\pi r_0^2 \left\{ \sum_{r=0}^{\infty} \frac{(-1)^r x^{2r}}{2^{2r+1} r!(r+1)!} \bigg|_{x=0} \right\}$$

$$= \pi r_0^2, \tag{2.74}$$

$$c_2 = G^{(2)}(0) = 2\pi r_0^2 \left\{ \frac{d^2}{dx^2} \sum_{r=0}^{\infty} \frac{(-1)^r x^{2r}}{2^{2r+1} r!(r+1)!} \bigg|_{x=0} \right\}$$

$$= -\frac{\pi r_0^2}{2^2} \tag{2.75}$$

and

$$d_1 = f^{(1)}(0)\theta_B = \theta_B \left\{ \frac{d}{d\theta} \frac{\pi D}{\lambda} \sin\theta \bigg|_{\theta=0} \right\}$$

$$= \frac{\pi D}{\lambda} \theta_B. \tag{2.76}$$

Substituting the coefficients above into Eqs. (2.42) and (2.43), the error signals for monopulse-conical scan and conical scan-monopulse methods become

$$\text{Azimuth angle-error signal} = \frac{V_r}{2} \left(\frac{1.02\pi}{2} \right)^2 \frac{\theta_q \theta_T}{\theta_B^2} \cos\phi_0, \tag{2.77}$$

and

$$\text{Elevation angle-error signal} = \frac{V_r}{2} \left(\frac{1.02\pi}{2} \right)^2 \frac{\theta_q \theta_T}{\theta_B^2} \sin\phi_0, \tag{2.78}$$

where the relation $\theta_B = 1.02\lambda/D$ was used.

Gaussian pattern. The pencile beam antenna pattern (32, p. 171) may be also approximated by the Gaussian function

$$G(\theta) = G_0 e^{-a^2\theta^2}, \tag{2.79}$$

where G_0 = maximum one-way voltage gain,

a^2 = constant = $2.776/2\theta_B^2$, where θ and θ_B are in degrees.

Since G(x) must be an even function of x and x must be an odd function of θ as described in the previous section, we have

$$G(x) = G_0 e^{-x^2}, \tag{2.80}$$

and

$$x = a\theta = \sqrt{\frac{2.776}{2}}\,\frac{\theta}{\theta_B}. \tag{2.81}$$

Similarly, the coefficients c_0, c_2, and d_1 are obtained as follows

$$c_0 = G(0) = G_0, \tag{2.82}$$

$$c_2 = G^{(2)}(x)\Big|_{x=0} = G_0\left\{\frac{d^2}{dx^2}\left(e^{-x^2}\right)\Big|_{x=0}\right\}$$

$$= G_0\left\{e^{-x^2}\sum_{r=0}^{1}\frac{2!(-1)^{2-r}}{r!(2-2r)!}(2x)^{2-2r}\Big|_{x=0}\right\}$$

$$= -2G_0, \tag{2.83}$$

and

$$d_1 = f^{(1)}(0)\theta_B = \sqrt{\frac{2.776}{2}} = a\theta_B. \tag{2.84}$$

Then, the error signals for both methods become

$$\text{Azimuth angle-error signal} = V_r(a^2\theta_q\theta_T)\cos\phi_o\ , \tag{2.85}$$

and

$$\text{Elevation angle-error signal} = V_r(a^2\theta_q\theta_T)\sin\phi_o. \tag{2.86}$$

II. ALTERNATE ANALYSIS OF BESSEL PATTERN

The analysis for an arbitrary antenna pattern case has been carried out in the previous section. The antenna pattern was expanded into the Maclaurin's series. However, the antenna pattern will be expanded into the suitable series for each case in this and following sections. This method is called the alternate analysis for the particular antenna pattern.

The antenna pattern for a circular aperture with uniform distribution is expanded in the series as

$$G(x) = 2\pi r_o^2 \frac{J_1(x)}{x}$$

$$= 2\pi r_o^2 \sum_{r=0}^{\infty} \frac{(-1)^r x^{2r}}{2^{2r+1} r!(r+1)!}\ , \tag{2.87}$$

where

$$x = \frac{\pi D}{\lambda}\sin\theta = \frac{1.02\pi}{\theta_B}\sin\theta, \tag{2.88}$$

and

$$\theta_B = 1.02 \frac{\lambda}{D} \text{ (radian)}, \tag{2.89}$$

from the previous section.

Since the θ is very small, x is approximated as

$$x \simeq 1.02\pi \frac{\theta}{\theta_B} . \tag{2.90}$$

Then, the antenna pattern in terms of θ and θ_B is expressed as

$$G(\theta) = A \sum_{r=0}^{\infty} \frac{(-1)^r (1.02\pi)^{2r} \left(\frac{\theta}{\theta_B}\right)^{2r}}{2^{2r+1} r!(r+1)!} , \tag{2.91}$$

where $A = 2\pi r_o^2$.

Substituting Eqs. (2.23) and (2.24) into Eq. (2.91), we have

$$G_1(t) + G_2(t)$$

$$= A \sum_{n=0}^{\infty} \frac{(-1)^n (1.02\pi)^{2n}}{2^{2n+1} n!(n+1)!} \left\{ \sum_{r=0}^{n} \left[1 + (-1)^r \right] \binom{n}{r} \left[\left(\frac{\theta_q}{\theta_B}\right)^2 + \left(\frac{\theta_T}{\theta_B}\right)^2 \right]^{n-r} \right.$$

$$\left. \times \left[\frac{2\theta_q \theta_T}{\theta_B^2} \cos(\phi - \phi_o) \right]^r \right\}, \tag{2.92}$$

and

$$G_1(t) - G_2(t)$$

$$= -A \sum_{n=0}^{\infty} \frac{(-1)^n (1.02\pi)^{2n}}{2^{2n+1} n!(n+1)!} \left\{ \sum_{r=0}^{n} \left[1 - (-1)^r \right] \binom{n}{r} \left[\left(\frac{\theta_q}{\theta_B} \right)^2 + \left(\frac{\theta_T}{\theta_B} \right)^2 \right]^{n-r} \right.$$

$$\left. \times \left[\frac{2\theta_q \theta_T}{\theta_B^2} \cos(\phi - \phi_o) \right]^r \right\}. \qquad (2.93)$$

Then, rearranging Eqs. (2.92) and (2.93) in order of r, they become

$$G_1(t) + G_2(t)$$

$$= A \sum_{r=0}^{\infty} \left[1 + (-1)^r \right] \left\{ \sum_{n=r}^{\infty} \frac{(-1)^n (1.02\pi)^{2n}}{2^{2n+1} n!(n+1)!} \binom{n}{r} \left[\left(\frac{\theta_q}{\theta_B} \right)^2 + \left(\frac{\theta_T}{\theta_B} \right)^2 \right]^{n-r} \right.$$

$$\left. \times \left[\frac{2\theta_q \theta_T}{\theta_B^2} \cos(\phi - \phi_o) \right]^r \right\}, \qquad (2.94)$$

and

$$G_1(t) - G_2(t)$$

$$= -A \sum_{r=0}^{\infty} \left[1 - (-1)^r \right] \left\{ \sum_{n=r}^{\infty} \frac{(-1)^n (1.02\pi)^{2n}}{2^{2n+1} n!(n+1)!} \binom{n}{r} \left[\left(\frac{\theta_q}{\theta_B} \right)^2 + \left(\frac{\theta_T}{\theta_B} \right)^2 \right]^{n-r} \right.$$

$$\left. \times \left[\frac{2\theta_q \theta_T}{\theta_B^2} \cos(\phi - \phi_o) \right]^r \right\}. \qquad (2.95)$$

Since the coefficients in Eqs. (2.94) and (2.95) are, from inspection,

$$\frac{(1.02\pi)^{2n}}{2^{2n+1}n!(n+1)!} < 1, \text{ for } n \geq 2, \tag{2.96}$$

they may be approximated, under the conditions of Eq. (2.32) through Eq. (2.35), as

$$G_1(t) + G_2(t) \simeq A\left\{1 - \frac{(1.02\pi)^2}{2^3}\left[\left(\frac{\theta_q}{\theta_B}\right)^2 + \left(\frac{\theta_T}{\theta_B}\right)^2\right]\right\}, \tag{2.97}$$

and

$$G_1(t) - G_2(t) \simeq A\frac{(1.02\pi)^2}{2^2}\frac{\theta_q\theta_T}{\theta_B^2}\cos(\phi-\phi_o). \tag{2.98}$$

1. Monopulse-Conical Scan Method

From Eq. (2.31), the time dependent error signal e(t) is given by

$$e(t) = \frac{\Delta}{\Sigma} = \frac{G_1(t) - G_2(t)}{G_1(t) + G_2(t)}. \tag{2.99}$$

Then, the error signal is also written as

$$e(t) = \frac{\left(\frac{1.02\pi}{2}\right)^2\left(\frac{\theta_q\theta_T}{\theta_B^2}\right)\cos(\phi-\phi_o)}{1 - \frac{1}{2}\left(\frac{1.02\pi}{2}\right)^2\left[\left(\frac{\theta_q}{\theta_B}\right)^2 + \left(\frac{\theta_T}{\theta_B}\right)^2\right]}. \tag{2.100}$$

The first order approximation on Eq. (2.100) is

$$e(t) \simeq \left(\frac{1.02\pi}{2}\right)^2 \left(\frac{\theta_q \theta_T}{\theta_B^2}\right) \cos(2\pi f_s t - \phi_o), \tag{2.101}$$

since

$$0 < \frac{1}{2} \left(\frac{1.02\pi}{2}\right)^2 \left[\left(\frac{\theta_q}{\theta_B}\right)^2 + \left(\frac{\theta_T}{\theta_B}\right)^2\right] < 1, \tag{2.102}$$

where $\phi_o = 2\pi f_s t$.

By the same procedure as described in the previous section, the azimuth and elevation angle-error signals are obtained as

$$\text{Azimuth angle-error signal} = \frac{V_r}{2} \left(\frac{1.02\pi}{2}\right)^2 \frac{\theta_q \theta_T}{\theta_B^2} \cos\phi_o, \tag{2.103}$$

and

$$\text{Elevation angle-error signal} = \frac{V_r}{2} \left(\frac{1.02\pi}{2}\right)^2 \frac{\theta_q \theta_T}{\theta_B^2} \sin\phi_o. \tag{2.104}$$

2. Conical Scan-Monopulse Method

In this case, the sum signal $\Sigma(t)$ and the difference signal $\Delta(t)$ are written, from Eqs. (2.97) and (2.98), as

$$\Sigma(t) = K' F_k(t) A \left\{1 - \frac{(1.02\pi)^2}{2^3}\left[\left(\frac{\theta_q}{\theta_B}\right)^2 + \left(\frac{\theta_T}{\theta_B}\right)^2\right]\right\}, \tag{2.105}$$

and

$$\Delta(t) = K'F_k(t)A \frac{(1.02\pi)^2}{2^2} \frac{\theta_q\theta_T}{\theta_B^2} \cos(2\pi f_{st}-\phi_o). \tag{2.106}$$

Letting

$$D_o = A\left\{1- \frac{(1.02\pi)^2}{2^3}\left[\left(\frac{\theta_q}{\theta_B}\right)^2 + \left(\frac{\theta_T}{\theta_B}\right)^2\right]\right\}, \tag{2.107}$$

and

$$D_1 = A \frac{(1.02\pi)^2}{2^2} \frac{\theta_q\theta_T}{\theta_B^2}, \tag{2.108}$$

Eqs. (2.105) and (2.106) become

$$\Sigma(t) = K'D_oF_k(t), \tag{2.109}$$

and

$$\Delta(t) = K'D_1F_k(t) \cos(2\pi f_s t-\phi_o) \tag{2.110}$$

These equations have the same forms as Eqs. (2.47) and (2.48). Therefore, using the results in the previous section, the angle-error signals are expressed as, from Eqs. (2.66) and (2.67),

$$\text{Azimuth angle-error signal} = \frac{V_r}{2}\frac{D_1}{D_o}\cos\phi_o, \text{ and} \tag{2.111}$$

$$\text{Elevation angle-error signal} = \frac{V_r}{2}\frac{D_1}{D_o}\sin\phi_o. \tag{2.112}$$

Then, the D_1/D_o may be easily obtained as

$$\frac{D_1}{D_o} \simeq \frac{(1.02\pi)^2}{2^2} \frac{\theta_q\theta_T}{\theta_B^2}. \tag{2.113}$$

Hence, Eqs. (2.111) and (2.112) become

$$\text{Azimuth angle-error signal} = \frac{V_r}{2} \frac{(1.02\pi)^2}{2^2} \left(\frac{\theta_q \theta_T}{\theta_B^2}\right) \cos\phi_o, \qquad (2.114)$$

and

$$\text{Elevation angle-error signal} = \frac{V_r}{2} \frac{(1.02\pi)^2}{2^2} \left(\frac{\theta_q \theta_T}{\theta_B^2}\right) \sin\phi_o. \qquad (2.115)$$

III. ALTERNATE ANALYSIS OF GAUSSIAN PATTERN

As described in the previous section, the antenna pattern is defined by

$$G(\theta) = G_o e^{-a^2\theta^2}, \qquad (2.116)$$

from Eq. (2.79).

Substituting θ^2 and θ'^2 given by Eqs. (2.9) and (2.10) into Eq. (2.116), the modulation factors due to antenna beams rotation become

$$G_1(\theta) = \exp\left[-a^2(\theta_q^2 + \theta_T^2)\right] \exp\left[2a^2\theta_q\theta_T \cos(\phi-\phi_o)\right], \qquad (2.117)$$

and

$$G_2(\theta') = \exp[-a^2(\theta_q^2 + \theta_T^2)] \exp[2a^2\theta_q\theta_T \cos(\phi-\phi_o+\pi)]. \qquad (2.118)$$

The Jacobi-Anger formula gives (1, p. 376; 40, p. 341)

$$e^{z\cos\psi} = \sum_{n=o}^{\infty} E_n I_n(z) \cos n\psi, \qquad (2.119)$$

where E_n is the Neumann factor as

$$E_n = \begin{cases} 1, & \text{for } n = 0 \\ 2, & \text{for } n = 1,2,3 \ldots, \end{cases} \tag{2.120}$$

and $I_n(z)$ is the modified Bessel function.

Upon using the Jacobi-Anger formula, $G_1(\theta)$ and $G_2(\theta')$ as a function of time become

$$G_1(t) = \exp[-a^2(\theta_q^2+\theta_T^2)] \sum_{n=o}^{\infty} E_n I_n(2a^2\theta_q\theta_T) \cos(2n\pi f_s t - n\phi_o), \tag{2.121}$$

and

$$G_2(t) = \exp[-a^2(\theta_q^2+\theta_T^2)] \sum_{n=o}^{\infty} E_n I_n(2a^2\theta_q\theta_T) \cos(2n\pi f_s t - n\phi_o + n\pi), \tag{2.122}$$

since $\theta = 2\pi f_s t$.

For the sake of convenience, letting (32, p. 171)

$$K'' = \left\{\exp[-a^2(\theta_q^2 + \theta_T^2)]\right\} I_o(2a^2\theta_q\theta_T), \tag{2.123}$$

and

$$K_n = \frac{2\, I_n(2a^2\theta_q\theta_T)}{I_o(2a^2\theta_q\theta_T)}, \tag{2.124}$$

the antenna scan modulation factors $G_1(t)$ and $G_2(t)$ are also written as

$$G_1(t) = K''[1 + \sum_{n=1}^{\infty} K_n \cos(2n\pi f_s t - n\phi_o)], \tag{2.125}$$

and

$$G_2(t) = K''[1 + \sum_{n=1}^{\infty} (-1)^n K_n \cos(2n\pi f_s t - n\phi_o)]. \quad (2.126)$$

Then, the sum and difference antenna patterns become

$$G_1(t) + G_2(t) = K''\left\{2 + \sum_{n=1}^{\infty} [1 + (-1)^n]K_n \cos(2n\pi f_s t - n\phi_o)\right\}, \quad (2.127)$$

and

$$G_1(t) - G_2(t) = K'' \sum_{n=1}^{\infty} [1-(-1)^n]K_n \cos(2n\pi f_s t - n\phi_o). \quad (2.128)$$

Similarly, the sum signal $\Sigma(t)$ and the difference signal $\Delta(t)$ are also written as

$$\Sigma(t) = K'K''F_k(t)\left\{2 + \sum_{n=1}^{\infty}[1 + (-1)^n]K_n \cos(2n\pi f_s t - n\phi_o)\right\}, \quad (2.129)$$

and

$$\Delta(t) = K'K''F_k(t) \sum_{n=1}^{\infty} [1 - (-1)^n]K_n \cos(2n\pi f_s t - n\phi_o). \quad (2.130)$$

1. Monopulse-Conical Scan Method

The time dependent error signal e(t) has been given by, in this case,

$$e(t) = \frac{G_1(t) - G_2(t)}{G_1(t) + G_2(t)}. \quad (2.131)$$

Substituting Eqs. (2.127) and (2.128) into Eq. (2.131), we have

$$e(t) = \frac{\sum_{n=1}^{\infty} K_{2n-1} \cos[2(2n-1)\pi f_s t-(2n-1)\phi_o]}{1 + \sum_{n=1}^{\infty} K_{2n} \cos(4n\pi f_s t-2n\phi_o)} . \tag{2.132}$$

Using the relation of Eq. (2.124), the e(t) is expressed in terms of the modified Bessel functions as

$$e(t) = \frac{\sum_{n=1}^{\infty} 2 I_{2n-1}(2a^2\theta_q\theta_T) \cos[2(2n-1)\pi f_s t-(2n-1)\phi_o]}{I_o(2a^2\theta_q\theta_T) + \sum_{n=1}^{\infty} 2 I_{2n}(2a^2\theta_q\theta_T) \cos(4n\pi f_s t-2n\phi_o)} . \tag{2.133}$$

Under the conditions

$$\left.\begin{aligned} 0 \leq 2a^2\theta_q\theta_T = \frac{2.776\theta_q\theta_T}{\theta_B^2} < 1, \\ \text{and} \\ (2a^2\theta_q\theta_T)^2 \text{ or higher order} \simeq 0, \end{aligned}\right\} \tag{2.134}$$

e(t) may be approximated by[†]

$$e(t) \simeq 2(a^2\theta_q\theta_T) \cos(2\pi f_s t-\phi_o). \tag{2.135}$$

Hence, the angle-error signals are

[†]Appendix B.

$$\text{Azimuth angle-error signal} = V_r(a^2\theta_q\theta_T)\cos\phi_o, \tag{2.136}$$

and

$$\text{Elevation angle-error signal} = V_r(a^2\theta_q\theta_T)\sin\phi_o. \tag{2.137}$$

2. Conical Scan-Monopulse Method

Rewriting Eqs. (2.129) and (2.130), the sum signal $\Sigma(t)$ and the different signal $\Delta(t)$ for this case are

$$\Sigma(t) = K'K''F_k(t)\left\{2 + \sum_{n=1}^{\infty}[1 + (-1)^n]K_n\cos(2n\pi f_s t - n\phi_o)\right\}, \tag{2.138}$$

and

$$\Delta(t) = K'K''F_k(t)\sum_{n=1}^{\infty}[1 - (-1)^n]K_n\cos(2n\pi f_s t - n\phi_o). \tag{2.139}$$

These equations† may be approximated, under the conditions for the small angles by Eq. (2.134), by

$$\Sigma(t) \simeq 2K'(t)K''F_k(t), \tag{2.140}$$

and

$$\Delta(t) \simeq 4K'(t)K''F_k(t)(a^2\theta_q\theta_T)\cos(2\pi f_s t - \phi_o). \tag{2.141}$$

Replacing the terms in Eqs. (2.140) and (2.141) as

$$\left.\begin{aligned} 2 &\longleftrightarrow A, \\ K'' &\longleftrightarrow D_o, \text{ and} \\ K''(2a^2\theta_q\theta_T) &\longleftrightarrow D_1 \end{aligned}\right\} \tag{2.142}$$

†Appendix C.

they are written as

$$\Sigma(t) = A\, D_0 K'(t) F_k(t), \tag{2.143}$$

and

$$\Delta(t) = A\, D_1 K'(t) F_k(t) \cos(2\pi f_s t - \phi_0). \tag{2.144}$$

Since K" is a function of θ_q, θ_T, and θ_B, Eqs. (2.143) and (2.144) are also the same forms as in Eqs. (2.47) and (2.48). Therefore, their results will be used for this case. From Eqs. (2.66) and (2.67), the angle-error signals are

$$\text{Azimuth angle-error signal} = \frac{V_r}{2} \frac{D_1}{D_0} \cos\phi_0, \tag{2.145}$$

and

$$\text{Elevation angle-error signal} = \frac{V_r}{2} \frac{D_1}{D_0} \sin\phi_0. \tag{2.146}$$

From the relations of Eq. (2.142), they can be directly obtained as

$$\text{Azimuth angle-error signal} = V_r(a^2 \theta_q \theta_T) \cos\phi_0, \tag{2.147}$$

and

$$\text{Elevation angle-error signal} = V_r(a^2 \theta_q \theta_T) \sin\phi_0. \tag{2.148}$$

IV. COMPARISON OF SMALL ANGLE RESULTS

The error signal extraction for small pattern squint and target angles has been discussed and the two kinds of approaches have been used for them; the analysis due to expanding an arbitrary antenna pattern to the Maclaurin's series and the analysis for the Bessel and Gaussian pattern due to their suitable series expansion. The results from the two approaches for the Bessel and Gaussian patterns are summarized in Table 2.1. It could be recognized from this table that the results from the two approaches coincide and our analysis may be correct.

V. GENERAL ANALYSIS FOR LARGE TARGET AND SQUINT ANGLES USING ARBITRARY PATTERN

We have discussed the extraction of the error in case of small target and pattern squint angles in the previous sections. In this actual tracking radar system they will not be so small. We will describe the extraction of the error signal for comparatively large target and pattern squint angles in this section. The sum of two rotating beams will be used usually as the transmitter antenna pattern and it will not be independent of time in this case because the pattern squint angle is not small and the illumination of the signal is modulated due to the antenna rotation. In the monopulse-conical scan method, however, the first signal processor will take the ratio of Δ/Σ and it will be cancelled out at the signal processor because it will be a common term of the Δ and Σ signals. On the other hand, it has to be taken into account in the conical scan-monopulse method since

Table 2.1

Summary of Error-Signals for Two Antenna Patterns in Case of Small Squint Angle and Target Angle

Type of Antenna	Monopulse-Conical Scan		Conical Scan-Monopulse	
	Alternate Calculation	Maclaurin Expansion	Alternate Calculation	Maclaurin Expansion
Gaussian Function Antenna Pattern	A.E.S. $= (a^2\theta_q\theta_T)V_r\cos\phi_o$	A.E.S. $= (a^2\theta_q\theta_T)V_r\cos\phi_o$	A.E.S. $= (a^2\theta_q\theta_T)V_r\cos\phi_o$	A.E.S. $= (a^2\theta_q\theta_T)V_r\cos\phi_o$
	E.E.S. $= (a^2\theta_q\theta_T)V_r\sin\phi_o$	E.E.S. $= (a^2\theta_q\theta_T)V_r\sin\phi_o$	E.E.S. $= (a^2\theta_q\theta_T)V_r\sin\phi_o$	E.E.S. $= (a^2\theta_q\theta_T)V_r\sin\phi_o$
Bessel Function Antenna Pattern	A.E.S. $= \frac{V_r}{2}\left(\frac{1.02\pi}{2}\right)^2\frac{\theta_q\theta_T}{\theta_B^2}\cos\phi_o$	A.E.S. $= \frac{V_r}{2}\left(\frac{1.02\pi}{2}\right)^2\frac{\theta_q\theta_T}{\theta_B^2}\cos\phi_o$	A.E.S. $= \frac{V_r}{2}\left(\frac{1.02\pi}{2}\right)^2\frac{\theta_q\theta_T}{\theta_B^2}\cos\phi_o$	A.E.S. $= \frac{V_r}{2}\left(\frac{1.02\pi}{2}\right)^2\frac{\theta_q\theta_T}{\theta_B^2}\cos\phi_o$
	E.E.S. $= \frac{V_r}{2}\left(\frac{1.02\pi}{2}\right)^2\frac{\theta_q\theta_T}{\theta_B^2}\sin\phi_o$	E.E.S. $= \frac{V_r}{2}\left(\frac{1.02\pi}{2}\right)^2\frac{\theta_q\theta_T}{\theta_B^2}\sin\phi_o$	E.E.S. $= \frac{V_r}{2}\left(\frac{1.02\pi}{2}\right)^2\frac{\theta_q\theta_T}{\theta_B^2}\sin\phi_o$	E.E.S. $= \frac{V_r}{2}\left(\frac{1.02\pi}{2}\right)^2\frac{\theta_q\theta_T}{\theta_B^2}\sin\phi_o$

A.E.S. = Azimuth angle-error signal; E.E.S. = Elevation angle-error signal.

the Δ and Σ signals including the transmitter signal modulated due to the antenna rotation are demodulated and low-pass filtered. Considering a beacon type target (cooperative target), for instance, a satellite, the modulated transmitter antenna pattern will not need to be taken into account since the target transmits the return signal and the broad antenna beam will be used on the target. Therefore, the two types of the error signals, for the beacon type target and the ordinary passive target, in the conical scan-monopulse method will be derived in this section.

In this system the maximum pattern squint angle would be half of each antenna beamwidth. Therefore, the target angle is also within half of each beamwidth since it is assumed that target is in the circle due to the two antenna beams rotation. Also, the antenna beamwidth expected to be used in this system may be in the order of several degrees. It could be assumed that the variable x in the arbitrary antenna pattern G(x) may have such a linear relation that

$$x = d_1 \left(\frac{\theta}{\theta_B} \right), \tag{2.149}$$

as Eqs. (2.19) and (2.20).

The general expression for the two antenna patterns, from Eqs. (2.27) and (2.28), become

$$G_1(\theta) = \sum_{r=0}^{\infty} (-1)^r \left\{ \sum_{n=r}^{\infty} \frac{C_{2n} d_1^{2n}}{(2n)!} \binom{n}{r} \left[\left(\frac{\theta_q}{\theta_B} \right)^2 + \left(\frac{\theta_T}{\theta_B} \right)^2 \right]^{n-r} \right\}$$

$$\times \left[\frac{2\theta_q \theta_T}{\theta_B^2} \cos(\phi - \phi_o) \right]^r, \tag{2.150}$$

and

$$G_2(\theta) = \sum_{r=0}^{\infty} \left\{ \sum_{n=r}^{\infty} \frac{c_{2n} d_1^{2n}}{(2n)!} \binom{n}{r} \left[\left(\frac{\theta_q}{\theta_B} \right)^2 + \left(\frac{\theta_T}{\theta_B} \right)^2 \right]^{n-r} \right\}$$

$$\times \left[\frac{2\theta_q \theta_T}{\theta_B^2} \cos(\phi - \phi_o) \right]^r . \qquad (2.151)$$

They have an infinite number of terms. How many terms in Eqs. (2.150) and (2.151) will satisfactorily express the antenna pattern in the angle region where our radar system will use? There is, however, no way to decide the number of the terms in general. But it could be supposed that the five terms may express the antenna pattern with some error in the region.

Taking the five terms in Eqs. (2.150) and (2.151), the sum and the difference of the two antenna patterns become

$$G_1(\theta) + G_2(\theta) = \sum_{r=0}^{4} [1 + (-1)^r]$$

$$\times \left\{ \sum_{n=r}^{4} \frac{c_{2n} d_1^{2n}}{(2n)!} \binom{n}{r} \left[\left(\frac{\theta_q}{\theta_B} \right)^2 + \left(\frac{\theta_T}{\theta_B} \right)^2 \right]^{n-r} \right\} \left[\frac{2\theta_q \theta_T}{\theta_B^2} \cos(\phi - \phi_o) \right]^r , \qquad (2.152)$$

and

$$G_1(\theta) - G_2(\theta) = - \sum_{r=0}^{4} [1 - (-1)^r]$$

$$\times \left\{ \sum_{n=r}^{4} \frac{c_{2n} d_1^{2n}}{(2n)!} \binom{n}{r} \left[\left(\frac{\theta_q}{\theta_B} \right)^2 + \left(\frac{\theta_T}{\theta_B} \right)^2 \right]^{n-r} \right\} \left[\frac{2\theta_q \theta_T}{\theta_B^2} \cos(\phi - \phi_o) \right]^r . \qquad (2.153)$$

1. Monopulse-Conical Scan Method

As described several times, the time dependent error signal is defined by

$$e(t) = \frac{\Delta}{\Sigma} = \frac{G_1(t) - G_2(t)}{G_1(t) + G_2(t)} . \tag{2.154}$$

If Eqs. (2.152) and (2.153) are substituted into Eq. (2.154) to obtain the error signal e(t), it may be very complicated. Therefore, letting[†]

$$x = \left(\frac{\theta_q}{\theta_B}\right)^2 + \left(\frac{\theta_T}{\theta_B}\right)^2 , \tag{2.155}$$

$$y = \frac{2\theta_q\theta_T}{\theta_B^2} \cos(2\pi f_s t - \phi_o), \tag{2.156}$$

and

$$A_r = \sum_{n=r}^{4} \frac{c_{2n} d_1^{2n}}{(2n)!} \binom{n}{r} x^{n-r}, \quad r = 0,1,2,3,4. \tag{2.157}$$

Then, the sum and difference antenna patterns given by Eqs. (2.152) and (2.153) are expressed as the simple representations

$$G_1(t) + G_2(t) = 2[A_o + A_2 y^2 + A_4 y^4], \tag{2.158}$$

and

$$G_1(t) - G_2(t) = -2[A_1 y + A_3 y^3]. \tag{2.159}$$

[†]This x is different from the one of Eq. (2.149). It is used for convenience to calculate.

Thus, the time dependent error signal

$$e(t) = - \frac{A_1 y + A_3 y^3}{A_0 + A_2 y^2 + A_4 y^4} . \qquad (2.160)$$

Supposed that A_j, j=0, 1, 2, 3, 4, are constant, y is variable, the inverse of the denominator is infinitely differentiable with respect to y in the region concerned, and they are continuous in the region, then e(t) may be expanded to, by the Taylor expansion,

$$e(t) = -\left\{\frac{A_1}{A_0} y - \left(\frac{A_1 A_2}{A_0^2} - \frac{A_3}{A_0}\right) y^3 + \left[\frac{A_1}{A_0}\left(\frac{A_2^2}{A_0^2} - \frac{A_4}{A_0}\right) - \frac{A_2 A_3}{A_0^2}\right] y^5 + \cdots\right\} . \qquad (2.161)$$

Neglecting all terms above fifth power of y since it is assumed that the antenna pattern is approximate to eighth order of θ and y is the second order of θ_q and θ_T which are the components of θ, Eq. (2.161) becomes

$$e(t) = - \left[\frac{A_1}{A_0} y - \left(\frac{A_1 A_2}{A_0^2} - \frac{A_3}{A_0}\right) y^3\right] . \qquad (2.162)$$

Substituting the expression for y given by Eq. (2.156) into the above equation gives

$$e(t) = -\left[\frac{A_1}{A_o} - \frac{3}{4}\left(\frac{2\theta_q\theta_T}{\theta_B^2}\right)^2\left(\frac{A_1A_2}{A_o^2} - \frac{A_3}{A_o}\right)\right]\left[\frac{2\theta_q\theta_T}{\theta_B^2}\cos(2\pi f_s t-\phi_o)\right]$$

$$-\frac{1}{4}\left(\frac{2\theta_q\theta_T}{\theta_B^2}\right)^3\left(\frac{A_1A_2}{A_o^2} - \frac{A_3}{A_o}\right)\cos(6\pi f_s t-3\phi_o) \quad . \qquad (2.163)$$

Thus, the angle-error signals become

Azimuth angle-error signal

$$= -\frac{V_r}{2}\left[\frac{A_1}{A_o} - \frac{3}{4}\left(\frac{2\theta_q\theta_T}{\theta_B^2}\right)^2\left(\frac{A_1A_2}{A_o^2} - \frac{A_3}{A_o}\right)\right]\left(\frac{2\theta_q\theta_T}{\theta_B^2}\right)\cos\phi_o, \qquad (2.164)$$

and

Elevation angle-error signal

$$= -\frac{V_r}{2}\left[\frac{A_1}{A_o} - \frac{3}{4}\left(\frac{2\theta_q\theta_T}{\theta_B^2}\right)^2\left(\frac{A_1A_2}{A_o^2} - \frac{A_3}{A_o}\right)\right]\left(\frac{2\theta_q\theta_T}{\theta_B^2}\right)\sin\phi_o. \qquad (2.165)$$

The first five terms on the antenna pattern series expansion were used in the above discussion. The variable θ in the antenna pattern also consists of the variables θ_q and θ_T which are the same power relation. The fifth term of the antenna pattern expansion corresponds to the eight power of θ, that is, the eight power of θ_q and θ_T. The terms of θ_T and θ_q above the ninth power may be neglected. This relation has been applied to Eq. (2.162).

Rewriting Eq. (2.157), we have

$$A_0 = a_0 + a_1 x + a_2 x^2 + a_3 x^3 + a_4 x^4, \tag{2.166}$$

$$A_1 = a_1 + 2a_2 x + 3a_3 x^2 + 4a_4 x^3, \tag{2.167}$$

$$A_2 = a_2 + 3a_3 x + 6a_4 x^2, \tag{2.168}$$

and

$$A_3 = a_3 + 4a_4 x, \tag{2.169}$$

where

$$a_n = \frac{c_{2n} d_1^{2n}}{(2n)!}, \quad \text{for } n=0,1,2,3,4. \tag{2.170}$$

Supposing that A_j is a function of x, A_0 and A_0^2 do not become to zero in the region considered, and $1/A_0$ and $1/A_0^2$ are infinitely differentiable, the terms† formed by A_j in Eq. (2.163) become

$$\frac{A_1}{A_0} \simeq \frac{a_1}{a_0} - \left(\frac{a_1^2}{a_0^2} - \frac{2a_2}{a_0}\right) x + \left(\frac{a_1^3}{a_0^3} - \frac{3a_1 a_2}{a_0^2} + \frac{3a_3}{a_0}\right) x^2$$

$$- \left(\frac{a_1^4}{a_0^4} - \frac{4a_1^2 a_2}{a_0^3} + \frac{4a_1 a_3}{a_0^2} + \frac{2a_2^2}{a_0^2} - \frac{4a_4}{a_0^2}\right) x^3, \tag{2.171}$$

$$\frac{A_1 A_2}{A_0^2} \simeq \frac{a_1 a_2}{a_0^2} - \left(\frac{2a_1^2 a_2}{a_0^3} - \frac{3a_1 a_3}{a_0^3} - \frac{2a_2^2}{a_0^2}\right) x, \tag{2.172}$$

and

$$\frac{A_3}{A_0} \simeq \frac{a_3}{a_0} - \left(\frac{a_1 a_3}{a_0^2} - \frac{4a_4}{a_0}\right) x. \tag{2.173}$$

---

†Appendix D.

Using the relations above, the angle-error signals given by Eqs. (2.164) and (2.165) become

Azimuth angle-error signal

$$= -\frac{V_r}{2}\left\{\frac{a_1}{a_0} - \left(\frac{a_1^2}{a_0} - \frac{2a_2}{a_0}\right)x + \left(\frac{a_1^3}{a_0^3} - \frac{3a_1a_2}{a_0^2} + \frac{3a_3}{a_0}\right)x^2 \right.$$

$$- \left(\frac{a_1^4}{a_0^4} - \frac{4a_1^2a_2}{a_0^3} + \frac{4a_1a_3}{a_0^2} + \frac{2a_2^2}{a_0^2} - \frac{4a_4}{a_0}\right)x^3$$

$$- \frac{3}{4}\left(\frac{2\theta_q\theta_T}{\theta_B^2}\right)^2 \left[\frac{a_1a_2}{a_0^2} - \frac{a_3}{a_0} - \left(\frac{2a_1^2a_2}{a_0^3} - \frac{4a_1a_2}{a_0^2} - \frac{2a_2^2}{a_0^2}\right.\right.$$

$$\left.\left.\left. + \frac{4a_4}{a_0}\right)x\right]\right\}\left(\frac{2\theta_q\theta_T}{\theta_B^2}\right)\cos\phi_0, \qquad (2.174)$$

and

Elevation angle-error signal

$$= -\frac{V_r}{2}\left\{\frac{a_1}{a_0} - \left(\frac{a_1^2}{a_0^2} - \frac{2a_2}{a_0}\right)x + \left(\frac{a_1^3}{a_0^3} - \frac{3a_1a_2}{a_0^2} + \frac{3a_3}{a_0}\right)x^2 \right.$$

$$- \left\{\frac{a_1^4}{a_0^4} - \frac{4a_1^2a_2}{a_0^3} + \frac{4a_1a_3}{a_0^2} + \frac{2a_2^2}{a_0^2} - \frac{4a_4}{a_0}\right\}x^3$$

$$- \frac{3}{4}\left(\frac{2\theta_q\theta_T}{\theta_B^2}\right)^2 \left[\frac{a_1a_2}{a_0^2} - \frac{a_3}{a_0} - \left(\frac{2a_1^2a_2}{a_0^3} - \frac{4a_1a_3}{a_0^2} - \frac{2a_2^2}{a_0^2}\right.\right.$$

$$\left.\left.\left. + \frac{4a_4}{a_0}\ x\right]\right\}\left(\frac{2\theta_q\theta_T}{\theta_B^2}\right)\sin\phi_0, \qquad (2.175)$$

where

$$\left.\begin{aligned} x &= \left(\frac{\theta_q}{\theta_B}\right)^2 + \left(\frac{\theta_T}{\theta_B}\right)^2, \\ a_0 &= c_0, \\ a_1 &= \frac{c_2 d_1^{\,2}}{2!}, \\ a_2 &= \frac{c_4 d_1^{\,4}}{4!}, \\ a_3 &= \frac{c_6 d_1^{\,6}}{6!}, \end{aligned}\right\} \tag{2.176}$$

and

$$a_4 = \frac{c_8 d_1^{\,8}}{8!}.$$

Here, it has to be remarked that the first order approximation of Eq. (2.174) and (2.175) becomes

$$\left.\begin{matrix} \text{Azimuth angle-error signal} \\ \text{Elevation angle-error signal} \end{matrix}\right\} = -\frac{V_r}{2}\,\frac{c_2 d_1^{\,2}}{c_0}\,\frac{\theta_q \theta_T}{\theta_B^2}\left\{\begin{matrix} \cos\phi_0 \\ \sin\phi_0 \end{matrix}\right\}, \tag{2.177}$$

and they are the same results as in the previous section.

2. Conical Scan-Monopulse Method for Active Target

The analysis of the conical scan-monopulse method for active target will be described in this section.

From Eqs. (2.158) and (2.159), the sum $\Sigma(t)$ and the difference $\Delta(t)$ are written as

$$\Sigma(t) = K'(t)F_k(t)[G_1(t) + G_2(t)]$$

$$= 2K'(t)F_k(t)[A_0 + A_2y^2 + A_4y^4], \tag{2.178}$$

and

$$\Delta(t) = K'(t)F_k(t)[G_1(t) - G_2(t)]$$

$$= -2K'(t)F_k(t)[A_1y + A_3y^3]. \tag{2.179}$$

Substituting Eq. (2.156) into Eqs. (2.178) and (2.179) and rearranging them in order of f_s, we have

$$\Sigma(t) = 2K'(t)F_k(t)\left\{\left[A_o + \frac{A_2}{2}\left(\frac{2\theta_q\theta_T}{\theta_B^2}\right)^2 + \frac{3A_4}{8}\left(\frac{2\theta_q\theta_T}{\theta_B^2}\right)^4\right]\right.$$

$$+ \left[\frac{A_2}{2} + \frac{A_4}{2}\left(\frac{2\theta_q\theta_T}{\theta_B^2}\right)^2\right]\left(\frac{2\theta_q\theta_T}{\theta_B^2}\right)^2\cos(4\pi f_s t - 2\phi_o)$$

$$\left. + \frac{A_4}{8}\left(\frac{2\theta_q\theta_T}{\theta_B^2}\right)^4\cos(8\pi f_s t - 4\phi_o)\right\}, \tag{2.180}$$

and

$$\Delta(t) = -2K'(t)F_k(t)\left\{\left[A_1 + \frac{3A_3}{4}\left(\frac{2\theta_q\theta_T}{\theta_B^2}\right)\right]\left(\frac{2\theta_q\theta_T}{\theta_B^2}\right)\right.$$

$$\left. \times \cos(2\pi f_s t - \phi_o) + \frac{A_3}{4}\left(\frac{2\theta_q\theta_T}{\theta_B^2}\right)^3\cos(6\pi f_s t - 3\phi_o)\right\}. \tag{2.181}$$

Letting

$$
\left.
\begin{aligned}
D_0 &= 2\left[A_0 + \frac{A_2}{2}\left(\frac{2\theta_q\theta_T}{\theta_B^2}\right)^2 + \frac{3A_4}{8}\left(\frac{2\theta_q\theta_T}{\theta_B^2}\right)^4\right], \\
D_1 &= -2\left[A_1 + \frac{3A_3}{4}\left(\frac{2\theta_q\theta_T}{\theta_B^2}\right)\right]\left(\frac{2\theta_q\theta_T}{\theta_B^2}\right), \\
D_2 &= \left[A_2 + A_4\left(\frac{2\theta_q\theta_T}{\theta_B^2}\right)\right]\left(\frac{2\theta_q\theta_T}{\theta_B^2}\right), \\
D_3 &= -\frac{A_3}{2}\left(\frac{2\theta_q\theta_T}{\theta_B^2}\right)^3, \\
D_4 &= \frac{A_4}{4}\left(\frac{2\theta_q\theta_T}{\theta_B^2}\right)^4
\end{aligned}
\right\} \qquad (2.182)
$$

and

$$
\left.
\begin{aligned}
f_1(t) &= K'(t)\cos(\omega_s t - \phi_o), \\
f_2(t) &= K'(t)\cos(2\omega_s t - 2\phi_o), \\
f_3(t) &= K'(t)\cos(3\omega_s t - 3\phi_o), \\
f_4(t) &= K'(t)\cos(4\omega_s t - 4\phi_o),
\end{aligned}
\right\} \qquad (2.183)
$$

the sum signal $\Sigma(t)$ and the difference signal $\Delta(t)$ given by Eqs. (2.180) and (2.181) reduce to the simpler representations

$$\Sigma(t) = D_0 K'(t) F_k(t) + D_2 f_2(t) F_k(t) + D_4 f_4(t) F_k(t), \tag{2.184}$$

and

$$\Delta(t) = D_1 f_1(t) F_k(t) + D_3 f_3(t) F_k(t). \tag{2.185}$$

Assuming that the spectrum of $K'(t)$ is less than half of the rotation frequency ω_s, $f_i(t)$, $i = 1, 2, 3, 4$, in Eq. (2.183) are ordinary amplitude modulation.

Taking the Fourier transform[†] on Eqs. (2.184) and (2.185), they become, in terms of the Fourier transform of $K'(t)$,

$$\begin{aligned}\Sigma(\omega) = &\sum_{n=-\infty}^{\infty} D_0 C_n K'(\omega - n\omega_p) \\ &+ \sum_{n=-\infty}^{\infty} D_2 C_n \left\{ \frac{e^{-j2\phi_0}}{2} K'(\omega - n\omega_p - 2\omega_s) + \frac{e^{j2\phi_0}}{2} K'(\omega - n\omega_p + 2\omega_s) \right\} \\ &+ \sum_{n=-\infty}^{\infty} D_4 C_n \left\{ \frac{e^{-j4\phi_0}}{2} K'(\omega - n\omega_p - 4\omega_s) + \frac{e^{j4\phi_0}}{2} K'(\omega - n\omega_p + 4\omega_s) \right\},\end{aligned} \tag{2.186}$$

and

$$\begin{aligned}\Delta(\omega) = &\sum_{n=-\infty}^{\infty} D_1 C_n \left\{ \frac{e^{-j\phi_0}}{2} K'(\omega - n\omega_p - \omega_s) + \frac{e^{j\phi_0}}{2} K'(\omega - n\omega_p + \omega_s) \right\} \\ &+ \sum_{n=-\infty}^{\infty} D_3 C_n \left\{ \frac{e^{-j3\phi_0}}{2} K'(\omega - n\omega_p - 3\omega_s) + \frac{e^{j3\phi_0}}{2} K'(\omega - n\omega_p + 3\omega_s) \right\}\end{aligned} \tag{2.187}$$

[†]Appendix E.

where C_n's are the coefficients of the complex Fourier series for $F_k(t)$ given by Eq. (2.56).

The spectra of $\Sigma(\omega)$ and $\Delta(\omega)$ are shown in Figure 2.4, assuming that the spectrum of $K'(\omega)$ is given by Figure 2.2(B), p. 59.

From Figure 2.4, it could be known that the spectra in this case include the same component of the spectra in Figure 2.2, p. 25, and the harmonics components increase. Therefore, the results given by Eqs. (2.66) and (2.67) can be applied to this analysis.

Thus, the angle-error signals are expressed by the representations as

$$\text{Azimuth angle-error signal} = \frac{V_r}{2}\frac{D_1}{D_0}\cos\phi_0, \tag{2.188}$$

and

$$\text{Elevation angle-error signal} = \frac{V_r}{2}\frac{D_1}{D_0}\sin\phi_0. \tag{2.189}$$

Here, the term D_1/D_0 is written as, from Eq. (2.182),

$$\frac{D_1}{D_0} = -\frac{\left[A_1 + \frac{3A_3}{4}\left(\frac{2\theta_q\theta_T}{\theta_B^2}\right)^2\right]\frac{2\theta_q\theta_T}{\theta_B^2}}{A_0 + \frac{A_2}{2}\left(\frac{2\theta_q\theta_T}{\theta_B^2}\right)^2 + \frac{3A_4}{8}\left(\frac{2\theta_q\theta_T}{\theta_B^2}\right)^4}$$

After some labor,† the above equation is approximated as

$$\frac{D_1}{D_0} \simeq \frac{a_1}{a_0} - \left(\frac{a_1^2}{a_0^2} - \frac{2a_2}{a_0}\right)x + \left(\frac{a_1^3}{a_0^3} - \frac{3a_1a_2}{a_0^2} + \frac{3a_3}{a_0}\right)x^2$$

†Appendix F.

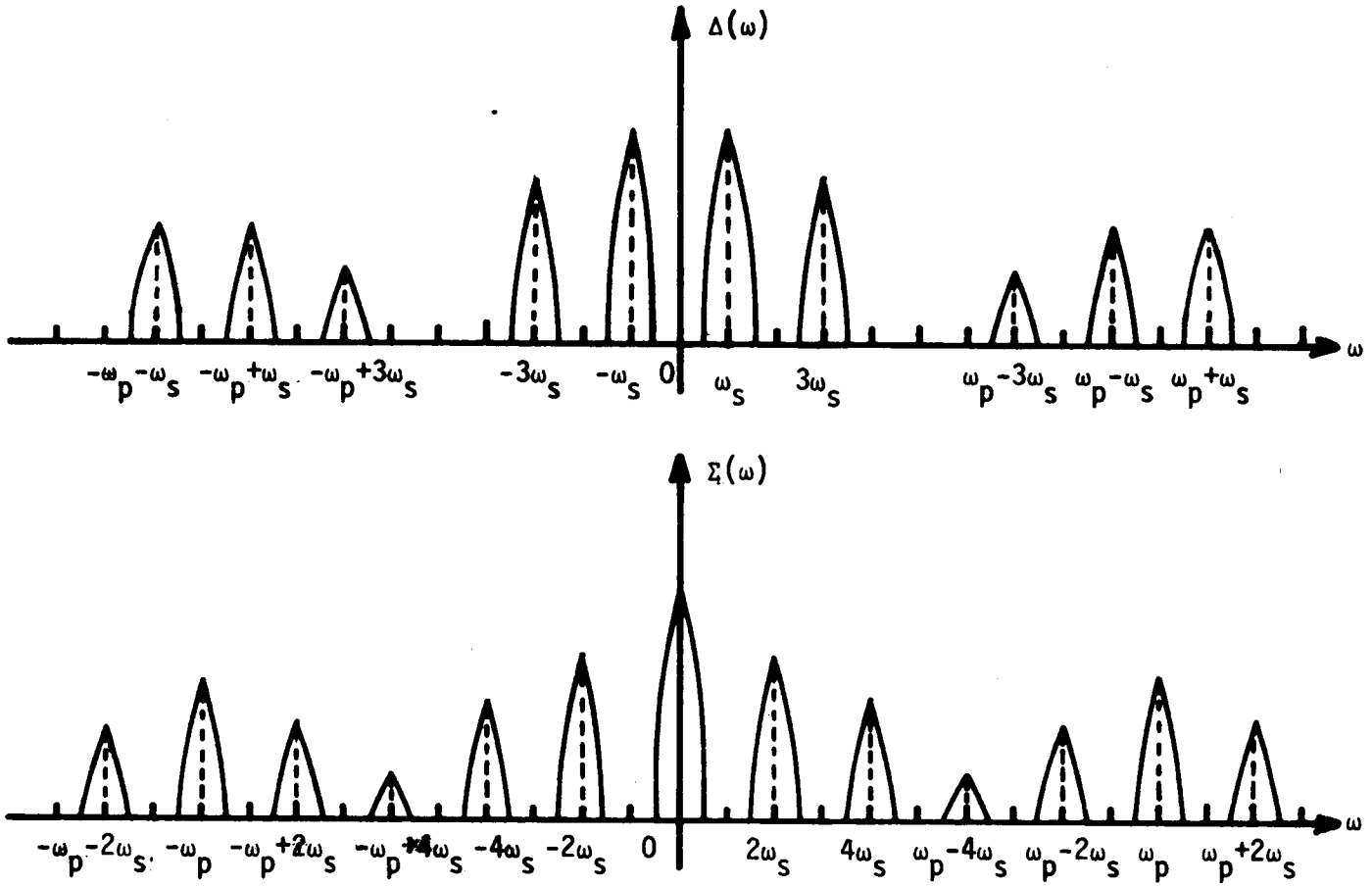


Figure 2.4. Spectra of $\Sigma(t)$ and $\Delta(t)$ in terms of $K'(\omega)$ in case of active target.

$$-\left(\frac{a_1^4}{a_0^4}-\frac{4a_1^2a_2}{a_0^3}+\frac{4a_1a_3}{a_0^2}+\frac{2a_2^2}{a_0^2}-\frac{4a_4}{a_0}\right)x^3$$

$$-\left(\frac{2\theta_q\theta_T}{\theta_B^2}\right)^2\left[\frac{1}{2}\,\frac{a_1a_2}{a_0^2}-\frac{3a_3}{4a_0}-\frac{1}{2}\left(\frac{2a_1^2a_2}{a_0^3}\right.\right.$$

$$\left.\left.-\frac{9}{2}\,\frac{a_1a_3}{a_0^2}-\frac{2a_2^2}{a_0^2}+\frac{6a_4}{a_0}\right)x\right]\left(\frac{2\theta_q\theta_T}{\theta_B^2}\right). \qquad (2.191)$$

Hence, the angle-error signals become

Azimuth angle-error signal

$$=-\frac{V_r}{2}\left\{\frac{a_1}{a_0}-\left(\frac{a_1^2}{a_0^2}-\frac{2a_2}{a_0}\right)x+\left(\frac{a_1^3}{a_0^3}-\frac{3a_1a_2}{a_0^2}+\frac{3a_3}{a_0}\right)x^2\right.$$

$$-\left(\frac{a_1^4}{a_0^4}-\frac{4a_1^2a_2}{a_0^3}+\frac{4a_1a_3}{a_0^2}+\frac{2a_2^2}{a_0^2}-\frac{4a_4}{a_0}\right)x^3$$

$$-\left(\frac{2\theta_q\theta_T}{\theta_B^2}\right)\left[\frac{1}{2}\,\frac{a_1a_2}{a_0^2}-\frac{3a_3}{4a_0}-\frac{1}{2}\left(\frac{2a_1^2a_2}{a_0^3}\right.\right.$$

$$\left.\left.\left.-\frac{9}{2}\,\frac{a_1a_3}{2a_0^2}-\frac{2a_2^2}{a_0^2}+\frac{6a_4}{a_0}\right)x\right]\right\}\left(\frac{2\theta_q\theta_T}{\theta_B^2}\right)\cos\phi_o, \qquad (2.192)$$

and

Elevation angle-error signal

$$= -\frac{V_r}{2}\left\{ \frac{a_1}{a_0} - \left(\frac{a_1^2}{a_0^2} - \frac{2a_2}{a_0}\right)x + \left(\frac{a_1^3}{a_0^3} - \frac{3a_1a_2}{a_0^2} + \frac{3a_3}{a_0}\right)x^2 \right.$$

$$- \left(\frac{a_1^4}{a_0^4} - \frac{4a_1^2a_2}{a_0^3} + \frac{4a_1a_3}{a_0^2} + \frac{2a_2^2}{a_0^2} - \frac{4a_4}{a_0}\right)x^3$$

$$\left. - \frac{2\theta_q\theta_T}{\theta_B^2}\left[\frac{1}{2}\frac{a_1a_2}{a_0^2} - \frac{3a_3}{4a_0} - \frac{1}{2}\left(\frac{2a_1^2a_2}{a_0^3}\right.\right.\right.$$

$$\left.\left.\left. - \frac{9a_1a_3}{2a_0^2} - \frac{2a_2^2}{a_0^2} + \frac{6a_4}{a_0}\right)x\right]\right\}\left(\frac{2\theta_q\theta_T}{\theta_B^2}\right)\sin\phi_o, \qquad (2.193)$$

where

$$\left.\begin{aligned} x &= \left(\frac{\theta_q}{\theta_B}\right)^2 + \left(\frac{\theta_T}{\theta_B}\right)^2, \\ a_o &= c_o, \\ a_1 &= \frac{c_2 d_1^2}{2!}, \\ a_2 &= \frac{c_4 d_1^4}{4!}, \\ a_3 &= \frac{c_6 d_1^6}{6!}, \end{aligned}\right\} \qquad (2.194)$$

and

$$a_4 = \frac{c_8 d_1^8}{8!}.$$

3. Conical Scan-Monopulse Method for Passive Target

In case of the conical scan-monopulse method for a passive target, the transmitter antenna pattern is also modulated by the rotation. If we assume that the fluctuation component K'(t) includes this modulation, we can make use of the results for active target case. Then, the term K'(t) may be written as, in this case,

$$K'(t) = R(P_t,r)S(t)G_t(t), \tag{2.195}$$

where

$R(P_t,r)$ = a function of distance r and transmitter power P_t,

$S(t)$ = echo fluctuation included target cross section, and

$G_t(t)$ = $G_1(t) + G_2(t)$, transmitter antenna pattern.

The $G_t(t)$ is also written as, from Eq. (2.158)

$$G_t(t) = G_1(t) + G_2(t) = 2[A_0 + A_2y^2 + A_4y^4]. \tag{2.196}$$

Upon using Eqs. (2.156) and (2.182), this equation is also written as

$$G_t(t) = D_0 + D_2 \cos(2\omega_s t - 2\phi_0) + D_4 \cos(4\omega_s t - 4\phi_0). \tag{2.197}$$

The $R(P_t,r)$ in Eq. (2.195) may become constant due to action of the AGC so that

$$K'(t) = R_0S(t)[D_0 + D_2 \cos(2\omega_0 - 2\phi_0) + D_4 \cos(4\omega_s t - 4\phi_0)], \tag{2.198}$$

where R_0 is constant.

Again, assuming that S(t) is bandlimited so as to avoid aliasing, the Fourier transform of K'(t) becomes

$$K'(\omega) = R_o D_o S(\omega)$$

$$+ \frac{R_o D_2 e^{-j2\phi_o}}{2} S(\omega-2\omega_s) + \frac{R_o D_2 e^{j2\phi_o}}{2} S(\omega+2\omega_s)$$

$$+ \frac{R_o D_4 e^{-j4\phi_o}}{2} S(\omega-2\omega_s) + \frac{R_o D_4 e^{j4\phi_o}}{4} S(\omega+4\omega_s), \qquad (2.199)$$

where

$$S(\omega) = \mathcal{F}[S(t)].$$

If this K'(ω) is substituted into the Δ(ω) and Σ(ω) given by Eqs. (2.186) and (2.187), the Δ(ω) and Σ(ω)† for this case will be obtained as

$$\Delta(\omega) = \sum_{n=-\infty}^{\infty} R_o C_n \left\{ B_1 \frac{e^{-j\phi_o}}{2} S(\omega-n\omega_p-\omega_s) + B_1 \frac{e^{j\phi_o}}{2} S(\omega-n\omega_p+\omega_s) \right.$$

$$+ B_3 \frac{e^{-j3\phi_o}}{2} S(\omega-n\omega_p-3\omega_s) + B_3 \frac{e^{j3\phi_o}}{2} S(\omega-n\omega_p+3\omega_s)$$

$$+ B_5 \frac{e^{-j5\phi_o}}{2} S(\omega-n\omega_p-5\omega_s) + B_5 \frac{e^{j5\phi_o}}{2} S(\omega-n\omega_p+5\omega_s)$$

$$\left. + B_7 \frac{e^{-j7\phi_o}}{2} S(\omega-n\omega_p-7\omega_s) + B_7 \frac{e^{j7\phi_o}}{2} S(\omega-n\omega_p+7\omega_s) \right\}, \qquad (2.200)$$

---

†Appendix G.

and

$$\Sigma(\omega) = \sum_{n=-\infty}^{\infty} R_o C_n \Big\{ B_0 S(\omega - n\omega_p)$$

$$+ B_2 \frac{e^{-j2\phi_o}}{2} S(\omega - n\omega_p - 2\omega_s) + B_2 \frac{e^{j2\phi_o}}{2} S(\omega - n\omega_p + 2\omega_s)$$

$$+ B_4 \frac{e^{-j4\phi_o}}{2} S(\omega - n\omega_p - 4\omega_s) + B_4 \frac{e^{j4\phi_o}}{2} S(\omega - n\omega_p + 4\omega_s)$$

$$+ B_6 \frac{e^{-j6\phi_o}}{2} S(\omega - n\omega_p - 6\omega_s) + B_6 \frac{e^{j6\phi_o}}{2} S(\omega - n\omega_p + 6\omega_s)$$

$$+ B_8 \frac{e^{-j8\phi_o}}{2} S(\omega - n\omega_p - 8\omega_s) + B_8 \frac{e^{j8\phi_o}}{2} S(\omega - n\omega_p + 8\omega_s) \Big\}, \qquad (2.201)$$

where

$$\left.\begin{aligned}
B_0 &= D_0^2 + \frac{D_2^2}{2} + \frac{D_4^2}{2}, \\
B_1 &= D_0 D_1 + \frac{D_1 D_2}{2} + \frac{D_2 D_3}{2} + \frac{D_3 D_4}{2}, \\
B_2 &= 2D_0 D_2 + D_2 D_4, \\
B_3 &= \frac{D_1 D_2}{2} + \frac{D_1 D_4}{2} + D_0 D_3, \\
B_4 &= 2D_0 D_4 + \frac{D_2^2}{4}, \\
B_5 &= \frac{D_1 D_4}{2} + \frac{D_2 D_3}{2},
\end{aligned}\right\} \qquad (2.202)$$

$$B_6 = D_2 D_4 ,$$

$$B_7 = \frac{D_3 D_4}{2} , \text{ and}$$

$$B_8 = \frac{D_4^2}{2} .$$

The spectra of the $\Delta(\omega)$ and $\Sigma(\omega)$ given by Eqs. (2.200) and (2.201) are shown in Figure 2.5.

Since we will use the lowest spectral components on both the $\Delta(\omega)$ and $\Sigma(\omega)$, we can use the same procedure as in the previous section.

Replacing D_0 and D_1 by B_0 and B_1 in Eqs. (2.188) and (2.189), the angle error signals in this case are obtained as

$$\text{Azimuth angle-error signal} = \frac{V_r}{2} \frac{B_1}{B_0} \cos\phi_0 , \tag{2.203}$$

and

$$\text{Elevation angle-error signal} = \frac{V_r}{2} \frac{B_1}{B_0} \sin\phi_0 . \tag{2.204}$$

Substituting the relations in Eq. (2.182) into B_0 and B_1 in the above equation, and neglecting the terms having above fifth power of y, B_0 and B_1 become

$$B_0 = 4 \left\{ A_0^2 + A_0 A_2 y^2 + \left(\frac{3A_0 A_4}{8} + \frac{3A_2^2}{8} + \frac{3A_2 A_4}{16} \right) y^4 \right\} , \tag{2.205}$$

and

$$B_1 = -4 \left\{ A_0 A_1 y + \frac{3}{4} (A_1 A_2 + A_0 A_3) y^3 \right\} , \tag{2.206}$$

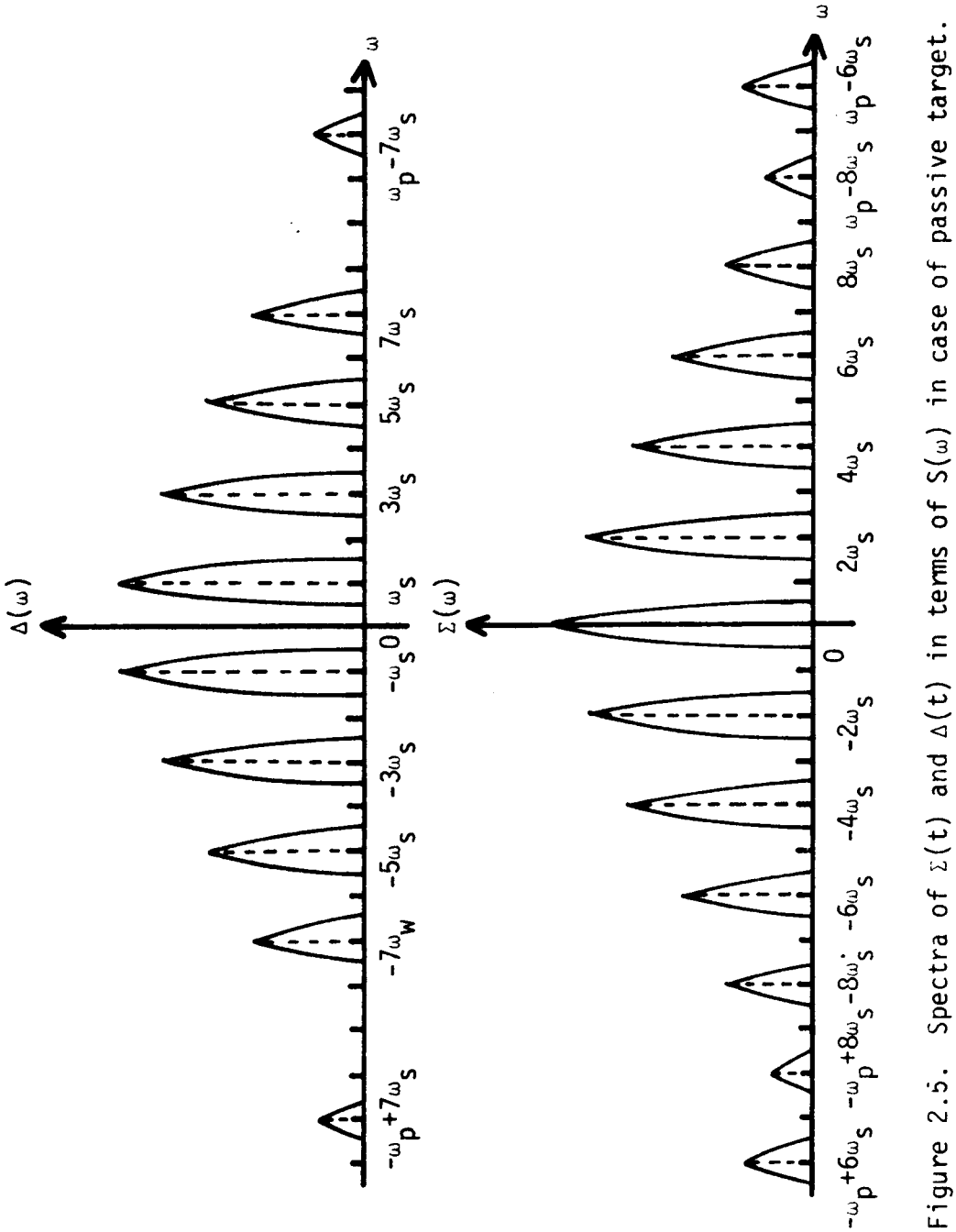


Figure 2.5. Spectra of $\Sigma(t)$ and $\Delta(t)$ in terms of $S(\omega)$ in case of passive target.

where in this case

$$y = \frac{2\theta_q \theta_T}{\theta_B^2} , \tag{2.207}$$

to avoid additional notation.

Then, the B_1/B_0 as a coefficient of the angle error signal is written as

$$\frac{B_1}{B_0} = -\frac{A_0A_1y + \frac{3}{4}(A_1A_2 + A_0A_3)y^3}{A_0^2 + A_0A_2y^2 + \left(\frac{3A_0A_4}{8} + \frac{3A_2^2}{8} + \frac{3A_2A_4}{16}\right)y^4} . \tag{2.208}$$

By the same procedure† for D_1/D_0 in the previous section, the above equation is expressed as

$$\frac{B_1}{B_0} = -\left\{\frac{a_1}{a_0} - \left(\frac{a_1^2}{a_0^2} - \frac{2a_2}{a_0}\right)x + \left(\frac{a_1^3}{a_0^3} - \frac{3a_1a_2}{a_0^2} + \frac{3a_2}{a_0}\right)x^2 \right.$$

$$-\left(\frac{a_1^4}{a_0^4} - \frac{4a_1^2a_2}{a_0^3} + \frac{4a_1a_3}{a_0^2} + \frac{2a_2^2}{a_0^2} - \frac{4a_4}{a_0}\right)x^3$$

$$- \frac{2\theta_q\theta_T}{\theta_B^2}\left[\frac{1}{4}\frac{a_1a_2}{a_0^2} - \frac{3}{4}\frac{a_3}{a_0} - \left(\frac{1}{2}\frac{a_1^2a_2}{a_0^3} - \frac{3}{2}\frac{a_1a_3}{a_0^2} - \frac{1}{2}\frac{a_2^2}{a_0^2}\right.\right.$$

$$\left.\left. + \frac{3a_4}{a_0}\right)x\right]\Bigg\}\left[\frac{2\theta_q\theta_T}{\theta_B^2}\right] . \tag{2.209}$$

---

†Appendix H.

Hence, the angle error signals finally become

Azimuth angle-error signal

$$= -\frac{V_r}{2}\left\{\frac{a_1}{a_o} - \left(\frac{a_1^2}{a_o^2} - \frac{2a_2}{a_o}\right)x + \left(\frac{a_1^3}{a_o^3} - \frac{3a_1a_2}{a_o^2} + \frac{3a_2}{a_o}\right)x^2\right.$$

$$-\left(\frac{a_1^4}{a_o^4} - \frac{4a_1^2a_2}{a_o^3} + \frac{4a_1a_3}{a_o^2} + \frac{2a_2^2}{a_o^2} - \frac{4a_4}{a_o}\right)x^3$$

$$-\left(\frac{2\theta_q\theta_T}{\theta_B^2}\right)^2\left[\frac{1}{4}\frac{a_1a_2}{a_o^2} - \frac{3}{4}\frac{a_3}{a_o} - \left(\frac{1}{2}\frac{a_1^2a_2}{a_o^3} - \frac{3}{2}\frac{a_1a_3}{a_o^2} - \frac{1}{2}\frac{a_2^2}{a_o^2}\right.\right.$$

$$\left.\left.+\frac{3a_4}{a_o}\right)x\right]\left.\right\}\left(\frac{2\theta_q\theta_T}{\theta_B^2}\right)\cos\phi_o, \qquad (2.210)$$

and

Elevation angle-error signal

$$= -\frac{V_r}{2}\left\{\frac{a_1}{a_o} - \left(\frac{a_1^2}{a_o^2} - \frac{2a_2}{a_o}\right)x + \left(\frac{a_1^3}{a_o^3} - \frac{3a_1a_2}{a_o^2} + \frac{3a_2}{a_o}\right)x^2\right.$$

$$-\left(\frac{a_1^4}{a_o^4} - \frac{4a_1^2a_2}{a_o^3} + \frac{4a_1a_3}{a_o^2} + \frac{2a_2^2}{a_o^2} - \frac{4a_4}{a_o}\right)x^3$$

$$-\left(\frac{2\theta_q\theta_T}{\theta_B^2}\right)^2\left[\frac{1}{4}\frac{a_1a_2}{a_o^2} - \frac{3}{4}\frac{a_3}{a_o} - \frac{1}{2}\frac{a_1^2a_2}{a_o^3} - \frac{3}{2}\frac{a_1a_3}{a_o^2} - \frac{1}{2}\frac{a_2^2}{a_o^2}\right.$$

$$\left.\left.+\frac{3a_4}{a_o}\right)x\right]\left.\right\}\left(\frac{2\theta_q\theta_T}{\theta_B^2}\right)\sin\phi_o, \qquad (2.211)$$

where

$$\left.\begin{aligned} x &= \left(\frac{\theta_q}{\theta_B}\right)^2 + \left(\frac{\theta_T}{\theta_B}\right)^2 , \\ a_0 &= c_0 , \\ a_1 &= \frac{c_2 d_1^{\,2}}{2!} , \\ a_2 &= \frac{c_4 d_1^{\,4}}{4!} , \\ a_3 &= \frac{c_6 d_1^{\,6}}{6!} , \text{ and} \\ a_4 &= \frac{c_8 d_1^{\,8}}{8!} . \end{aligned}\right\} \qquad (2.212)$$

VI. NUMERICAL RESULTS FOR LARGE PATTERN SQUINT AND TARGET ANGLES

We have discussed the angle-error signals for comparatively large pattern squint and target angles in both the monopulse-conical scan and the conical scan-monopulse methods. The Maclaurin's series expansion of the antenna pattern was used for those analyses. However, another approach to the extraction of the angle-error signal may be considered. The video-signals from each antenna have the wave shape in Figure 1.1(B), p. 2, but they have 180 degrees phase difference on the envelope of pulses. Therefore, the difference signal $\Delta(t)$, the sum signal $\Sigma(t)$, and the time dependent error signal $e(t)$ have the wave shapes as shown in Figure 2.6. If the envelope signals are bandlimited and the pulse repetition frequency is high enough to satisfy

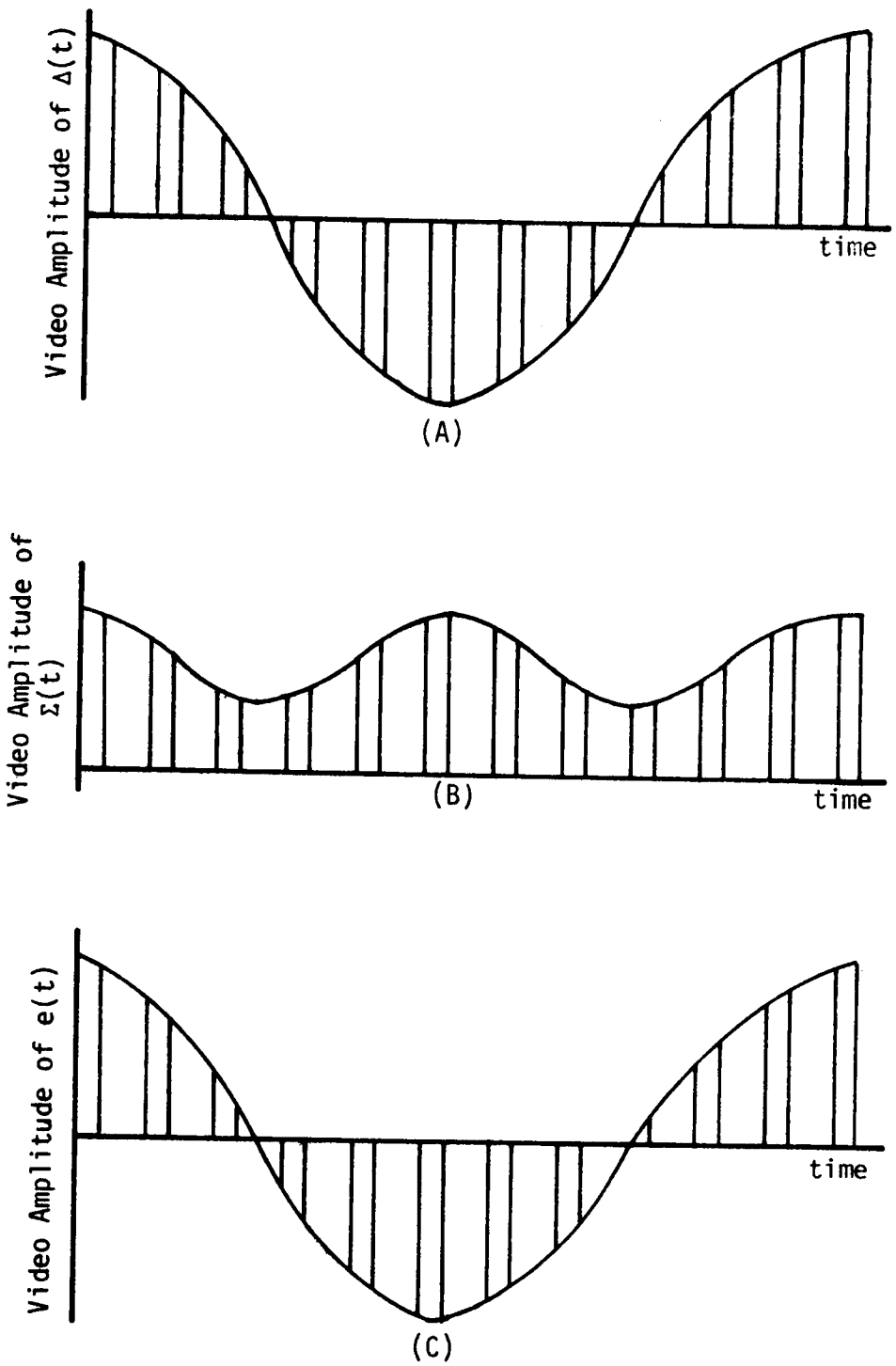


Figure 2.6. Wave shapes of $\Delta(t)$, $\Sigma(t)$, and $e(t)$. (A) Wave shape of $\Delta(t)$, (B) wave shape of $\Sigma(t)$; (C) wave shape of $e(t)$.

the sampling theorem, they may be considered as signals of pulse amplitude modulation (PAM). The envelope signals will be reconstructed by a PAM demodulator. Since the envelope signals of the pulse trains are reflected from the rotation of the antenna beams, they may be expanded into the Fourier series in terms of the antenna rotation frequency. Usually, the $\Delta(t)$ and $\Sigma(t)$ signals have the component of echo fluctuation $S(t)$ which may be a common factor of each term of the Fourier series.

From the properties of the sum signal $\Sigma(t)$ and the difference signal $\Delta(t)$, the difference signal $\Delta(t)$ have only odd harmonics terms of the antenna rotation frequency in the Fourier series and the sum signal $\Sigma(t)$ have only the even harmonics terms. Therefore, the time dependent error signal $e(t)$ which is a ratio of $\Delta(t)$ and $\Sigma(t)$ have only the odd harmonics terms.

Thus, they are expanded as

$$\Delta(t) = s(t) \sum_{\ell=1}^{L} d_{2\ell-1} \cos[(2\ell-1)\omega_s t + (2\ell-1)\phi_o], \tag{2.213}$$

$$\Sigma(t) = s(t) \left\{ \frac{f_o}{2} + \sum_{m=1}^{M} f_{2m} \cos(2m\omega_s t + 2m\phi_o) \right\}, \tag{2.214}$$

and

$$e(t) = \sum_{n=1}^{N} g_{2n-1} \cos[(2n-1)\omega_s t + (2n-1)\phi_o], \tag{2.215}$$

where $d_{2\ell-1}$, f_{2m}, and g_{2n-1} are the Fourier series coefficients, and L, M, and N are determined by their bandwidth.

In the monopulse-conical scan method, the time dependent error signal e(t) is fed to the product devices having the reference signals $V_r \cos\omega_s t$ and $V_r \sin\omega_s t$, respectively, and then they pass through LPFs. Therefore, the angle-error signals become

$$\text{Azimuth angle-error signal} = \frac{V_r}{2} g_1 \cos\phi_o, \tag{2.216}$$

and

$$\text{Elevation angle-error signal} = \frac{V_r}{2} g_1 \sin\phi_o. \tag{2.217}$$

In the conical scan-monopulse method, the difference signal $\Delta(t)$ is also fed into the same product device and then they pass through LPFs. After that, they are divided by the fundamental component of the sum signal $\Sigma(t)$ to cancel out the component of echo fluctuation. Thus, the angle error signals become

$$\text{Azimuth angle-error signal} = \frac{V_r}{2} \frac{d_1}{f_o} \cos\phi_o, \tag{2.218}$$

and

$$\text{Elevation angle-error signal} = \frac{V_r}{2} \frac{d_1}{f_o} \sin\phi_o. \tag{2.219}$$

For the sake of convenience, we will call this method the Fourier series method and the method described in the previous sections the Maclaurin series method.

This Fourier series method is for numerical computation by computer. If the suitable numerical integration method is used to obtain the Fourier coefficients, the results may express the true values.

The azimuth angle-error signal is maximum when the phase angle

ϕ_0 is zero. We will calculate the angle-error signal at ϕ_0=0 throughout this section.

1. Monopulse-Conical Scan Method

The azimuth angle-error signal for an arbitrary antenna pattern due to the Maclaurin's series method is given by Eq. (2.174). From this equation, the error-signal voltage of the Bessel and Gaussian patterns given by Eqs. (2.71) and (2.79) have been calculated for several squint angles by computer, and they are shown in Figures 2.7 and 2.8.

In the Fourier series method, the angle-error signal given by Eq. (2.216) in this case becomes

$$\text{Azimuth angle-error signal} = \frac{1}{2} g_1, \tag{2.220}$$

where $V_r = 1$,

$$g_1 = \frac{\omega_s}{\pi} \int_{-\pi/\omega_s}^{\pi/\omega_s} e(t) \cos\omega_s t \, dt, \tag{2.221}$$

and

$$e(t) = \frac{G_1(t) - G_2(t)}{G_1(t) + G_2(t)} . \tag{2.222}$$

Substituting the Bessel and Gaussian antenna pattern representations into Eq. (2.222), the value of g_1 is calculated by computer. The Simpson's rule is used for the integration of Eq. (2.221).

The results are shown in Figures 2.9 and 2.10.

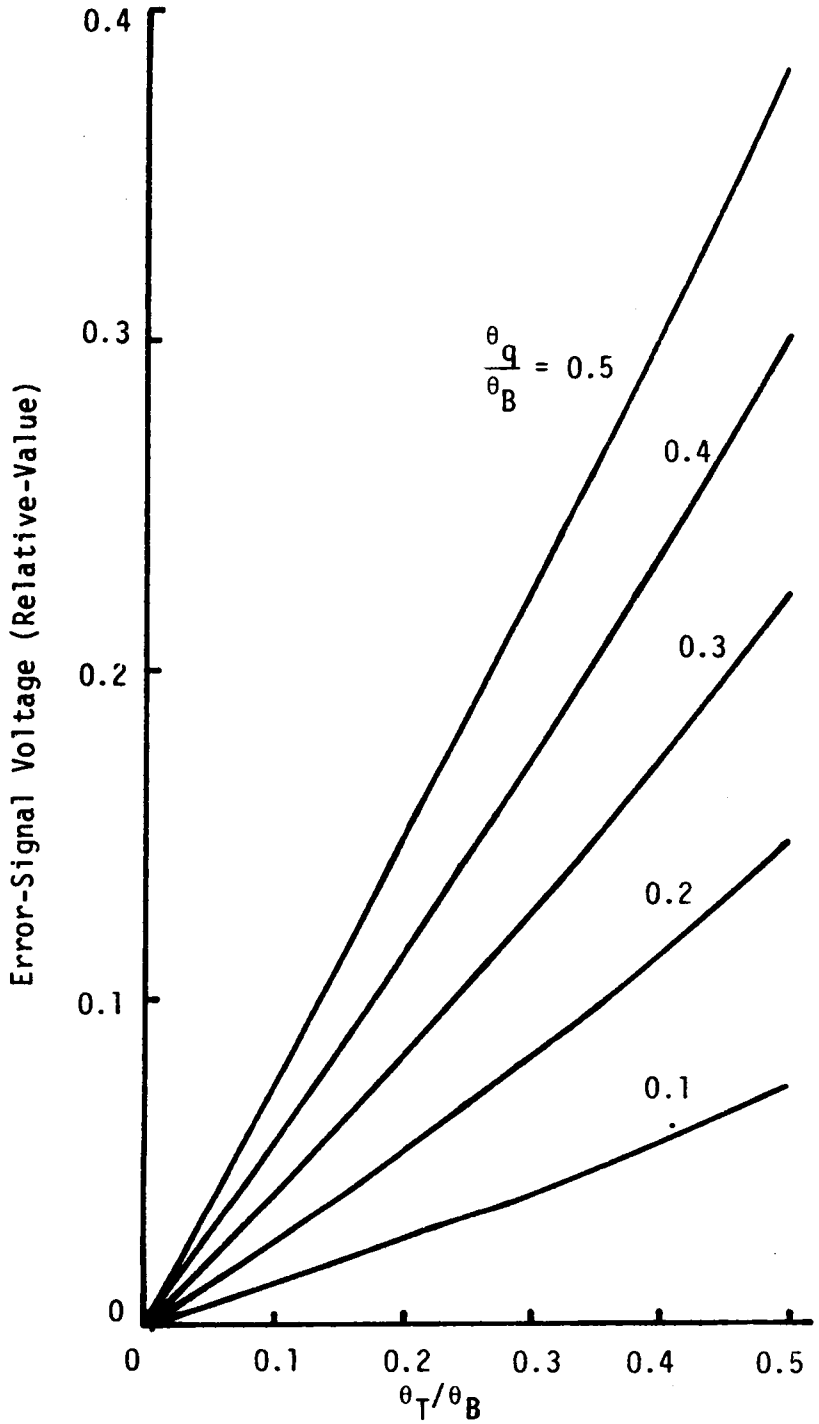


Figure 2.7. Error-signal voltage of monopulse-conical scan method (Bessel function antenna pattern) by Maclaurin series method.

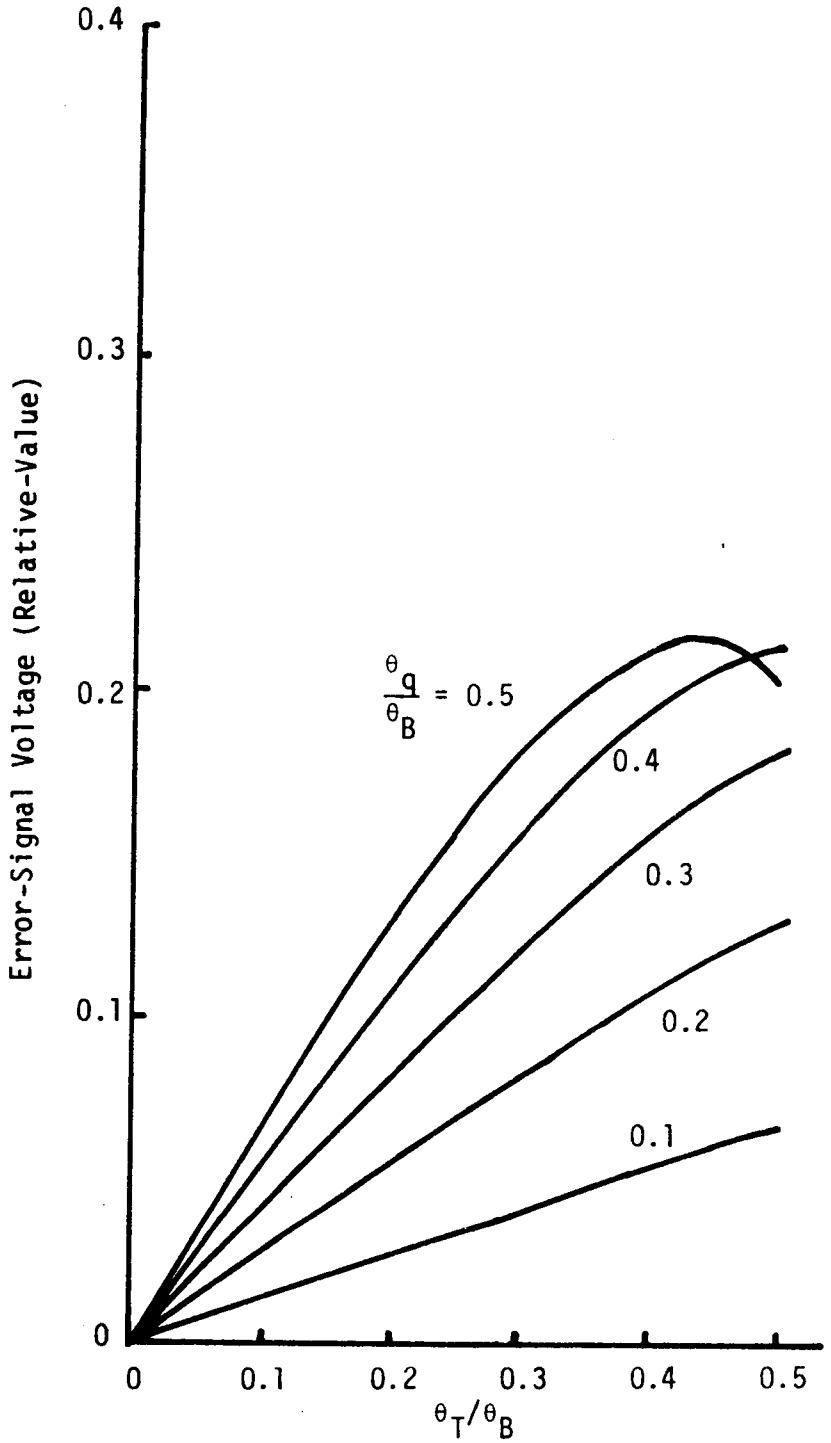


Figure 2.8. Error-signal voltage of monopulse-conical scan method (Gaussian function antenna pattern) by Maclaurin series method.

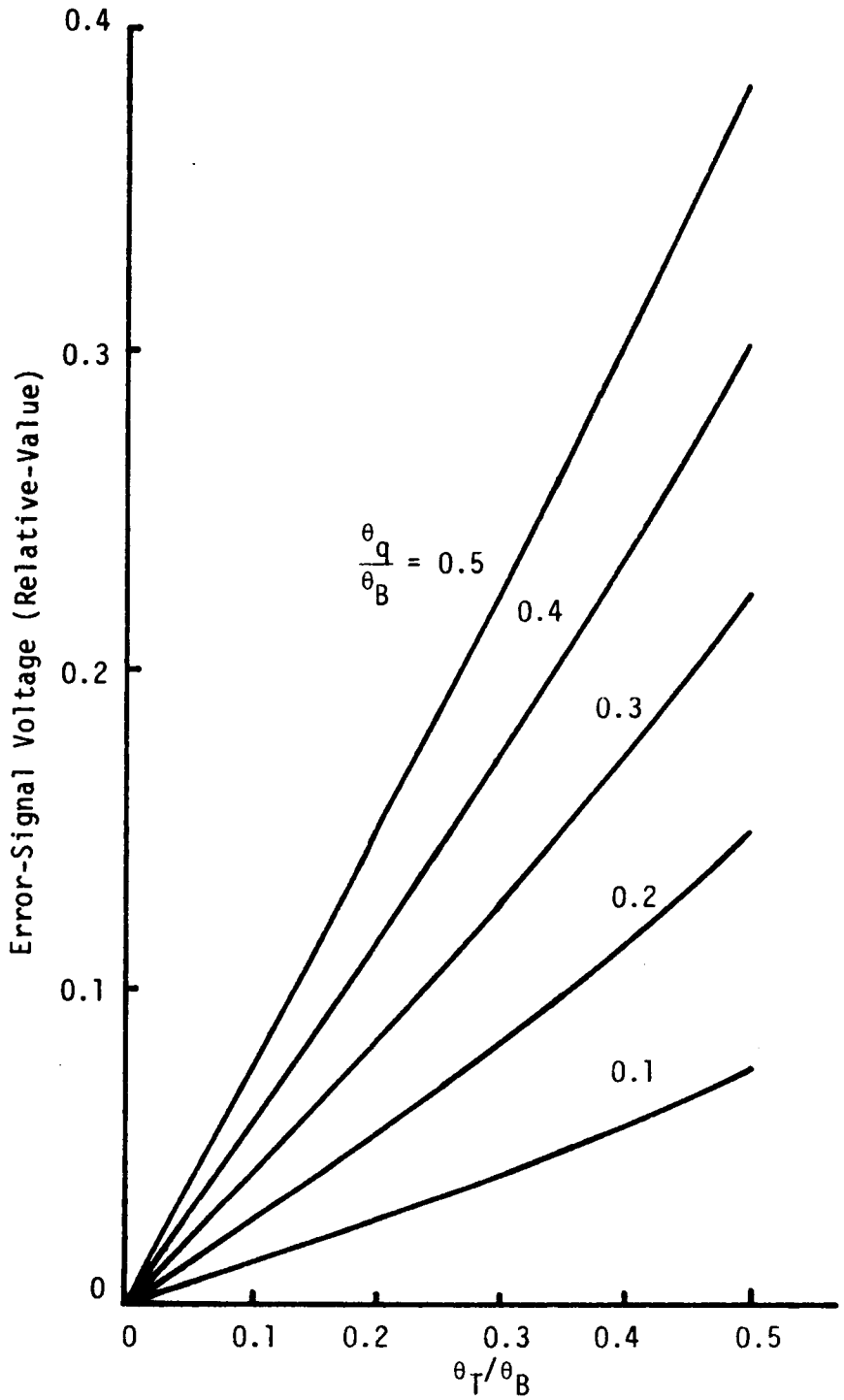


Figure 2.9. Error-signal voltage of monopulse-conical scan method (Bessel function antenna pattern) by Fourier series method.

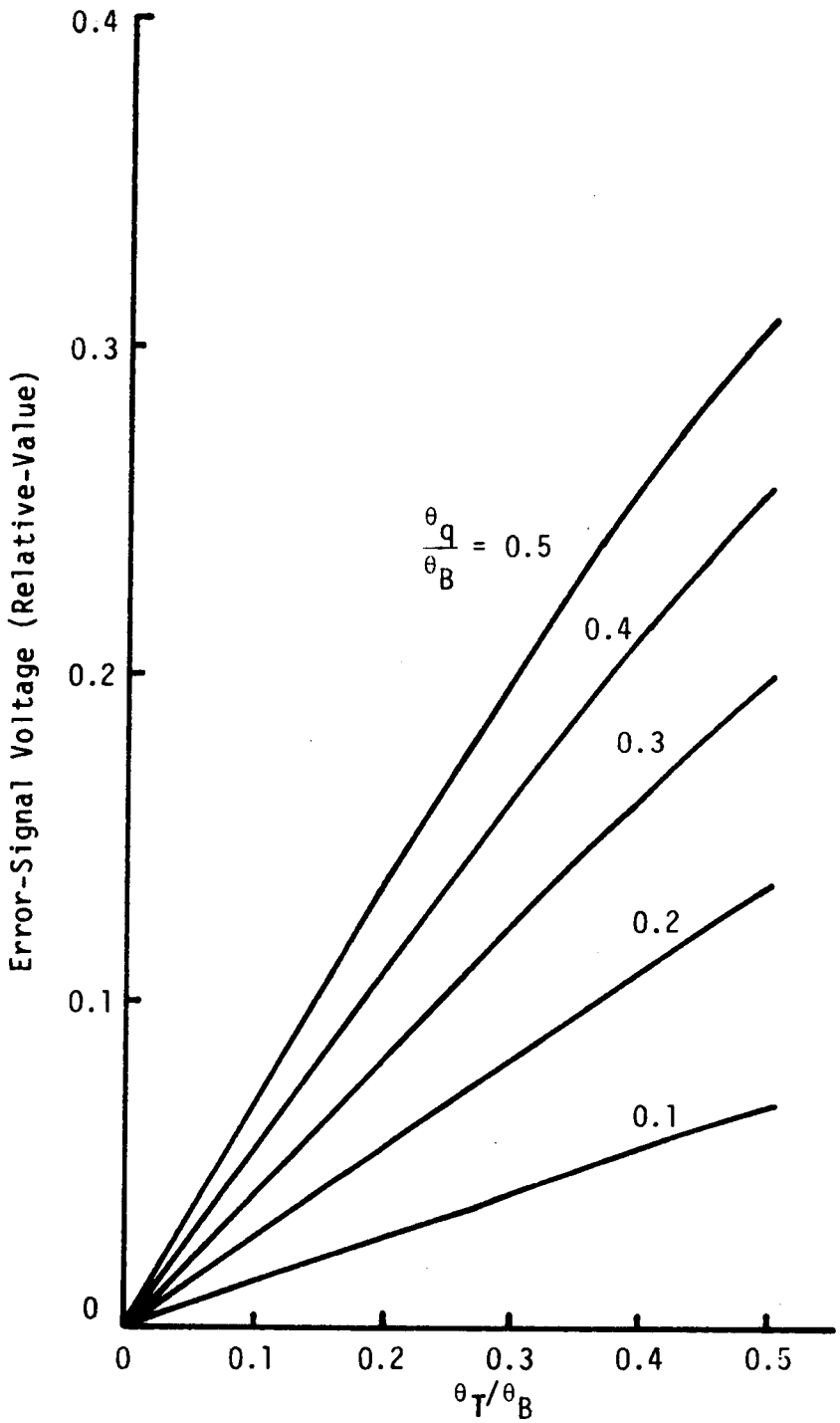


Figure 2.10. Error-signal voltage of monopulse-conical scan method (Gaussian function antenna pattern) by Fourier series method.

2. Conical Scan-Monopulse Method for Active Target

The azimuth angle-error signal for an arbitrary antenna pattern in this case is given by Eq. (2.192).

Similarly, the numerical results for the Bessel and Gaussian antenna patterns are shown in Figures 2.11 and 2.12.

In the Fourier series method, the azimuth angle-error signal becomes

$$\text{Azimuth angle-error signal} = \frac{1}{2}\,\frac{d_1}{f_0}, \tag{2.223}$$

where

$$d_1 = \frac{\omega_s}{\pi}\int_{-\pi/\omega_s}^{\pi/\omega_s} \Delta(t)\,\cos\omega_s t\,dt, \tag{2.224}$$

$$f_0 = \frac{\omega_s}{\pi}\int_{-\pi/\omega_s}^{\pi/\omega_s} \Sigma(t)\,dt, \tag{2.225}$$

$$\Delta(t) = G_1(t) - G_2(t), \tag{2.226}$$

and

$$\Sigma(t) = G_1(t) + G_2(t), \tag{2.227}$$

assumed that all other factors are unity.

The results for the two antenna patterns were calculated by computer and are shown in Figures 2.13 and 2.14.

3. Conical Scan-Monopulse Method for Passive Target

The numerical results given by Eq. (2.210) are shown in Figures 2.15 and 2.16.

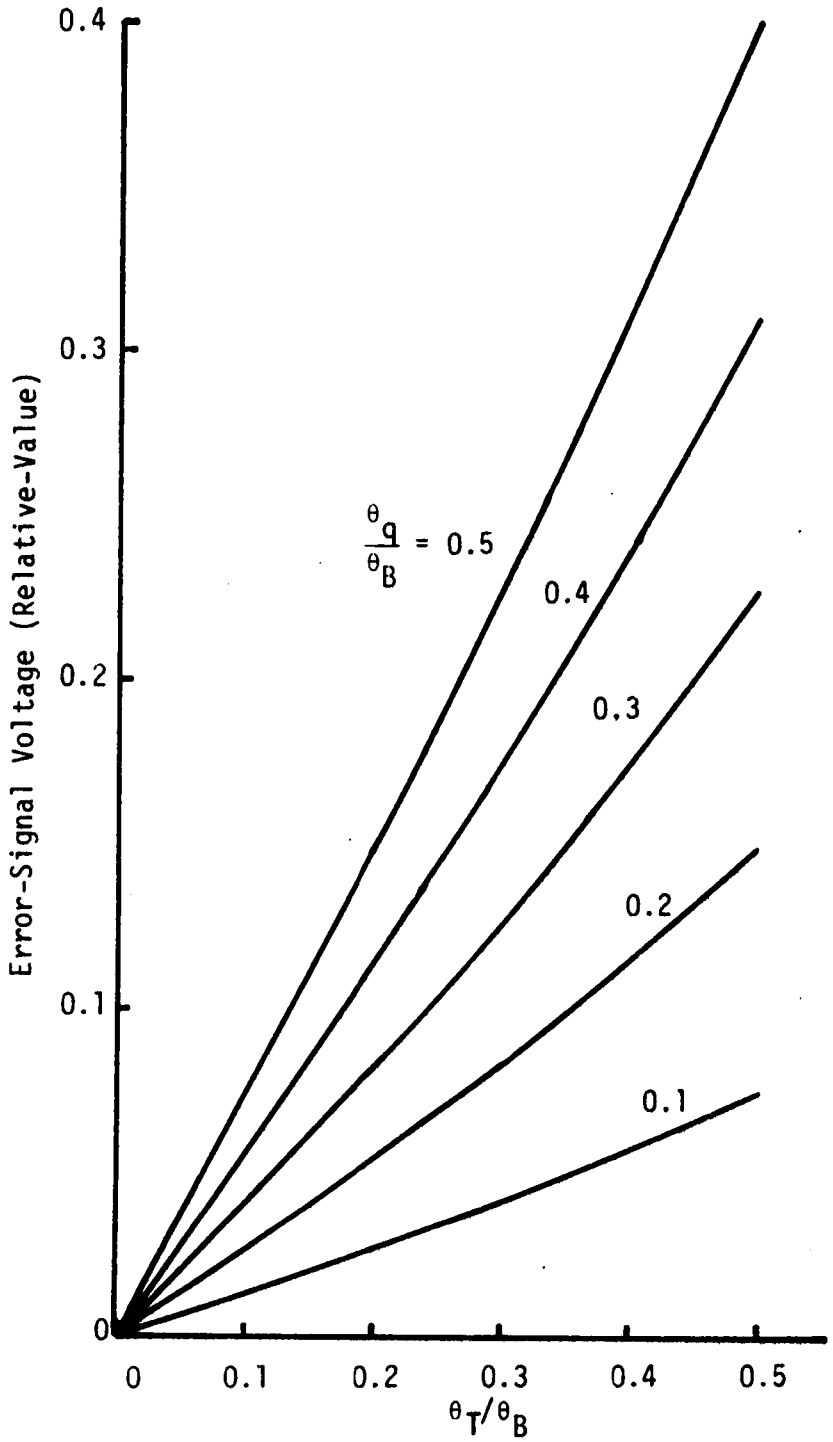


Figure 2.11. Error-signal voltage of conical scan-monopulse method (Bessel function antenna pattern) for active target by Maclaurin series method.

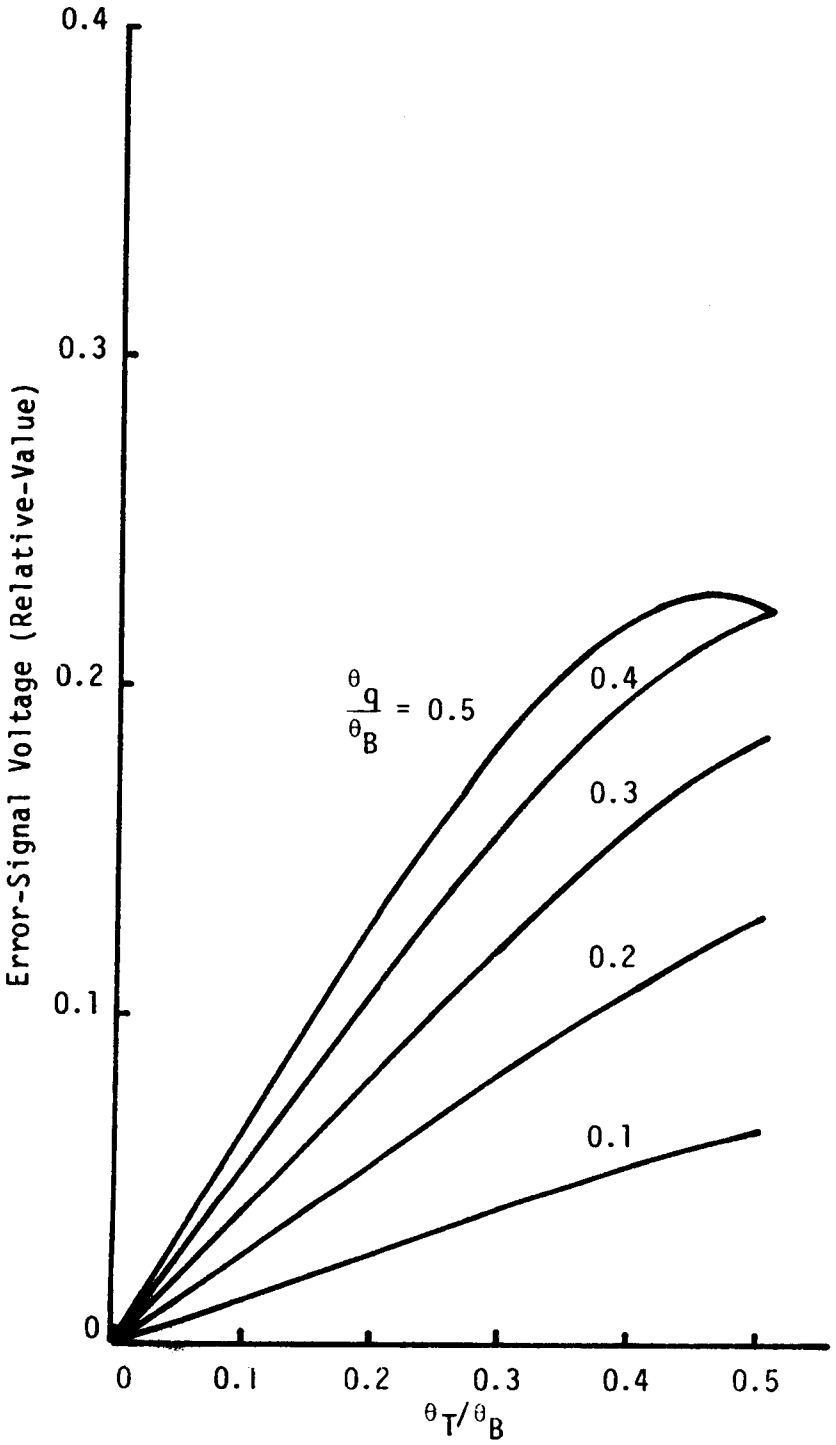


Figure 2.12. Error-signal voltage of conical scan-monopulse method (Gaussian function antenna pattern) for active target by Maclaurin series method.

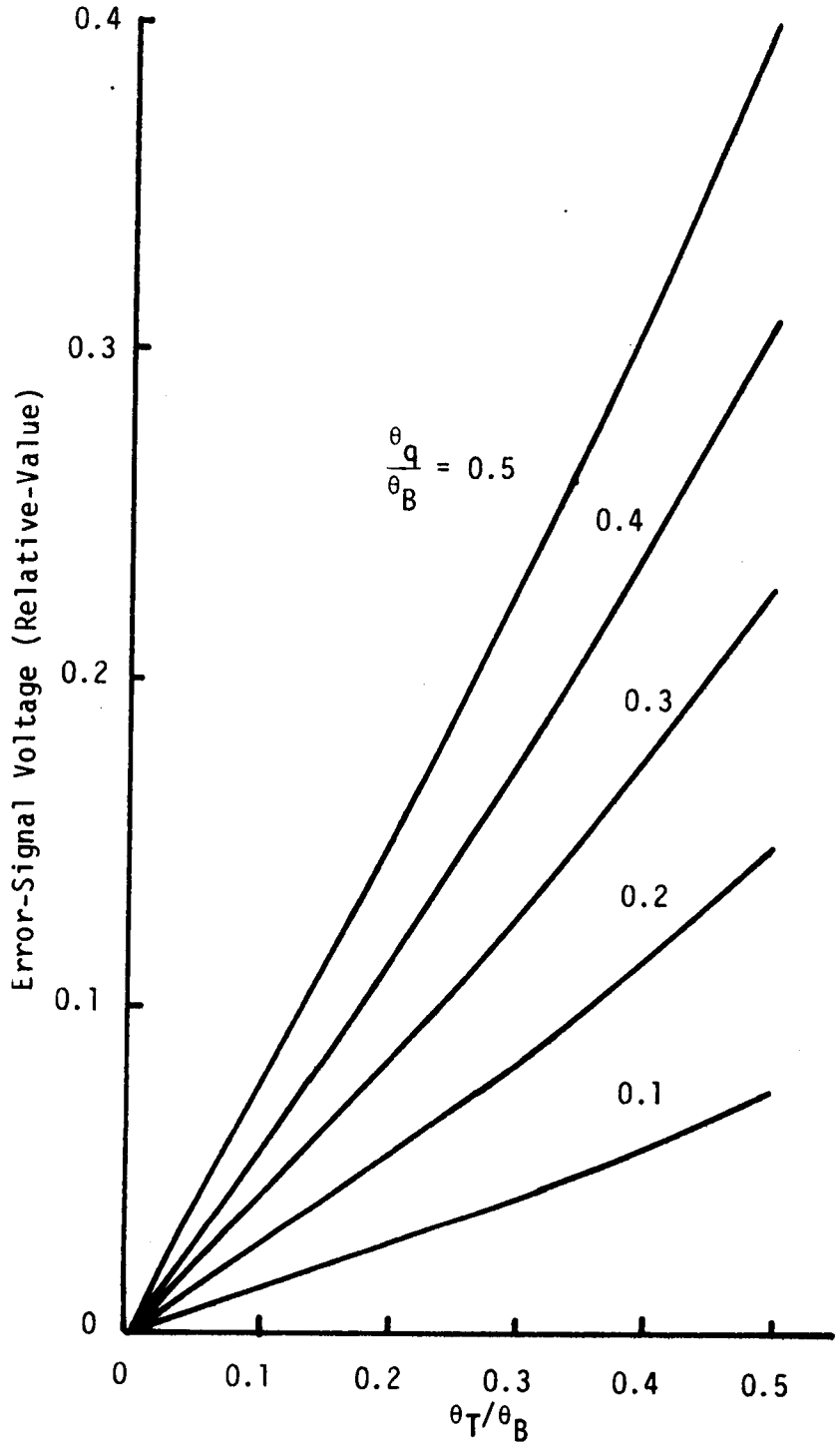


Figure 2.13. Error-signal voltage of conical scan-monopulse method (Bessel function antenna pattern) for active target by Fourier series method.

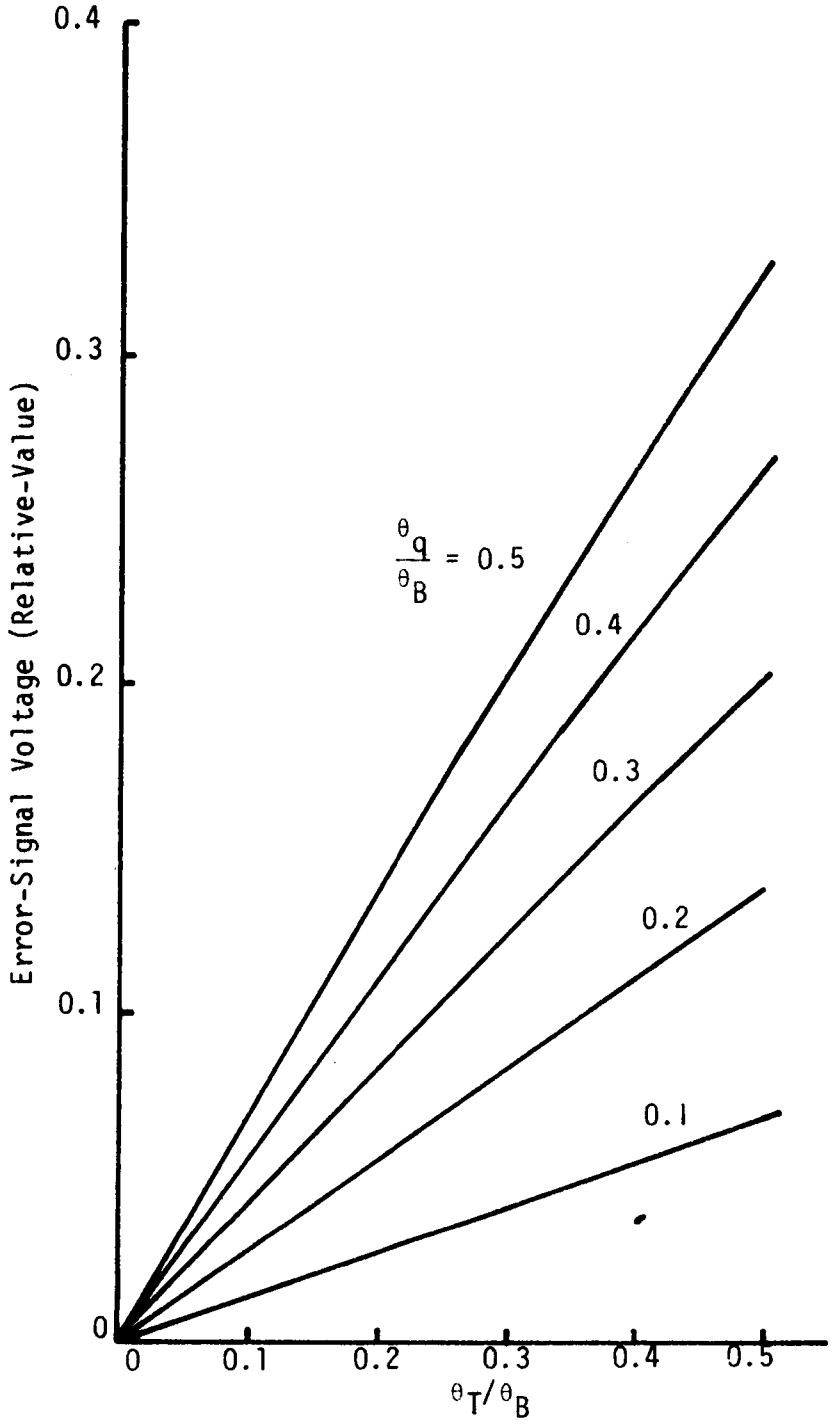


Figure 2.14. Error-signal voltage of conical scan-monopulse method (Gaussian function antenna pattern) for active target by Fourier series method.

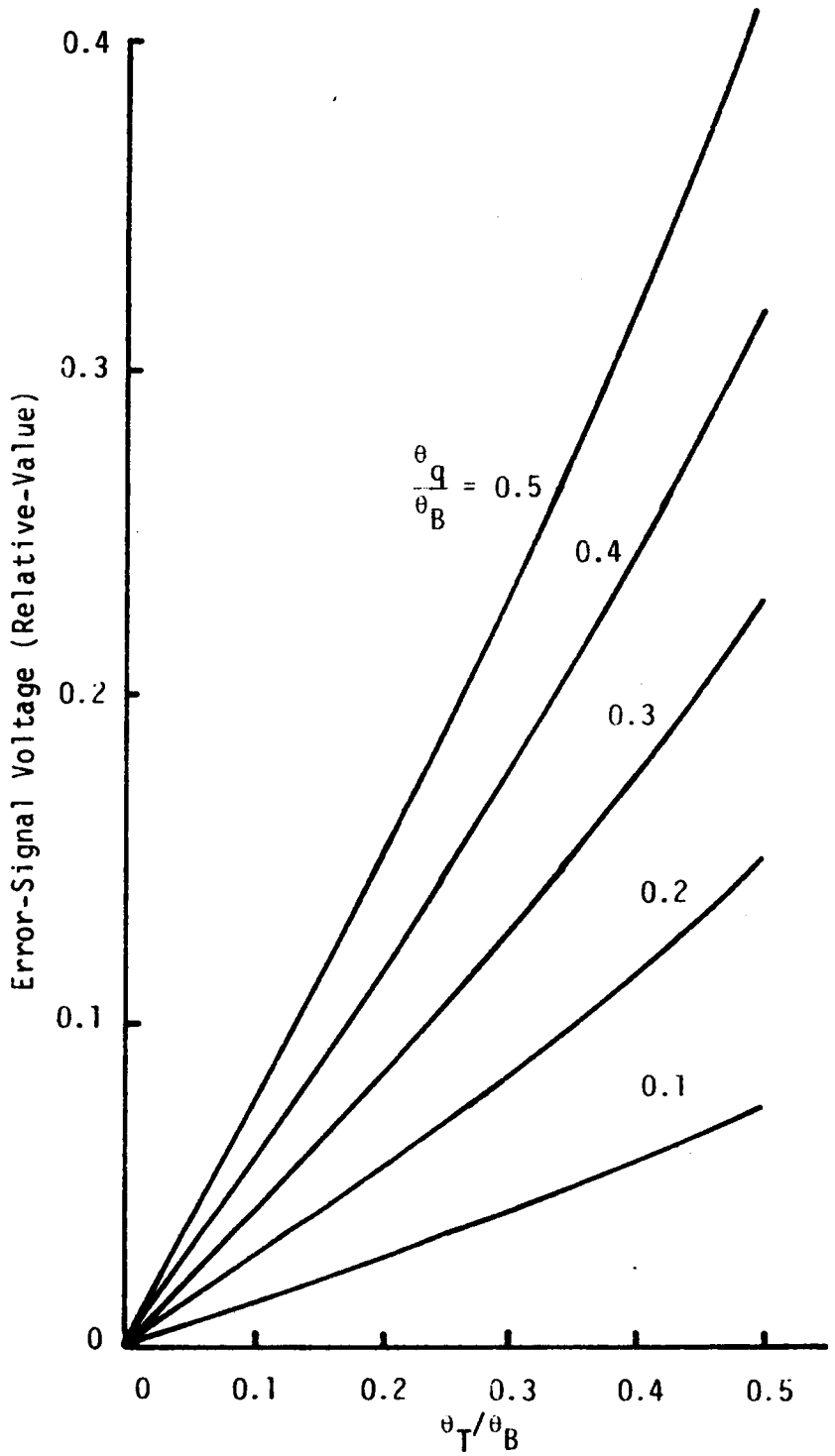


Figure 2.15. Error-signal voltage of conical scan-monopulse method (Bessel function antenna pattern) for passive target by Maclaurin series method.

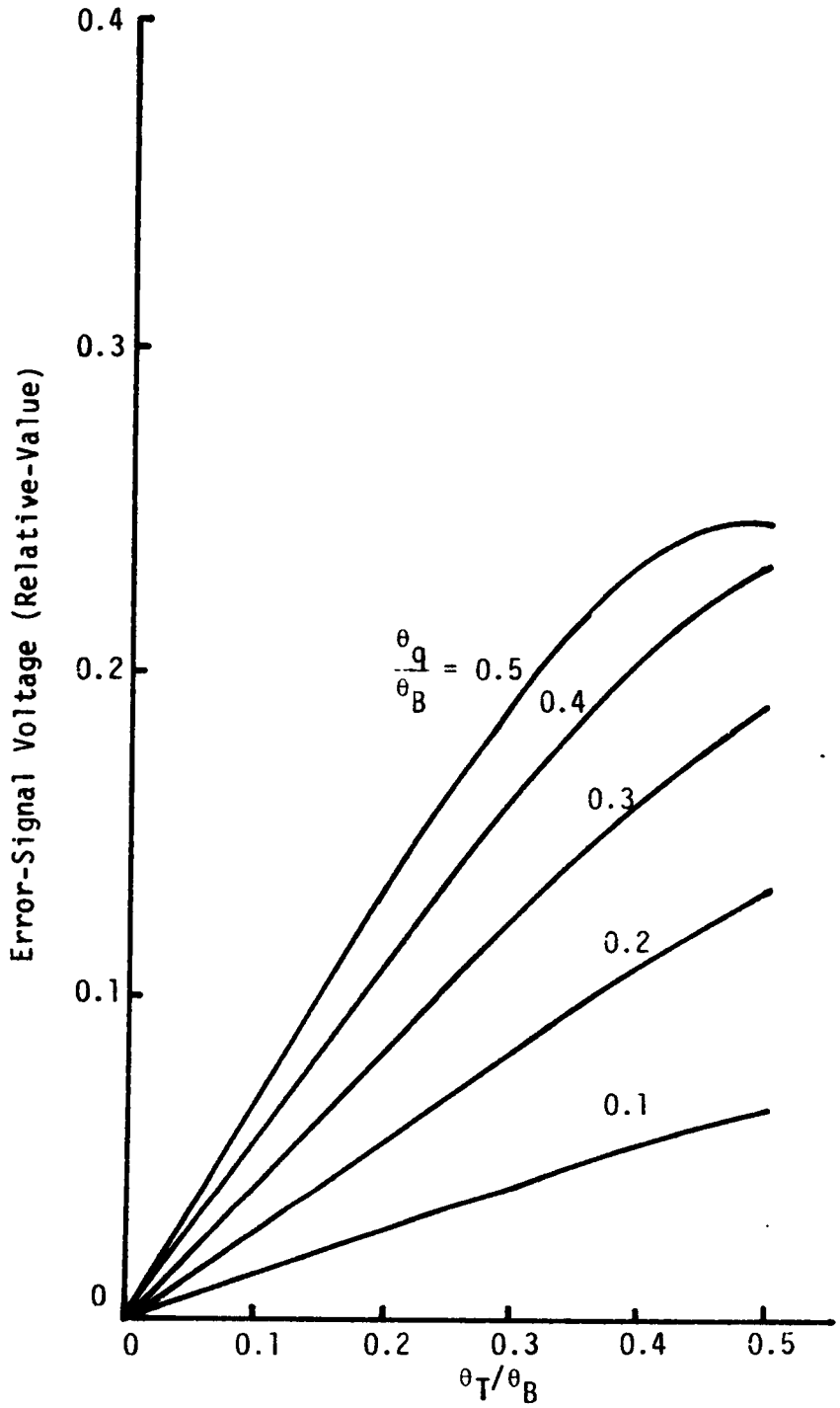


Figure 2.16. Error-signal voltage of conical scan-monopulse method (Gaussian function antenna pattern) for passive target by Maclaurin series method.

In the Fourier series method for this case, the sum signal $\Sigma(t)$ and the difference signal $\Delta(t)$ are given by

$$\Sigma(t) = [G_1(t) + G_2(t)]^2, \tag{2.228}$$

and

$$\Delta(t) = [G_1(t) + G_2(t)][G_1(t) - G_2(t)]. \tag{2.229}$$

Substituting the above equations into Eqs. (2.224) and (2.225), respectively, the numerical results are obtained, and they are shown in Figures 2.17 and 2.18.

4. Comparison of Numerical Results from Two Methods

Comparing the results from the error signal extraction methods, the error-signal voltages of the Bessel function antenna pattern in both the monopulse-conical scan method and the conical scan-monopulse method completely coincide for the target angle within half antenna beamwidth.

In the Gaussian antenna pattern, however, they do not coincide well for the large squint and target angles. It would be considered that the Maclaurin's series used does not have enough terms to approximate to the Gaussian function antenna pattern for large squint and target angles. It will be still useful for the analysis of the tracking mode, that is, the radar is tracking a target. In practice, however, parabolic-reflector antenna may be used in the conopulse radar system. The main beam may be expressed by the Bessel function antenna pattern. In order to check how well both the results for the Bessel function antenna pattern coincide and how the error-signals behave for the target angle above half antenna beamwidth, they are

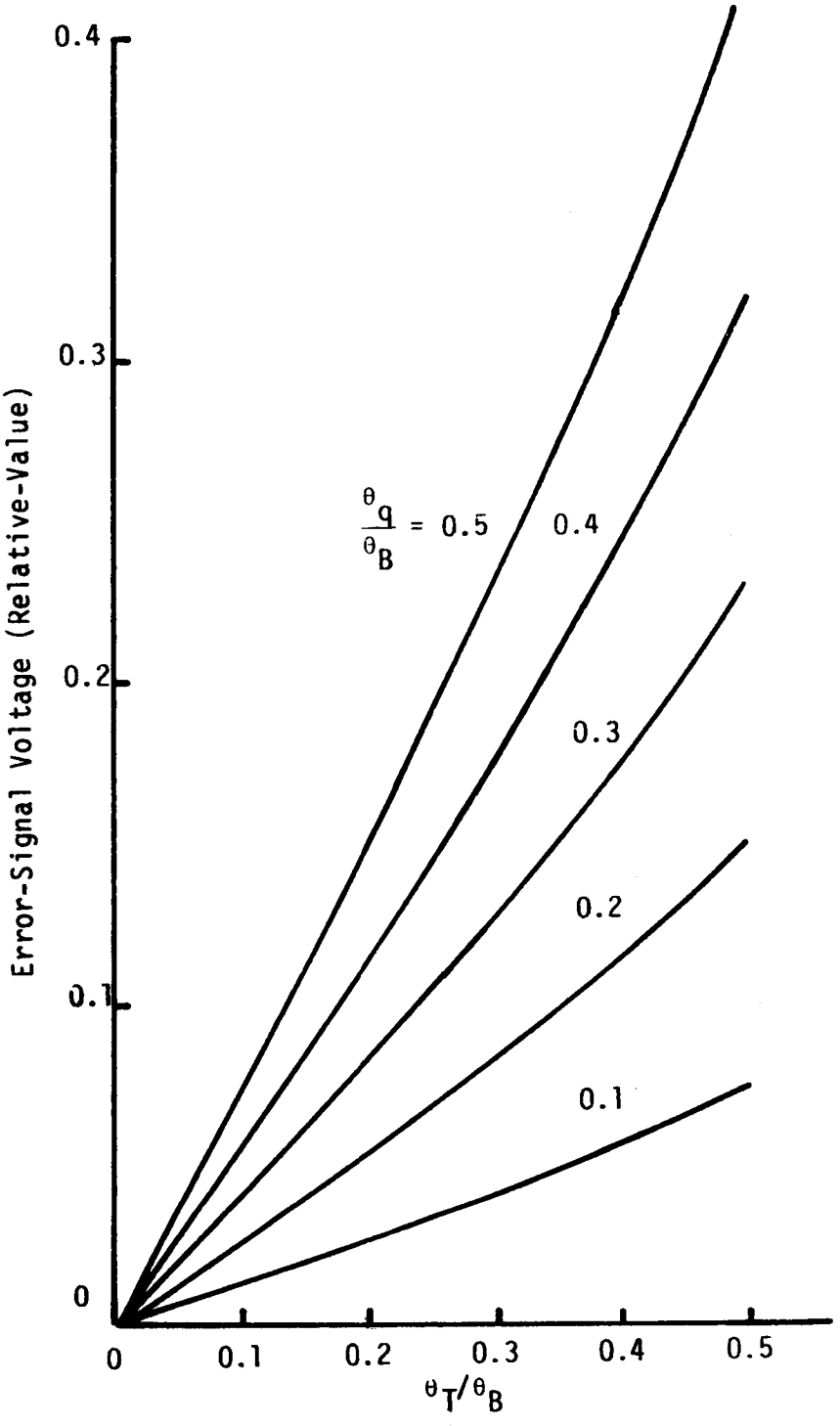


Figure 2.17. Error-signal voltage of conical scan-monopulse method (Bessel function antenna pattern) for passive target by Fourier series method.

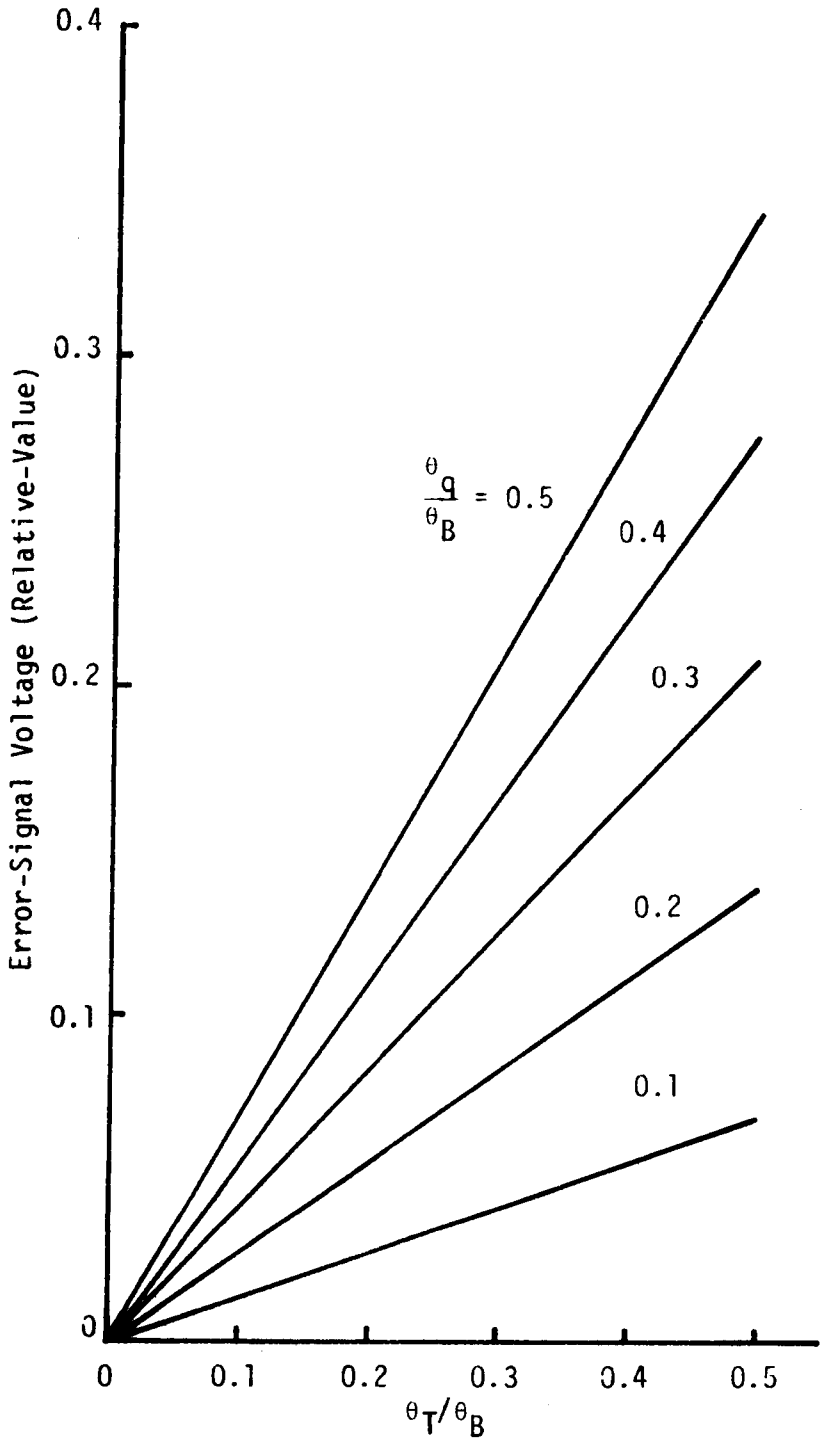


Figure 2.18. Error-signal voltage of conical scan-monopulse method (Gaussian function antenna pattern) for passive target by Fourier series method.

calculated for the angle region. The error-signal voltages of the monopulse-conical scan method from the two error signal extraction methods are shown in Figures 2.19, 2.20, 2.21, 2.22, and 2.23 for each squint angle separately because the curves are too complicated to draw them on a graph paper. On the other hand, the error signals of the conical scan-monopulse method for active target are shown in Figure 2.24. In both the monopulse-conical scan and conical scan-monopulse methods, the error-signal voltages from the two extraction methods coincide even for the target angle above the half beamwidth. The error-signal voltage in the monopulse-conical scan method is very complicated for about $1.2 < \theta_T/\theta_B$ due to the sidelobes. Finally, it should be recognized that the error-signal voltages in both the methods are almost linear within the target angle less than the half beamwidth.

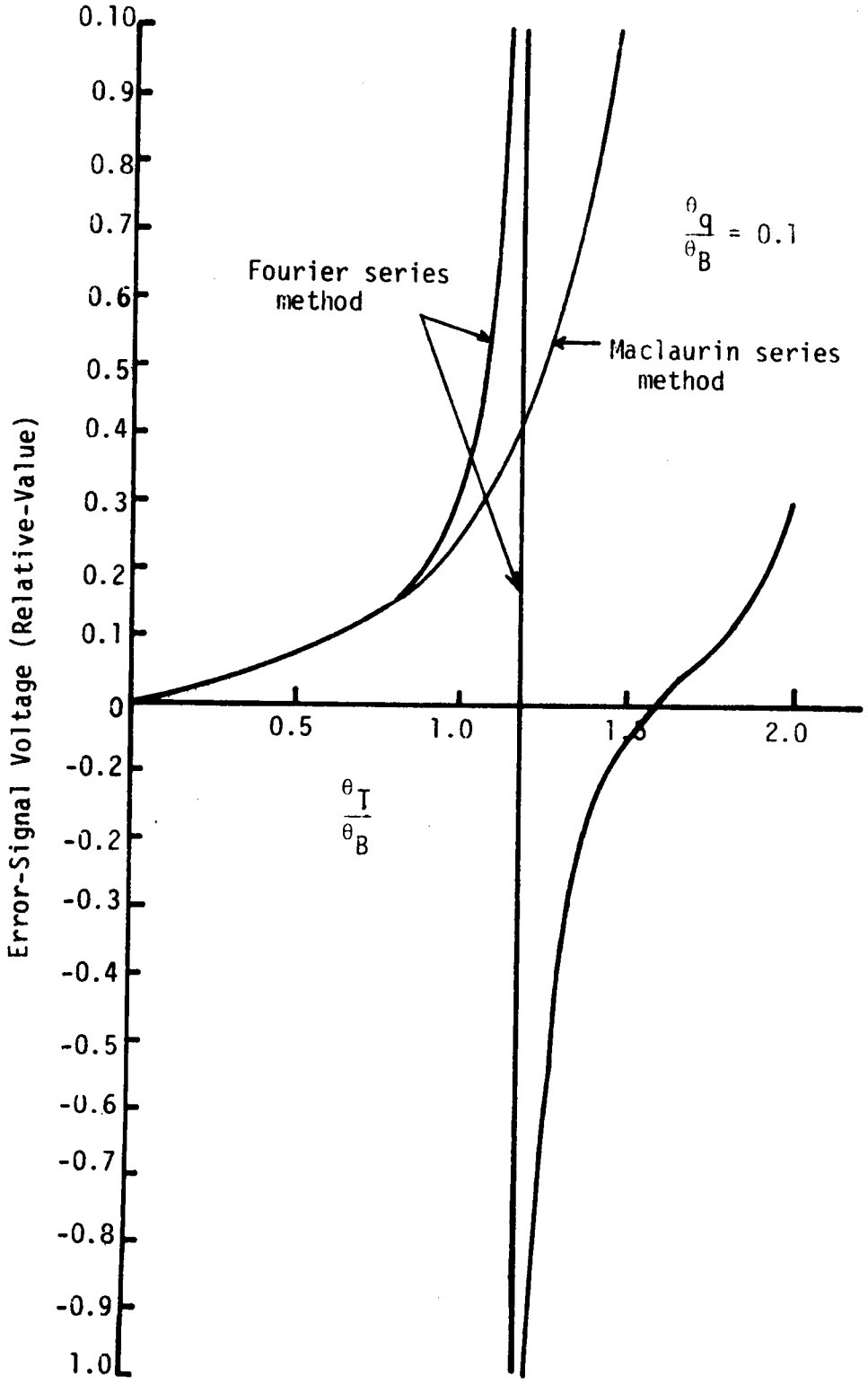


Figure 2.19. Comparison of error-signal voltages for monopulse-conical scan method (Bessel function antenna pattern) from two error signal extraction methods at the squint angle $\theta_q/\theta_B = 0.1$.

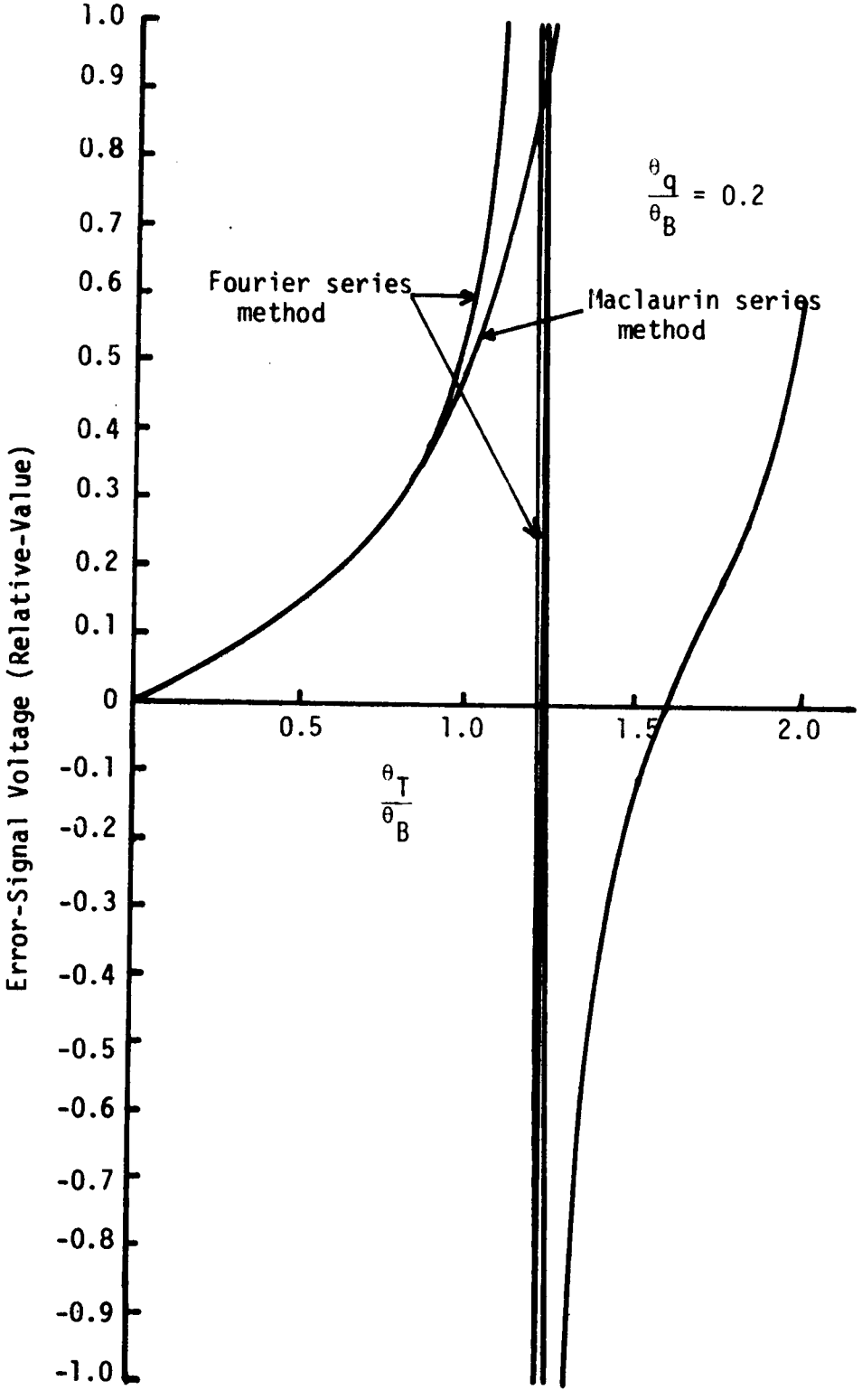


Figure 2.20. Comparison of error-signal voltages for monopulse-conical scan method (Bessel function antenna pattern) from two error signal extraction methods at the squint angle $\theta_q/\theta_B = 0.2$.

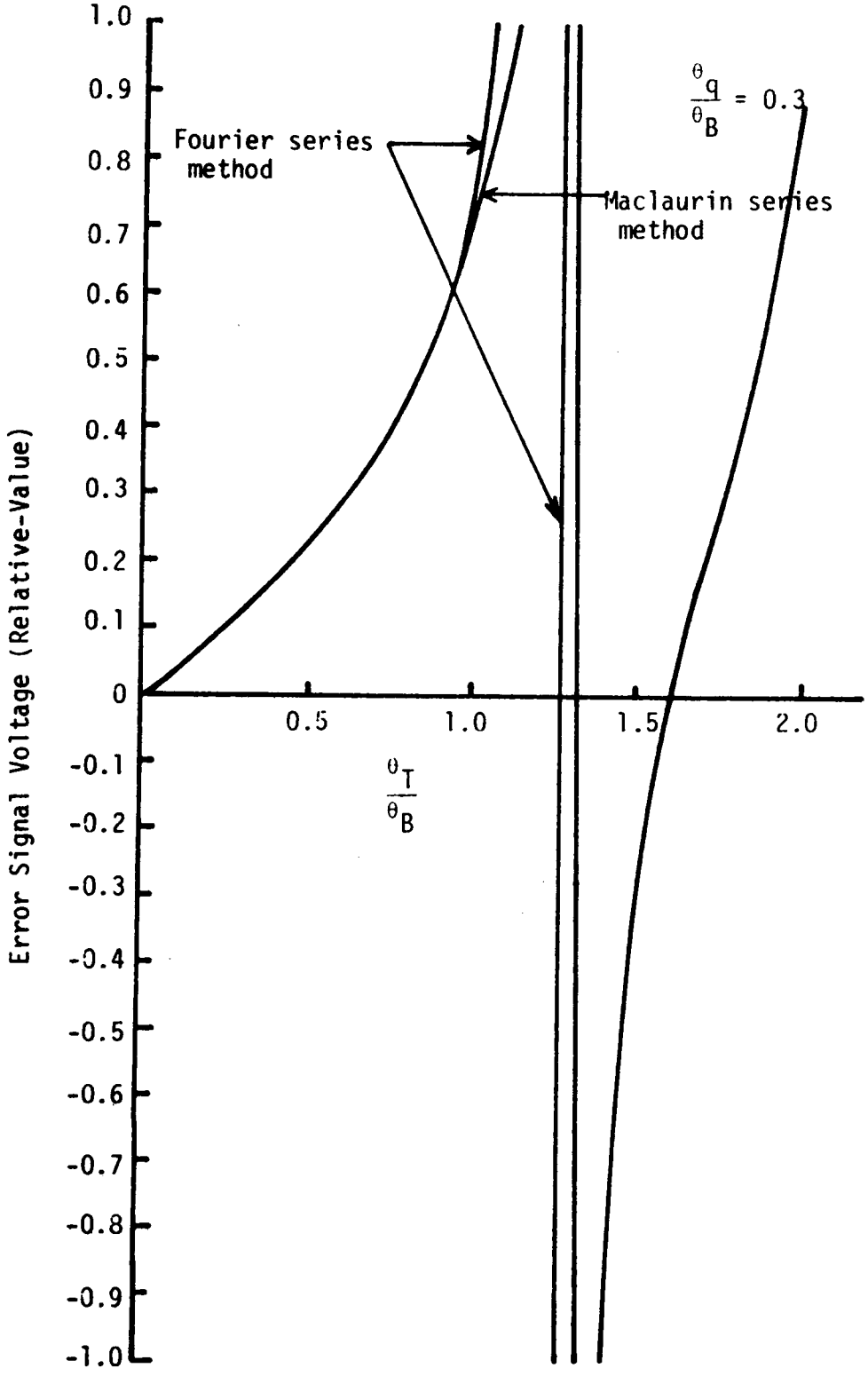


Figure 2.21. Comparison of error-signal voltages for monopulse-conical scan method (Bessel function antenna pattern) from two error signal extraction methods at the squint angle $\theta_q/\theta_B = 0.3$.

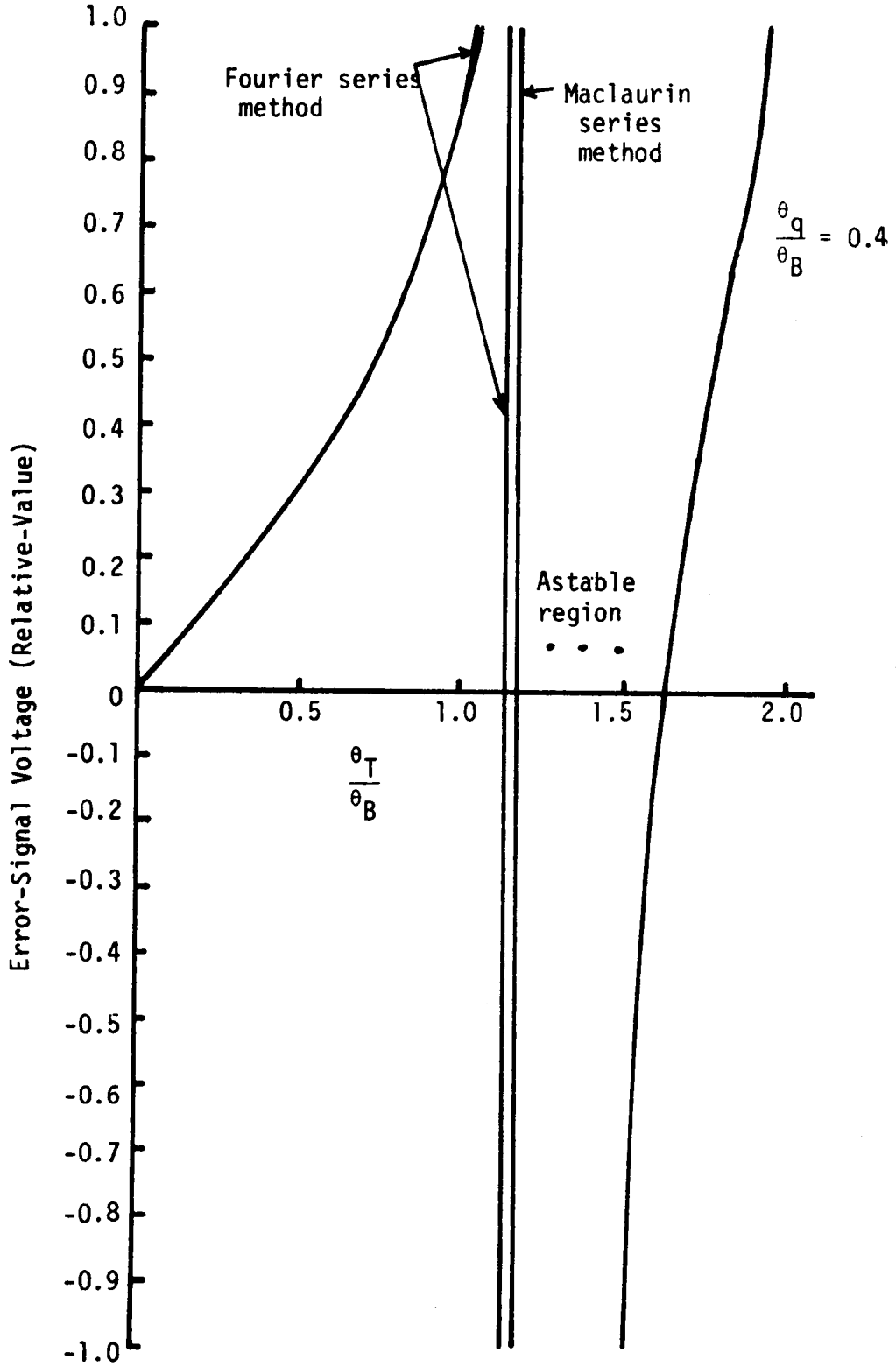


Figure 2.22. Comparison of error-signal voltages for monopulse-conical scan method (Bessel function antenna pattern) from two error signal extraction methods at the squint angle $\theta_q/\theta_B = 0.4$.

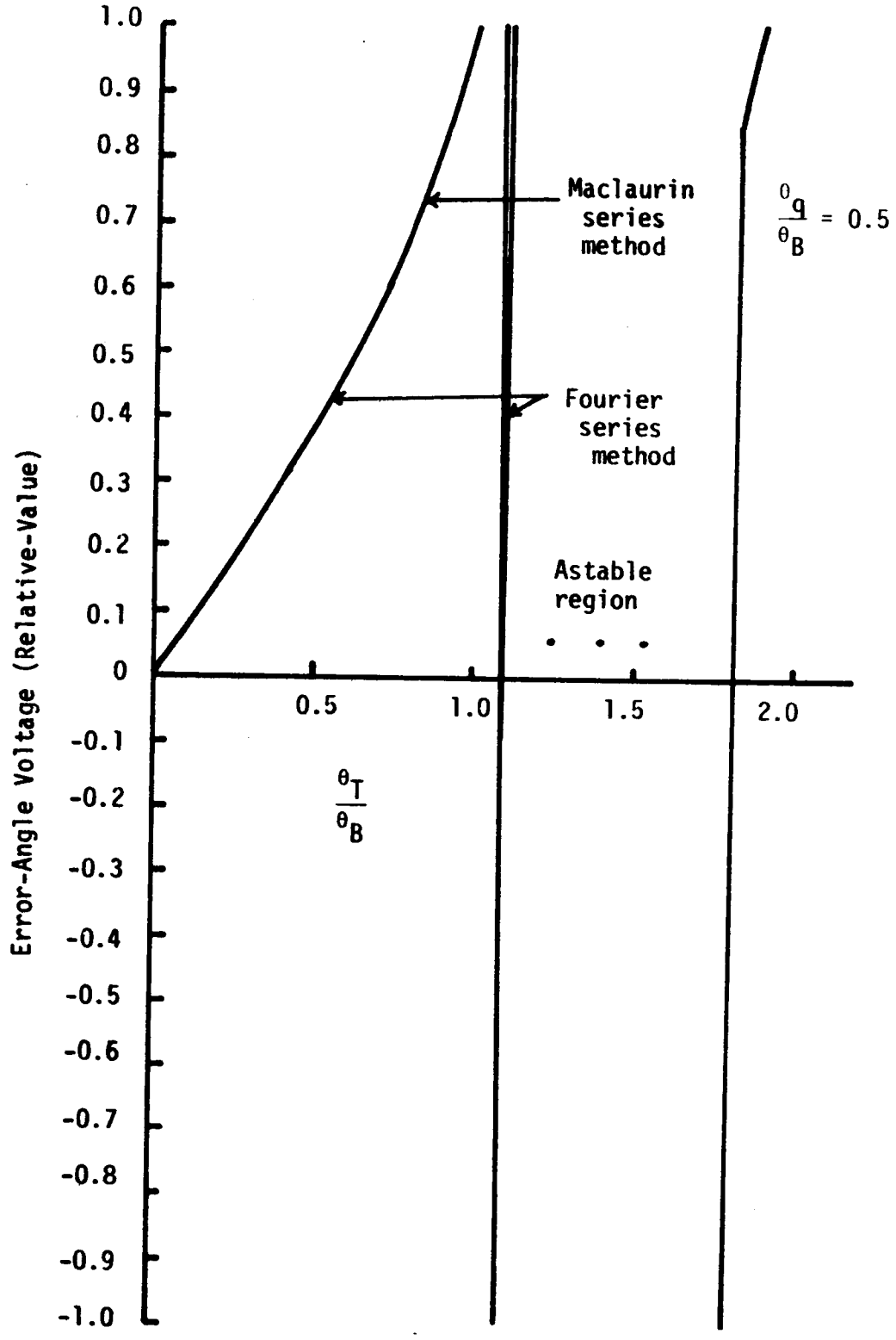


Figure 2.23. Comparison of error-signal voltages for monopulse-conical scan method (Bessel function antenna pattern) from two error signal extraction methods at the squint angle $\theta_q/\theta_B = 0.5$.

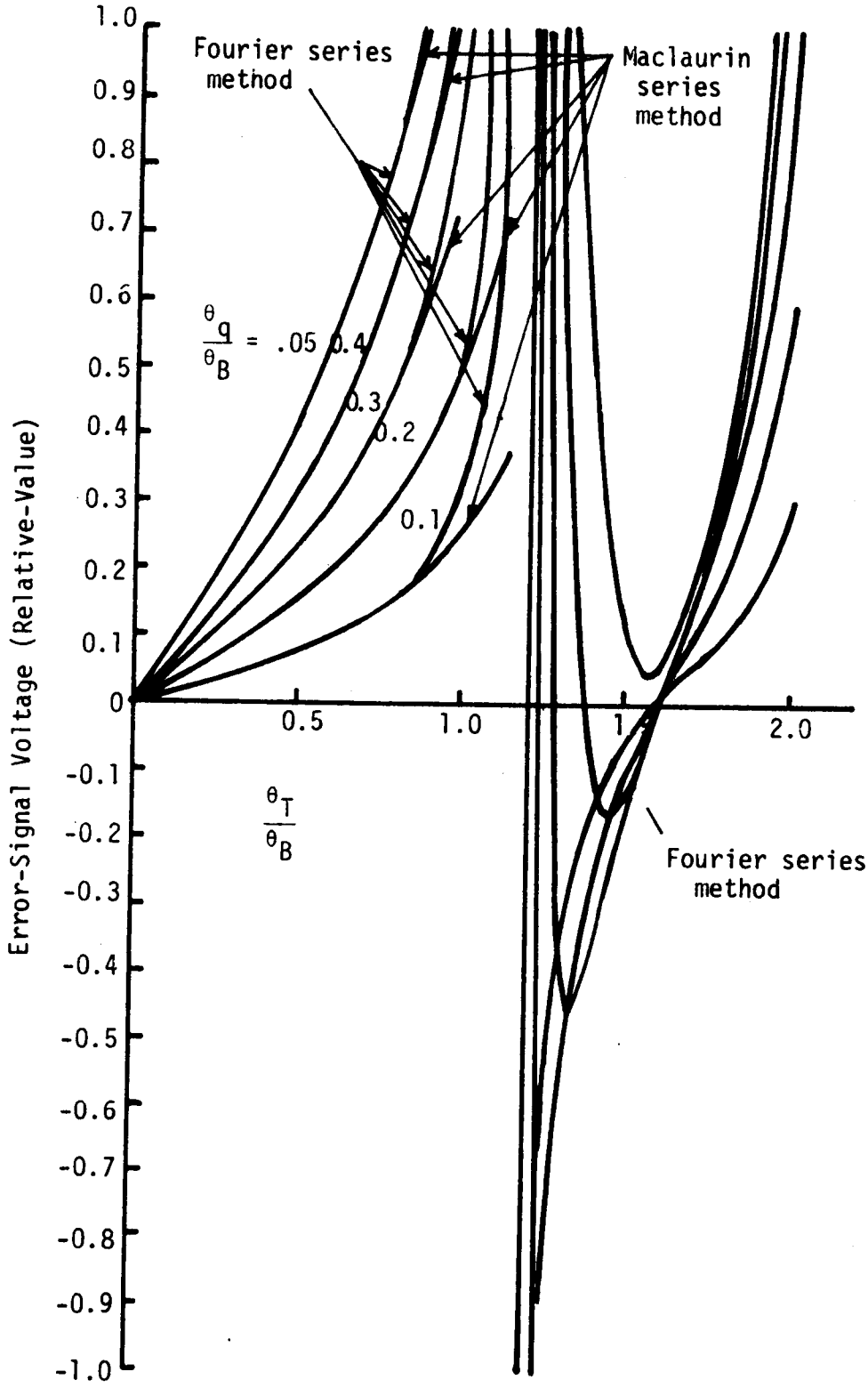


Figure 2.24. Comparison of error-signal voltages for conical scan-monopulse method (Bessel function antenna pattern: passive target) from two error signal extraction methods.

CHAPTER III

PRACTICAL DESIGN OF CONOPULSE SYSTEM

The theoretical block diagrams for two methods, Monopulse-Conical Scan Method and Conical Scan-Monopulse Method and the error-signal extraction by using their block diagrams have been described in Chapters I and II, respectively. However, we have ignored the component of the carrier on the sum $\Sigma(t)$ and the difference $\Delta(t)$ signals and assumed that they are completely demodulated in the discussion of the previous chapter. In order to design the two methods practically, the component of the carrier cannot be ignored and we will make use of it in the important stages actively. We will describe the practical design of the two systems stage by stage in this chapter.

I. MONOPULSE-CONICAL SCAN METHOD

The block diagram of this system (31, pp. 21-4-21-27; 32, p. 176) is shown in Figure 3.1. We will analyze this system by using the complex expression for the carrier component and the actual signal level will be used for the analysis since it will be very useful for the later discussion.

1. Hybrid Junction Stage

The two antenna feeds are connected to the two terminals of a hybrid junction such as a magic T, a rat race, or a short-slot coupler. The sum $\Sigma(t)$ and difference $\Delta(t)$ signals appear at the two other terminals of the hybrid. Then, the input signals to the two RF amplifiers after the hybrid may be written as

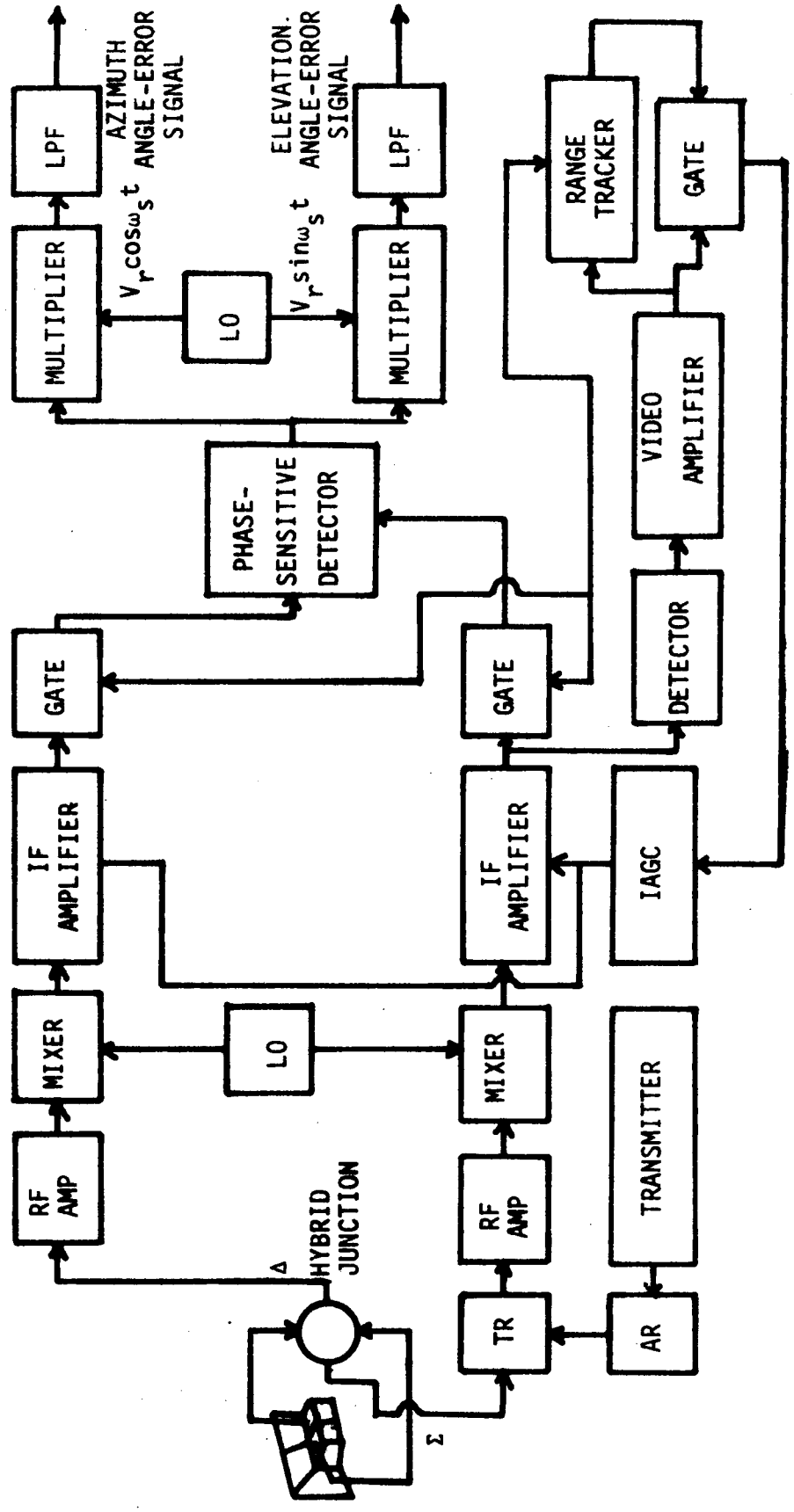


Figure 3.1. Block diagram of monopulse-conical scan method.

$$\Sigma(t) = \frac{\Sigma_a^2(t)\lambda\sqrt{P_t\sigma(t)}}{(4\pi)^3 R^2 L_t L_{at}^2 L_r} F_k(t) e^{j(\omega_c+\omega_d)t+j\theta}, \text{ [volts]}, \tag{3.1}$$

and

$$\Delta(t) = \frac{\Sigma_a(t)\Delta_a(t)\lambda\sqrt{P_t\sigma(t)}}{(4\pi)^3 R^2 L_t L_{at}^2 L_r} F_k(t) e^{j(\omega_c+\omega_d)t+j\theta}, \text{ [volts]}, \tag{3.2}$$

where

P_t = peak transmitter power,

$\Sigma_a(t) = G_1(t) + G_2(t)$ = antenna sum-pattern (one way voltage gain),

$\Delta_a(t) = G_1(t) - G_2(t)$ = antenna difference-pattern (one way voltage gain),

R = range of target,

$F_k(t)$ = pulse shape (peak voltage is one),

$\sigma(t)$ = target cross section including scintillation,

ω_c = carrier frequency,

λ = wave length of carrier,

ω_d = doppler frequency,

θ = phase shift,

L_t = loss between transmitter and antenna included its loss,

L_{at} = atmospheric loss, and

L_r = loss between receiver and antenna included its loss.

2. RF Amplifier Stage and Mixer Stage

It is considered that the RF amplifier consists of a wideband amplifier and a bandpass filter (BPF) and the BPF has enough bandwidth to pass all frequency components of the sum $\Sigma(t)$ and difference $\Delta(t)$ signals. Therefore, the function of the RF amplifier may be an ordinary wideband amplifier for the two signals.

For the sake of convenience let

$$S(t) = \frac{\Sigma_a^2(t)\lambda\sqrt{P_t\sigma(t)}}{(4\pi)^{\frac{3}{2}}R^2L_tL_{at}^2L_r} , \tag{3.3}$$

and

$$D(t) = \frac{\Sigma_a(t)\Delta_a(t)\lambda\sqrt{P_t\sigma(t)}}{(4\pi)^{\frac{3}{2}}R^2L_tL_{at}^2L_r} . \tag{3.4}$$

The output signals of RF amplifier on both channels become

$$\Sigma_{RF}(t) = A_{RF}S(t)F_k(t)e^{j(\omega_c+\omega_d)t+j\theta} , \tag{3.5}$$

and

$$\Delta_{RF}(t) = A_{RF}D(t)F_k(t)e^{j(\omega_c+\omega_d)t+j\theta} , \tag{3.6}$$

where A_{RF} is the gain of the RF amplifier.

The function of mixer stage included its LPF may be determined by

$$C = AB^* , \tag{3.7}$$

where A, B, and C are in the complex expression, A is the input signal, B is the local signal, and C is the output signal.

Letting the local signal be

$$V_2(t) = e^{j(\omega_c - \omega_i)t}, \tag{3.8}$$

where ω_i is the intermediate frequency (IF), the two output signals become, from the relation of Eq. (3.7),

$$\Sigma_m(t) = A_{RF}S(t)F_k(t)e^{j(\omega_i+\omega_d)t+j\theta}, \tag{3.9}$$

and

$$\Delta_m(t) = A_{RF}D(t)F_k(t)e^{j(\omega_i+\omega_d)t+j\theta}. \tag{3.10}$$

3. IF Amplifier Stage with IAGC

This IF amplifier has high gain and selectivity as well as an ordinary one. The matched filter may, however, be used to obtain the optimum output. Then, the $F_k(t)$ expressed the pulse train may change to some different wave shape at the output of the IF amplifier. But the same expression will be used to avoid additional notation. The most important action of this IF amplifier is the instantaneous automatic gain control (IAGC) which accomplishes the division operation when taken in conjunction with the phase sensitive detector.

The IAGC system detects the peak voltage of the sum signal given by Eq. (3.9) and provides a DC voltage proportional to the peak signal voltage. The voltage is fed to the IF amplifiers as shown in Figure 3.1, p. 96, where it is used for decreasing gain as the signal

increases. Then, the IF output of Σ channel are constant so that

$$\Sigma_{IF}(t) = A_{RF}A_{IF}S(t)F_k(t)e^{j(\omega_i+\omega_d)t+j\theta}$$

$$= K_{IF}F_k(t)e^{j(\omega_i+\omega_d)t+j\theta}, \tag{3.11}$$

where A_{IF} is the gain of IF amplifier and K_{IF} is constant.

Therefore, the gain of the IF amplifier becomes, in terms of $S(t)$ and A_{RF},

$$A_{IF} = \frac{K_{IF}}{A_{RF}S(t)} . \tag{3.12}$$

Similarly, the IF output of Δ channel is written as

$$\Delta_{IF}(t) = A_{RF}A_{IF}D(t)F_k(t)e^{j(\omega_i+\omega_d)t+j\theta}$$

$$= K_{IF}\frac{D(t)}{S(t)}F_k(t)e^{j(\omega_i+\omega_d)t+j\theta}. \tag{3.13}$$

Substituting Eqs. (3.3) and (3.4) into Eq. (3.13), we have

$$\Delta_{IF}(t) = K_{IF}\frac{\Delta_a(t)}{\Sigma_a(t)}F_k(t)e^{j(\omega_i+\omega_d)t+j\theta}. \tag{3.14}$$

Thus, we have obtained the ratio of $\Delta_a(t)$ and $\Sigma_a(t)$ on the Δ channel signal, but it still has the carrier component and modulation pulse. They will vanish in the next phase-sensitive detector.

4. Phase-Sensitive Detector

The phase-sensitive detector, which is generally assumed to be a product device followed by a low-pass filter, gives an output

$$V_{out}(t) = \Delta_{IF}(t)\Sigma^*_{IF}(t). \tag{3.15}$$

Assuming that the pulse shape of $F_k(t)$ is an arbitrary one as described before, it is written as, in the complex Fourier series form,

$$F_k(t) = \sum_{n=-\infty}^{\infty} C_n e^{jn\omega_p t} \tag{3.16}$$

Upon using Eqs. (3.11), (3.14), (3.15), and (3.16), we have

$$V_{out}(t) = K^2_{IF} \frac{\Delta_a(t)}{\Sigma_a(t)} \left\{ \sum_{n=-\infty}^{\infty} C_n e^{jn\omega_p t} \sum_{m=-\infty}^{\infty} C^*_m e^{-jm\omega_p t} \right\}$$

$$= K^2_{IF} \frac{\Delta_a(t)}{\Sigma_a(t)} \left\{ \sum_{n=-\infty}^{\infty} C_n C^*_{-n} + \sum_{\substack{\ell=-\infty \\ \ell \neq 0}}^{\infty} \sum_{n=-\infty}^{\infty} C_n C^*_{(n-\ell)} e^{j\ell\omega_p t} \right\}. \tag{3.17}$$

Since $F_k(t)$ is usually real, we have

$$C_n = C^*_{-n}$$

and

$$\text{average power of } F_k(t) = P = \sum_{n=-\infty}^{\infty} C_n{}^2 \,. \tag{3.18}$$

By action of the low-pass filter, $V_{out}(t)$ becomes

$$V_{out}(t) = K^2_{IF} \, P \, \frac{\Delta_a(t)}{\Sigma_a(t)} \,. \tag{3.19}$$

This is the desired angle-error signal which is called the time dependent error signal e(t) in the previous chapters.

Since the time dependent error-signal has been obtained at the

phase-sensitive detector and the analysis for the remaining stages are the same as the discussion in Chapter II, we will not explain them in this section to avoid complexity.

II. CONICAL SCAN-MONOPULSE METHOD

The block diagram of this system is shown in Figure 3.2. We will analyze this system step by step. However, the stages from the antenna to the IF stage are the same as in the monopulse-conical scan. So, we will start to analyze them from the IF amplifier stage.

1. IF Amplifier Stage with AGC

The difference between the IF amplifier on the conical scan-monopulse method and the monopulse-conical scan method is in the action of its automatic gain control (AGC). This AGC system is an ordinary one as in radio and TV.

Since the $\sigma(t)$ in Eqs. (3.1) and (3.2) is the target cross section including its scintillation, the term of $\sqrt{P_t\sigma(t)}$ may be expressed by

$$\sqrt{P_t\sigma(t)} = S\ K(t), \tag{3.20}$$

where S is constant and determined by parameters of the transmitter peak power and the target cross section, and K(t) is defined by the target echo scintillation.

If the only components for the changes of target cross section S, distance R, and other DC components are passed through the AGC filter followed by the video amplifier in Figure 3.2, and the signal level

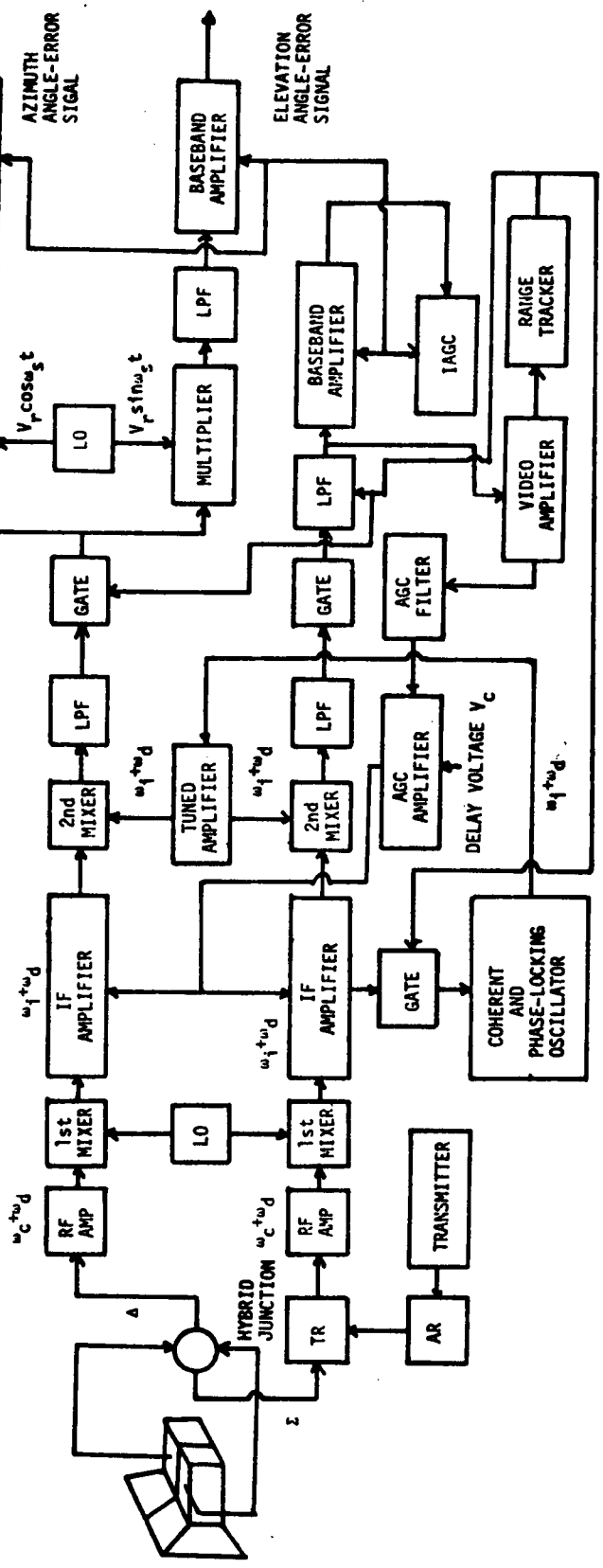


Figure 3.2. Block diagram of conical scan-monopulse method.

exceeds a delay voltage V_c prespecified, those changes may become constant and the output signals of the IF amplifiers on Σ and Δ channels may be represented by the expressions†

$$\Sigma_{IF}(t) = K_{IF}\Sigma_a^2(t)K(t)F_k(t)e^{j(\omega_i+\omega_d)t+j\theta}, \tag{3.21}$$

and

$$\Delta_{IF}(t) = K_{IF}\Sigma_a(t)\Delta_a(t)K(t)F_k(t)e^{j(\omega_i+\omega_d)t+j\theta}, \tag{3.22}$$

for the passive target case, where K_{IF} is determined by design of AGC.

2. Second Mixer Stage

This is a device for coherent detection. The local signal is completely phase-locked with the IF signal on the Σ channel as shown in Figure 3.2. So, the output signals passed through the low-pass filters having their cut-off frequency $\omega_i-\omega_d$ become

$$\Sigma(t) = K_{IF}\Sigma_a^2(t)K(t)F_k(t), \tag{3.23}$$

and

$$\Delta(t) = K_{IF}\Sigma_a(t)\Delta_a(t)K(t)F_k(t). \tag{3.24}$$

3. Multiplier Stage and Baseband Amplifier Stage

The output signals of the gates are written as

---

†The output pulse shape may change to some different shape at the IF output. The same notation is used to avoid additional notation.

$$\Sigma(t) = K_{IF}\Sigma_a^2(t)K(t) \sum_{n=-\infty}^{\infty} C_n e^{jn\omega_p t} , \tag{3.25}$$

and

$$\Delta(t) = K_{IF}\Sigma_a(t)\Delta_a(t)K(t) \sum_{n=-\infty}^{\infty} C_n e^{jn\omega_p t} , \tag{3.26}$$

Then, they are rewritten as

$$\Sigma(t) = K_{IF}C_o\Sigma_a^2(t)K(t) + \text{other higher frequency terms}, \tag{3.27}$$

and

$$\Delta(t) = K_{IF}C_o\Sigma_a(t)\Delta_a(t)K(t) + \text{other higher frequency terms.} \tag{3.28}$$

The fundamental components of Eqs. (3.27) and (3.28) are the desired signal.

The signals $\Delta_{(\cos)}$ and $\Delta_{(\sin)}$ described in Figure 1.5, p. 9, are obtained at the two multiplier stages, and the baseband amplifiers with IAGC which responses K(t) on the Σ channel perform the divider circuit the same as in the monopulse-conical scan. Finally, the azimuth angle-error and the elevation angle-error signals are obtained at the outputs of the two baseband amplifiers controlled by IAGC on the Δ channel.

CHAPTER IV

NOISE IN CONOPULSE SYSTEM

In this chapter we will be interested in finding the accuracy of the relative target angles with respect to an arbitrary reference axis and boresight axis. The most obvious and direct source of inaccurate determinations is noise. There are several theoretical approaches to obtain the accuracy (31, p. 4-3) such as the Cramer-Rao lower bounds (8, pp. 475-524; 25; 26; 33; 37), the maximum-likelihood estimates (15; 16; 37; 43, pp. 62-80), and the Barankin's greatest lower bound for unbiased estimates (4; 36).

The relationships among these approaches are briefly described here. The Cramer-Rao bounds are lower bounds for so-called "regular" estimation cases. The great majority of cases arising in actual radar measurement are regular, and also the Cramer-Rao bounds are asymptotically greatest lower bounds under appropriate additional conditions, i.e., they can actually be attained by possible estimation procedures. Specifically, they are asymptotically attained by maximum-likelihood estimates. It means that the Cramer-Rao lower bounds and the accuracy of maximum-likelihood estimates become the same for the white Gaussian noise and sufficiently high total signal-to-noise ratio (SNR). The Barankin's approach gives the greatest lower bounds for the variance and covariance of parameters for all unbiased estimates for all cases (regular or non-regular) and all SNR, as well as the estimates that attain these bounds. However, its chief draw-back is that it does not lead to neat closed-form solutions except in special cases. The

solutions may, in general, be obtained by numerical computation.

In case of our tracking radar, the radar may track a target after search radar detects it. It is considered that the SNR may be large enough to satisfy the condition of the terminology "asymptotically" in the Cramer-Rao lower bounds and the maximum-likelihood estimates.

In our tracking radar system, two kinds of estimates or accuracy can be considered, i.e., for the signal data taken just after the antenna such that the result of the analysis gives the theoretical lower limit to accuracy, and for the actual system implementation since it gives approximately the true accuracy of the real system.

In this chapter, we will describe these two kinds of accuracy and how the accuracy in the real system approaches the theoretical lower limit. The Cramer-Rao lower bounds and the maximum-likelihood estimates are applied to the analyses for the signal data taken just after the two antennas and for the signal data in the real system implementation, respectively.

I. THEORETICAL LOWER LIMIT OF ACCURACY

In this section, we will find the accuracy of the raw data, that is, the signal data taken at the two antenna outputs as shown in Figure 4.1.

The following discussion is heavily based on Dr. Peebles' work (25, pp. 127-136). However, his result is for one pulse basis. Therefore, our main intention is that his result is expanded to the closed form taking his result as the starting point of our discussion.

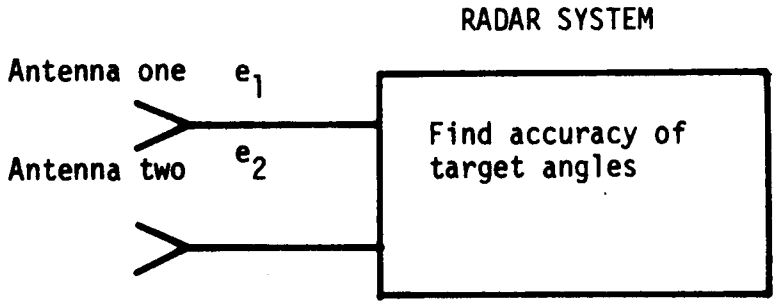


Figure 4.1. Accuracy of raw data.

The signal processor to omit the carriers may be required at least to calculate the accuracy as shown in Figure 4.2.

Since this analysis is ideal, it could be considered that the pulse is an impulse, its pulse period is τ, and (2n+1) pulses are included in the observation interval, $-T \leq t \leq T$.

The voltage U_m from mth antenna is comprised of a signal $e_m(t)$ and a noise $n_m(t)$ so that

$$U_m(t) = e_m(t) + n_m(t), \quad m = 1, 2. \tag{4.1}$$

In this case, $e_m(t)$ may be written as

$$e_m(t) = \sum_{k=-n}^{n} R\Sigma_a(t)e^{j(\omega_o+\omega_d)t+j\theta}G_m(t)\delta(t-k\tau), \tag{4.2}$$

where R is determined by parameters of radar equation, $\Sigma_a(t)$ is normalized transmitter antenna pattern modulated by its rotation (the gain at the beam axis is one), ω_o and ω_d are carrier and doppler frequencies, respectively, θ is phase shift, and $G_m(t)$ is normalized receiver antenna pattern modulated by its rotation.

Here, we supposed that the target does not move in the observation interval, and the target echo fluctuation does not exist since it does not reflect to the error signals in the actual system.

Eq. (4.2) is in the complex form. We could use complex notation, however, we use a real expression on it because the real part of Eq. (4.2) is what the actual system utilizes.

Hence, letting $e_m(t)$ equal the real part of Eq. (4.2) to avoid additional notation, we have

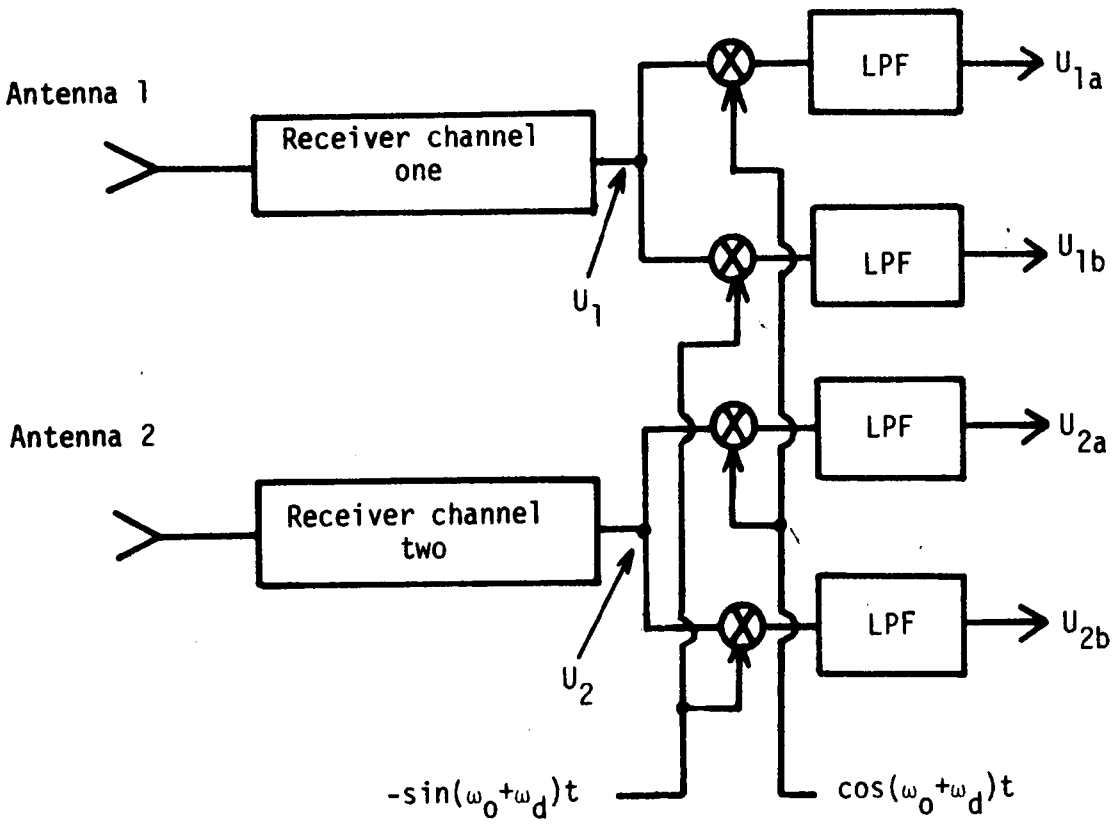


Figure 4.2. Signal processor at early stages.

$$e_m(t) = \sum_{k=-n}^{n} R\Sigma_a(t)G_m(t)\delta(t-k\tau)\left\{\cos\theta\sin(\omega_o+\omega_d)t\right.$$

$$\left. - \sin\theta\sin(\omega_o+\omega_d)t\right\}, \qquad (4.3)$$

since the antenna patterns are real.

The noise at the mth channel output may be written as

$$n_m(t) = a_m(t)\cos(\omega_o+\omega_d)t - b_m(t)\sin(\omega_o+\omega_d)t. \qquad (4.4)$$

The signal of the mth channel is the sum of Eqs. (4.3) and (4.4). This is fed to the mixers of Figure 4.2. When the indicated product is taken and terms involving $(2\omega_o+2\omega_d)$ are neglected due to action of the LPF having the cut-off frequency ω_o, the outputs of the mth channel become

$$U_{ma} = \sum_{k=-n}^{n} R\Sigma_a(t)G_m(t)\frac{\omega_o}{\pi}S_a[\omega_o(t-k\tau)]\cos\theta + a_m(t), \qquad (4.5)$$

and

$$U_{mb} = \sum_{k=-n}^{n} R\Sigma_a(t)G_m(t)\frac{\omega_o}{\pi}S_a[\omega_o(t-k\tau)]\sin\theta + b_m(t), \qquad (4.6)$$

where it is assumed that the LPF's have the gain of 2, and

$$S_a(x) = \frac{\sin x}{x}. \qquad (4.7)$$

However, since the radar carrier frequency is usually in the microwave band, it could be true that $\pi/\omega_o \simeq 0$ and

$$\frac{\omega_o}{\pi} S_a[\omega_o(t-k\tau)] \simeq \delta(t-k\tau). \tag{4.8}$$

Thus, Eqs. (4.5) and (4.6) become

$$U_{ma} = R\cos\theta \sum_{k=-n}^{n} \Sigma_a(t) G_m(x,y,t)\delta(t-k\tau) + a_m(t), \tag{4.9}$$

and

$$U_{mb} = R\sin\theta \sum_{k=-n}^{n} \Sigma_a(t) G_m(x,y,t)\delta(t-k\tau) + b_m(t), \tag{4.10}$$

where the antenna pattern is also a function of x and y which express the azimuth axis and the elevation axis.

In the previous chapter, the antenna pattern was treated as a function of time and target angles θ_T and ϕ_o with respect to the boresight axis and an arbitrary reference axis. However, their values do not directly appear at the output of the actual system. The error-angle signals are proportional to the off angles from the origin on the azimuth axis and the elevation axis. Their relationships are shown in Figure 4.3. Therefore, we will treat the real error-angle signals x and y instead of the target angles θ_T and ϕ_o in this chapter.

For the sake of convenience, let us define

$$e_{ma} = R\cos\theta \sum_{k=-n}^{n} \Sigma_a(t) G_m(x,y,t)\delta(t-k\tau), \tag{4.11}$$

and

$$e_{mb} = R\sin\theta \sum_{k=-n}^{n} \Sigma_a(t) G_m(x,y,t)\delta(t-k\tau), \tag{4.12}$$

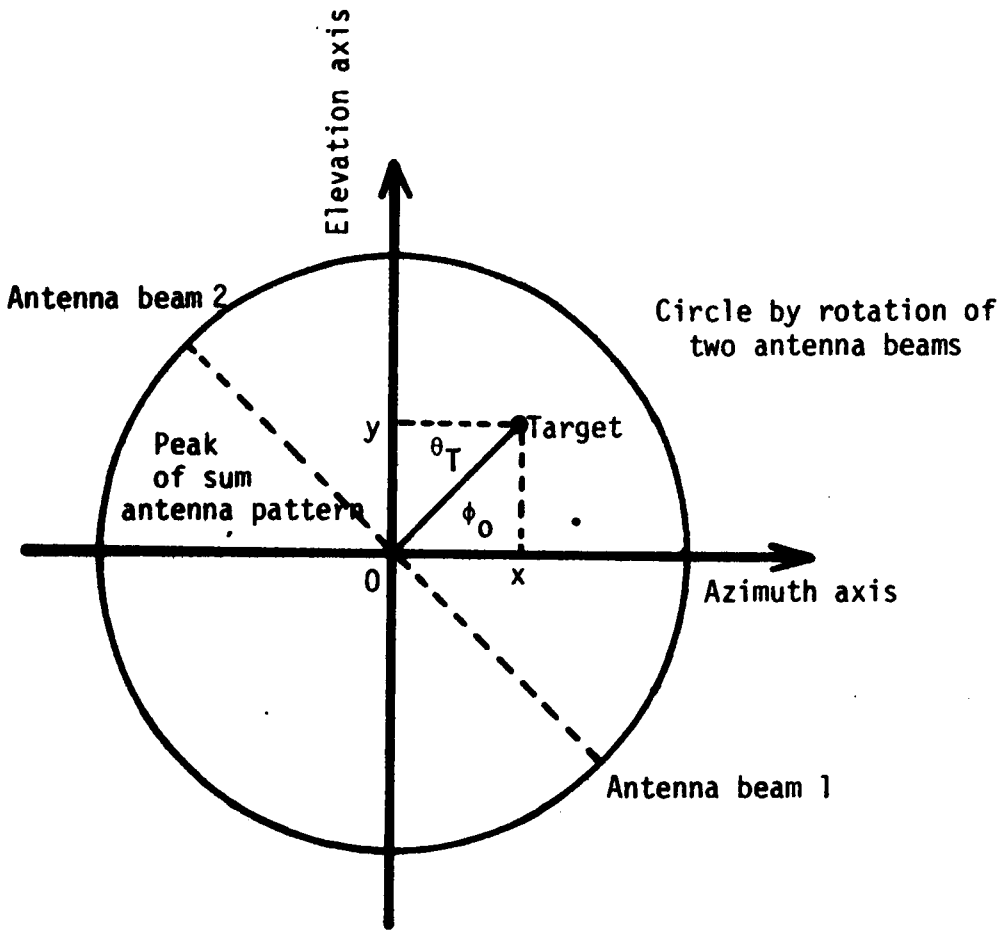


Figure 4.3. Relation of target angles and their axes on target plane.

so that Eqs. (4.9) and (4.10) become

$$U_{ma} = e_{ma} + a_m(t), \tag{4.13}$$

and

$$U_{mb} = e_{mb} + b_m(t). \tag{4.14}$$

From the result of Dr. Peebles (23, p. 55; 25, p. 133), the elements of the information matrix that the inverse matrix expresses the minimum variances and covariances of estimates are given by

$$I_{pq} = \frac{1}{\sigma^2} \sum_{m=1}^{2} \left\{ \left(\frac{e_{ma}}{\partial\theta_p} \right) \left(\frac{e_{ma}}{\partial\theta_q} \right) + \left(\frac{\partial e_{mb}}{\partial\theta_p} \right) \left(\frac{\partial e_{mb}}{\partial\theta_q} \right) \right\}, \tag{4.15}$$

where it is assumed that the noises in each channel are independent and they have the same power so that

$$\sigma^2 = \sigma_{ma}^2 = \sigma_{mb}^2.$$

Here, θ_p and θ_q are corresponding to the parameters x and y, respectively.

Substituting Eqs. (4.11) and (4.12) into Eq. (4.15), we have

$$I_{pq} = \frac{R^2}{\sigma^2} \sum_{m=1}^{2} \left\{ \sum_{k=-n}^{n} \Sigma_a{}^2(t) \left[\frac{\partial G_m(x,y,t)}{\partial\theta_p} \right] \left[\frac{\partial G_m(x,y,t)}{\partial\theta_q} \right] \right.$$

$$\left. \times \delta(t-k\tau) \right\}, \tag{4.16}$$

where it is supposed that

$$\delta(t-k\tau) = \delta^2(t-k\tau).$$

Since $\Sigma_a(t)$ is normalized transmitter antenna pattern modulated by its rotation, it may be almost constant so that

$$M = \Sigma_a^2(t). \tag{4.17}$$

Thus, Eq. (4.16) becomes

$$I_{pq} = \frac{R^2 M}{\sigma^2} \sum_{m=1}^{2} \left\{ \sum_{k=-n}^{n} \left[\frac{\partial G_m(x,y,t)}{\partial \theta_p} \right] \left[\frac{\partial G_m(x,y,t)}{\partial \theta_q} \right] \times \delta(t-k\tau) \right\}. \tag{4.18}$$

For the sake of convenience, let us define

$$f(x,y,t) = \frac{\partial G_m(x,y,t)}{\partial \theta_p} \frac{\partial G_m(x,y,t)}{\partial \theta_q}. \tag{4.19}$$

$f(x,y,t)$ may be continuous in the interval $-T \leq t \leq T$ and it may be also bandlimited. Assuming that the pulse repetition frequency $(1/\tau)$ is much higher than the maximum frequency of $f(x,y,t)$, the Rieman integral theorem may be satisfied as

$$\tau \sum_{k=-n}^{n} f(x,y,t)\delta(t-k\tau) \simeq \int_{-T}^{T} f(x,y,t)dt. \tag{4.20}$$

From the relation of Eq. (4.20), the I_{pq} given by Eq. (4.18) becomes

$$I_{pq} = \frac{R^2 M}{\sigma^2 \tau} \sum_{m=1}^{2} \int_{-T}^{T} \left[\frac{\partial G_m(x,y,t)}{\partial \theta_p} \right] \left[\frac{\partial G_m(x,y,t)}{\partial \theta_q} \right] dt. \tag{4.21}$$

This is the general solution of closed form sought in this chapter.

The next problem is the evaluation of the integrand of Eq. (4.20) for our radar system.

From Eqs. (2.27) and (2.28) in Chapter II, the antenna patterns as a function of target angles are

$$G_1(\theta) = \sum_{r=0}^{\infty} (-1)^r \left\{ \sum_{n=r}^{\infty} \frac{c_{2n} d_1}{(2n)!} \binom{n}{r} \left[\left(\frac{\theta_q}{\theta_B} \right)^2 + \left(\frac{\theta_T}{\theta_B} \right)^2 \right]^{n-r} \right.$$

$$\left. \times \left[\frac{2\theta_q \theta_T}{\theta_B^2} \cos(\omega_s t - \phi_o) \right]^r \right\}$$

$$\simeq c_o + \frac{c_2 d_1^2}{2} \left[\left(\frac{\theta_q}{\theta_B} \right)^2 + \left(\frac{\theta_T}{\theta_B} \right)^2 \right] - \frac{c_2 d_1^2 \theta_q \theta_T}{\theta_B^2} \cos(\omega_s t - \phi_o), \tag{4.22}$$

and

$$G_2(\theta) \simeq c_o + \frac{c_2 d_1^2}{2} \left[\left(\frac{\theta_q}{\theta_B} \right)^2 + \left(\frac{\theta_T}{\theta_B} \right)^2 \right] + \frac{c_2 d_1^2 \theta_q \theta_T}{\theta_B^2} \cos(\omega_s t - \phi_o), \tag{4.23}$$

for the first order approximation because we have already known that the first order approximation of antenna pattern is enough for target close to the boresight axis in the discussion of Chapter II.

Eqs. (4.22) and (4.23) have the angles θ_T and ϕ_o as variables, and the angles θ_B and θ_q as parameters. So, we have to convert the variables θ_T and ϕ_o to the variables x and y which are the output voltages in the real system as described before. Referring to Figure 4.3, p. 113, it is easy to obtain such relations as

$$\left.\begin{aligned} \theta_T &= x^2 + y^2 \ , \quad \text{and} \\ \phi_o &= \ell\pi + \tan^{-1}\frac{y}{x} \ , \end{aligned}\right\} \tag{4.24}$$

where ℓ is integer and is dependent on the target position.

Next, we will consider the observation interval as follows.

Referring to Figure 4.3, p. 113, the peak of the same antenna pattern may come across a target at least once at the half cycle rotation of two antenna, that is, the observation interval has to be some integer times the half cycle of antenna beam rotation to get the even data about the target on the statistical standing point. Then, it is determined by

$$T = \frac{n\pi}{2\omega_s} \ , \tag{4.25}$$

where n is integer.

Substituting Eq. (4.24) into Eqs. (4.22) and (4.23), the antenna patterns in terms of x and y are

$$G_1(x,y,t) = c_o + \frac{c_2 d_1^{\,2}}{2}\left(\frac{\theta_q}{\theta_B}\right)^2 + \frac{c_2 d_1^{\,2}}{2\theta_B^2}(x^2+y^2)$$

$$- \frac{c_2 d_1^{\,2}\theta_q\sqrt{x^2+y^2}}{\theta_B^2}\cos[\omega_s t - \ell\pi - \tan^{-1}\frac{y}{x}], \tag{4.26}$$

and

$$G_2(x,y,t) = c_o + \frac{c_2 d_1^2}{2}\left(\frac{\theta_q}{\theta_B}\right)^2 + \frac{c_2 d_1^2}{2\theta_B^2}(x^2+y^2)$$

$$+ \frac{c_2 d_1^2 \theta_q}{2\theta_B^2}\sqrt{x^2+y^2}\cos(\omega_s t - \ell\pi\tan^{-1}\frac{y}{x}]. \qquad (4.27)$$

From the general solution of Eq. (4.21), the elements of the information matrix in this case are given by

$$I_{xx} = \frac{R^2 M}{\sigma^2_\tau}\int_{-T}^{T}\left\{\left(\frac{\partial G_1(x,y,t)}{\partial x}\right)^2 + \left(\frac{\partial G_2(x,y,t)}{\partial x}\right)^2\right\} dt, \qquad (4.28)$$

$$I_{xy} = I_{yx} = \frac{R^2 M}{\sigma^2_\tau}\int_{-T}^{T}\left\{\left(\frac{\partial G_1(x,y,t)}{\partial x}\right)\left(\frac{\partial G_1(x,y,t)}{\partial y}\right)\right.$$

$$\left. + \left(\frac{\partial G_2(x,y,t)}{\partial x}\right)\left(\frac{\partial G_2(x,y,t)}{\partial y}\right)\right\} dt, \qquad (4.29)$$

and

$$I_{yy} = \frac{R^2 M}{\sigma^2_\tau}\int_{-T}^{T}\left\{\left(\frac{\partial G_1(x,y,t)}{\partial y}\right)^2 + \left(\frac{\partial G_2(x,y,t)}{\partial y}\right)^2\right\} dt. \qquad (4.30)$$

Substituting† Eqs. (4.26) and (4.27) into Eqs. (4.28), (4.29), and (4.30), the elements become

$$I_{xx} = \frac{R^2}{\sigma^2_\tau}\left\{4Tx^2\left(\frac{c_2 d_1^2}{\theta_B^2}\right)^2 + 2T\left(\frac{c_2 d_1^2}{\theta_B^2}\right)^2\right\} \qquad (4.31)$$

---

†Appendix I.

$$I_{xy} = I_{yx} = \frac{4R^2\Sigma_a{}^2(t)xyT}{\sigma^2_\tau}\left(\frac{c_2d_1{}^2}{\theta_B^2}\right)^2 , \tag{4.32}$$

$$I_{yy} = \frac{R^2\Sigma_a{}^2(t)}{\sigma^2_\tau}\left\{ 4Ty^2\left(\frac{c_2d_1{}^2}{\theta_B^2}\right)^2 + 2T\left(\frac{c_2d_1{}^2}{\theta_B^2}\right)^2 \right\} . \tag{4.33}$$

Since the inverse of the information matrix is the variance and covariance matrix of x and y, it becomes

$$[I]^{-1} = \begin{bmatrix} \dfrac{\frac{R^2M}{\sigma^2_\tau}\left[4Ty^2\left(\frac{c_2d_1{}^2}{\theta_B^2}\right)^2 + 2T\left(\frac{c_2d_1{}^2}{\theta_B^2}\right)^2\right]}{D}, & -\dfrac{\frac{4R^2Mxyt}{\sigma^2_\tau}\left(\frac{c_2d_1{}^2}{\theta_B^2}\right)^2}{D} \\ -\dfrac{\frac{4R^2Mxyt}{\sigma^2_\tau}\left(\frac{c_2d_1{}^2}{\theta_B^2}\right)^2}{D}, & \dfrac{\frac{R^2M}{\sigma^2_\tau}\left[4Ty^2\left(\frac{c_2d_1{}^2}{\theta_B^2}\right)^2 + 2T\left(\frac{c_2d_1{}^2}{\theta_B^2}\right)^2\right]}{D} \end{bmatrix} , \tag{4.34}$$

where

$$[I]^{-1} = \begin{bmatrix} I_{xx}, I_{xy} \\ I_{yx}, I_{yy} \end{bmatrix}^{-1} = \begin{bmatrix} \sigma^2_{xx}, \sigma^2_{xy} \\ \sigma^2_{yx}, \sigma^2_{yy} \end{bmatrix} , \tag{4.35}$$

$$\sigma^2_{xx} = E\{(\hat{x}-x)^2\} ,$$

$$\sigma^2_{xy} = \sigma^2_{yx} = E\{(\hat{x}-x)(\hat{y}-y)\}, \text{ and} \tag{4.36}$$

$$\sigma^2_{yy} = E\{(\hat{y}-y)^2\},$$

where $\hat{x}$ and $\hat{y}$ are measured (estimate) values, and x and y are true values,

and

$$D = \frac{R^4M^2}{\sigma^4\tau^2}\left\{\left[4Tx^2\left(\frac{c_2d_1^2}{\theta_B^2}\right)^2 + 2T\left(\frac{c_2d_1^2}{\theta_B^2}\right)^2\right.\right.$$

$$\times\left[4Ty^2\left(\frac{c_2d_1^2}{\theta_B^2}\right)^2 + 2T\left(\frac{c_2d_1^2}{\theta_B^2}\right)^2\right]$$

$$\left.\left. - 16x^2y^2T^2\left(\frac{c_2d_1^2}{\theta_B^2}\right)^4\right\}\right. . \qquad (4.37)$$

If the target is on the boresight axis, that is, the tracking mode, the matrix of Eq. (4.34) becomes, as $x \longrightarrow 0$ and $y \longrightarrow 0$,

$$[I]^{-1} = \begin{bmatrix} \dfrac{1}{\dfrac{2TR^2M}{\sigma^2\tau}\left(\dfrac{c_2d_1^2\theta_q}{\theta_B^2}\right)^2} & , & 0 \\ 0 & , & \dfrac{1}{\dfrac{2TR^2M}{\sigma^2\tau}\left(\dfrac{c_2d_1\theta_q}{\theta_B^2}\right)^2} \end{bmatrix} \qquad (4.38)$$

where

$$M = \Sigma_a^2(t),$$

and it is dependent on the pattern squint angle as follows

$$\left.\begin{aligned} M &> 1, \quad \text{for } \theta_q/\theta_B < 0.5 \\ M &= 1, \quad \text{for } \theta_q/\theta_B = 0.5 \\ M &< 1, \quad \text{for } \theta_q/\theta_B > 0.5 \end{aligned}\right\} . \tag{4.39}$$

This is the final result for the accuracy. It is remarked on Eq. (4.37) that the accuracy of x and y are the same and the cross terms are zero.

II. TRUE ACCURACY OF REAL SYSTEM

In this section, we will find the accuracy of x and y in the actual system implementation.

We will apply the maximum-likelihood method to the analysis, and describe briefly this method (37).

Suppose the observed signal is

$$S(t) = F(t,\alpha_1, \ldots, \alpha_n) + \mathcal{E}(t), \; A \le t \le B, \tag{4.40}$$

where $F(t, \alpha_1, \ldots, \alpha_n)$ is a real function of time which depends on a set of unknown parameters $\alpha_1, \ldots, \alpha_n$ and $\mathcal{E}(t)$ is additive noise.

In the case of white Gaussian noise, the variance and covariance matrix of the parameters is given by

$$E\{(\hat{\alpha}_i-\alpha_i)(\hat{\alpha}_j-\alpha_j)\} = (B^{-1})_{ij}, \tag{4.41}$$

and

$$B_{ij} = \frac{2}{\psi}\int_A^B \frac{\partial F(t,\alpha_1, \ldots,\alpha_n)}{\partial \alpha_i} \; \frac{\partial F(t,\alpha_1, \ldots, \alpha_n)}{\partial \alpha_j}\, dt, \tag{4.42}$$

where ψ is the one-sided noise power spectral density, $\hat{\alpha}_i$, i=1, ..., n, represent the asymptotically minimum variance unbiased estimates of the parameters, and α_i are the true values.

In order to apply this method to our actual system, the signal $F(t, \alpha_1, \ldots, \alpha_n)$ must have x and y as the parameters. The azimuth and elevation angle error signals are not able to be adopted as the signal. Therefore, we will use the time dependent error signal as the signal given by Eq. (2.41) so that

$$e(t) = -\frac{c_2 d_1^2}{c_o} \frac{\theta_q \theta_T}{\theta_B^2} \cos(\omega_s t - \phi_o). \tag{4.43}$$

This signal exists in the monopulse-conical scan method. However, the conical scan-monopulse method does not have any signals having the parameters x and y simultaneously except in the raw data signals. So, it could be assumed that it exists in the method.

Substituting the relations given by Eq. (4.24) into Eq. (4.41), the signal F(t,x,y) is written as

$$F(t,x,y) = (-1)^{\ell} \frac{A\theta_q}{\theta_B^2} \sqrt{x^2+y^2} \cos(\omega_s t - \tan^{-1} \frac{y}{x}), \tag{4.44}$$

where

$$A = -\frac{c_2 d_1^2}{c_o}.$$

Under the same observation interval in the previous section, substituting Eq. (4.44) into Eq. (4.42), the elements† of the

†Appendix J.

inverse of the variance and covariance matrix become

$$B_{11} = \frac{2}{\psi}\int_{-T}^{T}\left(\frac{\partial F(t,x,y)}{\partial x}\right)^2 dt = \frac{2T}{\psi}\left(\frac{A\theta_q}{\theta_B^2}\right)^2, \tag{4.45}$$

$$B_{12} = B_{21} = \frac{2}{\psi}\int_{-T}^{T}\frac{\partial F(t,x,y)}{\partial x}\frac{\partial F(t,x,y)}{\partial y}\,dt = 0, \tag{4.46}$$

and

$$B_{22} = \frac{2}{\psi}\int_{-T}^{T}\left(\frac{\partial F(t,x,y)}{\partial y}\right)^2 dt = \frac{2T}{\psi}\left(\frac{A\theta_q}{\theta_B^2}\right)^2. \tag{4.47}$$

Then, the variance and covariance matrix is

$$[B]^{-1} = \begin{bmatrix} \dfrac{1}{\dfrac{2T}{\psi}\left(\dfrac{A\theta_q}{\theta_B^2}\right)^2} & 0 \\ 0 & \dfrac{1}{\dfrac{2T}{\psi}\left(\dfrac{A\theta_q}{\theta_B^2}\right)^2} \end{bmatrix}, \tag{4.48}$$

where

$$[B]^{-1} = \begin{bmatrix} \sigma_{xx}^2 & \sigma_{xy}^2 \\ \sigma_{yx}^2 & \sigma_{yy}^2 \end{bmatrix} \tag{4.49}$$

and the elements of the matrix $[B]^{-1}$ are defined by Eq. (4.36).

This is the general solution of the actual system implementation. However, the noise power spectrum density may be different in the two methods.

1. Monopulse-Conical Scan Method

First we will consider the theoretical model of this method as shown in Figure 4.4 to obtain the noise power spectrum density.

The input signals of the RF amplifiers on both channels may be written in the complex form as

$$\Sigma_{RF}(t) = R\Sigma_a^2(t)F_k(t)e^{j(\omega_o+\omega_d)t+j\theta} + n_s(t), \tag{4.50}$$

and

$$\Delta_{RF}(t) = R\Sigma_a(t)\Delta_a(t)F_k(t)e^{j(\omega_o+\omega_d)t+j\theta} + n_D(t), \tag{4.51}$$

where R is determined by parameters of radar equation, $\Sigma_a(t)$ and $\Delta_a(t)$ are normalized antenna pattern (that is, the gain at the beam axis is one), $n_s(t)$ and $n_D(t)$ are noises in the corresponding channels, the other notations are the same as in Chapter III.

In this analysis, it is assumed that the SNR is large. Therefore, it may be supposed that the action of IAGC is complete, i.e., we can ignore the noise on the Σ channel.

From Eq. (3.12), the IF gain due to action of IAGC is written as

$$A_{IF} = \frac{K_{IF}}{A_{RF}R\Sigma_a^2(t)} . \tag{4.52}$$

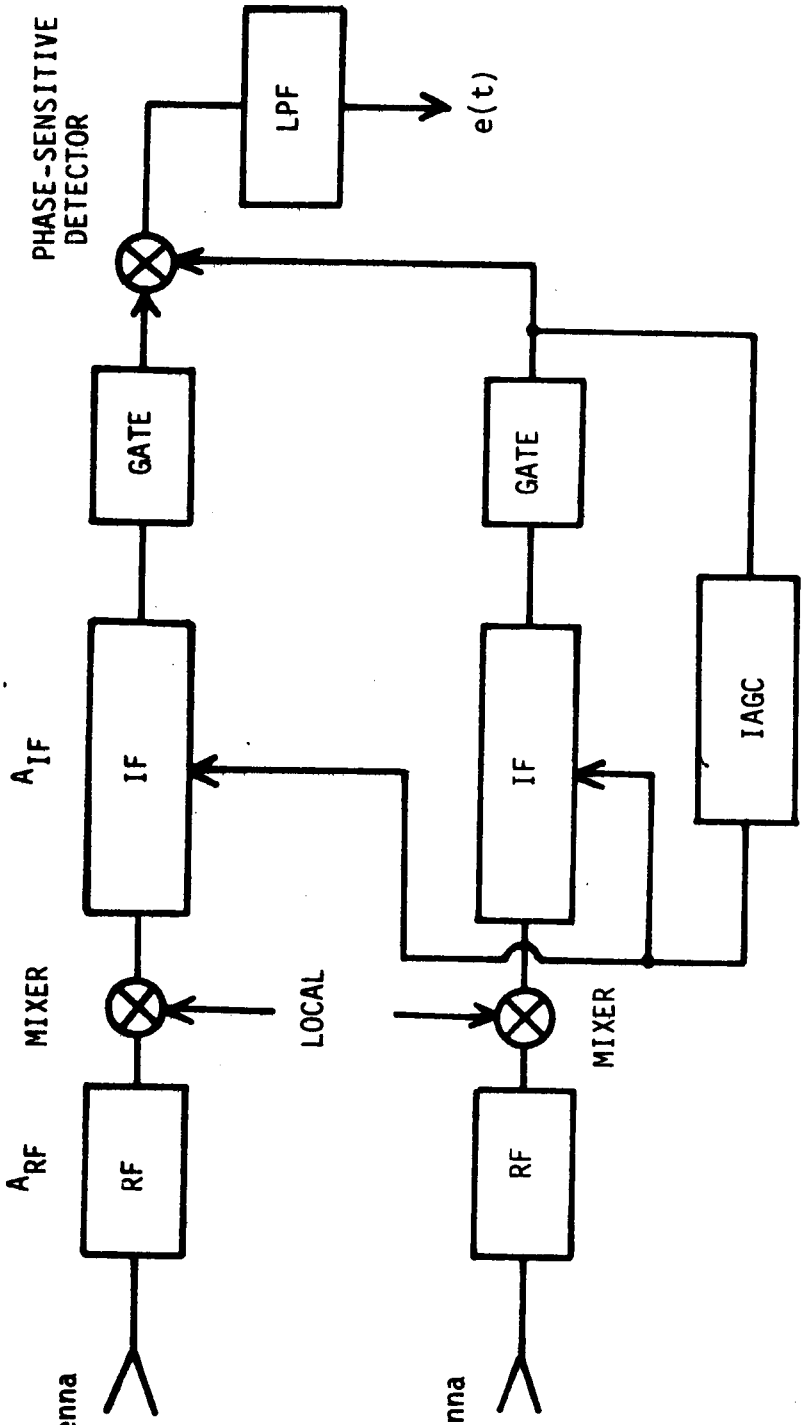


Figure 4.4. Theoretical model of monopulse-conical scan method.

Since the component of IF frequency is omitted at the phase-sensitive detector, we will use the expression on video band for this analysis to avoid complexity.

The output signal† after the gate on the Δ channel become

$$\Delta(t) = RA_{RF}A_{IF}\Sigma_a(t)\Delta_a(t)F_k(t) + A_{RF}A_{IF}n_D(t)G_k(t), \tag{4.53}$$

where $n_D(t)$ is the noise in the video band here, and $G_k(t)$ represents the gate.

Substituting Eq. (4.52) into Eq. (4.53), we have

$$\Delta(t) = K_{IF}\frac{\Delta_a(t)}{\Sigma_a(t)}F_k(t) + \frac{K_{IF}}{R\Sigma_a^2(t)}n_D(t)G_k(t). \tag{4.54}$$

Similarly, the output after the gate on the Σ channel is

$$\Sigma(t) = K_{IF}F_k(t). \tag{4.55}$$

It should be remarked that all terms in Eqs. (4.54) and (4.55) are real in this case.

Since the phase-sensitive detector consists of a product device and a LFP, a function is defined by

$$e(t) = \Delta(t)\Sigma^*(t). \tag{4.56}$$

Using the results of Eqs. (3.17), (3.18), and (3.19) in Chapter III, the signal e(t) is

---

†The pulse shape $F_k(t)$ may be changed to some different pulse shape if matched filter is used. However, the same notation for the $F_k(t)$ is used to avoid additional notation.

$$e(t) = K_{IF}^2 \frac{\Delta_a(t)}{\Sigma_a(t)} \left\{ P + \sum_{\substack{\ell=-\infty \\ \ell \neq 0}}^{\infty} \sum_{n=-\infty}^{\infty} C_n C^*_{(n-\ell)} e^{j\ell\omega_p t} \right\}$$

$$+ \frac{K_{IF}^2}{RM} n_D(t) \sum_{m=-\infty}^{\infty} C^*_m e^{-jm\omega_p t} , \qquad (4.57)$$

where P is the average power of $F_k(t)$.

If the pulse width τ_{pe} as shown in Figure 4.5 is defined by

$$\tau_{pe} = \frac{\int_{-\tau_p/2}^{\tau_p/2} F_k^2(t)dt}{F_k^2(0)} , \qquad (4.58)$$

the average power P of $F_k(t)$ is expressed as

$$P = \frac{1}{\tau} \int_{-\tau_p/2}^{\tau_p/2} F_k^2(t)dt = \frac{\tau_{pe}}{\tau} , \qquad (4.59)$$

since $F_k^2(0) = 1$ in this case.

Substituting Eq. (4.59) into Eq. (4.57), the error signal e(t) becomes

$$e(t) = K_{IF}^2 \frac{\Delta_a(t)}{\Sigma_a(t)} \left(\frac{\tau_{pe}}{\tau} \right) + \frac{K_{IF}^2}{RM} n_D(t) F_k(t)$$

$$+ \text{higher frequency terms.} \qquad (4.60)$$

After passing through the LPF having the cut-off frequency such as

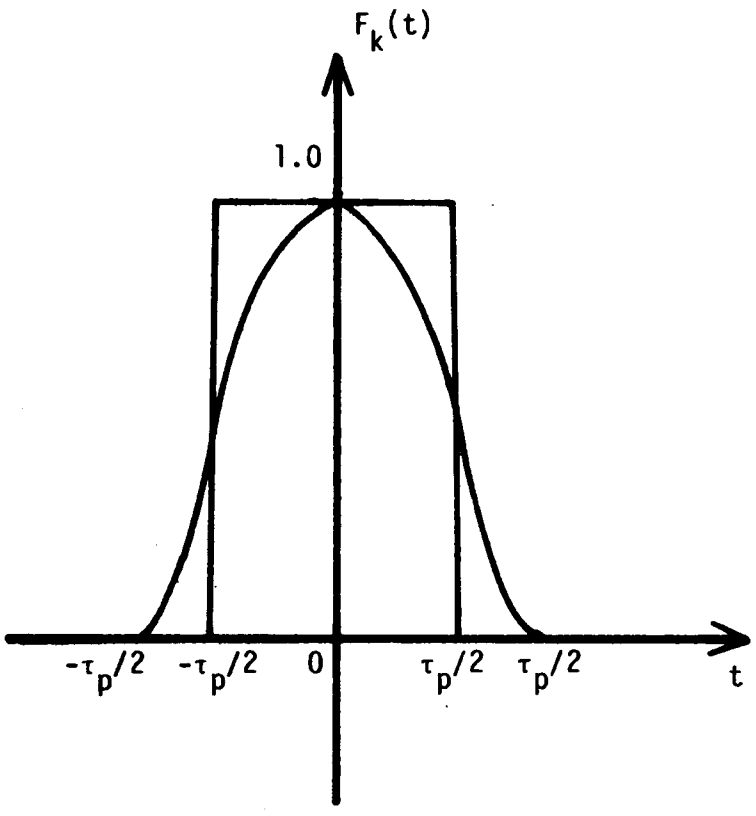


Figure 4.5. Relation of pulse width.

$$B_\tau = \frac{1}{2\tau}, \tag{4.61}$$

e(t) become

$$e(t) = K_{IF}^2 \frac{\Delta_a(t)}{\Sigma_a(t)} \frac{\tau_{pe}}{\tau} + \frac{K_{IF}^2}{RM} n_D'(t). \tag{4.62}$$

Normalizing or amplifying Eq. (4.62) by $1/K^2_{IF}(\tau_{pe}/\tau)$ gives

$$e(t) = \frac{\Delta_a(t)}{\Sigma_a(t)} + \frac{1}{RM} \frac{\tau}{\tau_{pe}} n'_D(t). \tag{4.63}$$

The next problem is finding the noise power spectral density in Eq. (4.63). First we will find the noise power of $n_D(t)F_k(t)$ as follows

$$\begin{aligned} \sigma_D'^2 &= E\{[n_D(t)F_k(t)]^2\} \\ &= E\{n_D^2(t)\}E\{F_k^2(t)\} \\ &= \sigma^2 \text{ x average power of } F_k(t) \\ &= \sigma^2 \frac{\tau_{pe}}{\tau}, \end{aligned} \tag{4.64}$$

since $n_D^2(t)$ and $F_k^2(t)$ are statistically independent and $F_k^2(t)$ is ergodic, where $\sigma^2 = E\{n_D^2(t)\}$.

If the half bandwidth of the IF filter or the video amplifier is expressed by

$$B = \frac{k}{\tau_{pe}}, \tag{4.65}$$

where k is constant, the noise power of $n_D'(t)$ may be given by

$$\sigma_D^2 = E\{n_D'^2(t)\} = \sigma^2 \frac{\tau_{pe}}{\tau} \cdot \frac{\tau_{pe}}{2k\tau}$$

$$= \sigma^2 \frac{\tau_{pe}^2}{2k\tau^2} . \tag{4.66}$$

Thus, the noise power in Eq. (4.63) is

$$\sigma_{noise}^2 = \frac{1}{R^2M^2} \frac{\tau^2}{\tau_{pe}^2} E\{n_D'^2(t)\}$$

$$= \frac{\sigma^2}{2kR^2M^2} . \tag{4.67}$$

The noise power spectral density (one-sided) is given by

$$\psi = \frac{\sigma_{noise}^2}{\frac{1}{2\tau}} = \frac{\sigma^2\tau}{kR^2M^2} . \tag{4.68}$$

The constant k in the above equation is determined by the pulse shape and the design of IF filter. It is impossible to find the upper limit of the k due to the uncertainty principle, however, the IF filter may be designed so as to maximize the efficiency which may be the maximum in the matched filter.

Therefore, it could be said that

$$k = \tau_{pe}B \leq 1, \tag{4.69}$$

from Skolnik's book (32, p. 414), assuming that the input pulse width into the IF amplifier is close to the pulse width τ_{pe} except in the case of a rectangular pulse and a rectangular shape filter, and where the value of k may become unity as in the case of a matched filter.†

Upon using Eqs. (4.48) and (4.68), the variance and covariance matrix for the monopulse-conical scan method becomes

$$[B]^{-1} = \begin{bmatrix} \dfrac{1}{\dfrac{2TkM^2R^2}{\sigma^2_\tau}\left(\dfrac{c_2 d_1^2 \theta_q}{\theta_B^2}\right)^2} & , & 0 \\ 0 & , & \dfrac{1}{\dfrac{2TkM^2R^2}{\sigma^2_\tau}\left(\dfrac{c_2 d_1^2 \theta_q}{\theta_B^2}\right)^2} \end{bmatrix} . \quad (4.70)$$

2. Conical Scan-Monopulse Method

We could consider such theoretical block diagram for the conical scan-monopulse method as in Figure 4.6. We assumed that there exists a divider circuit after PAM-demodulator although the actual system does not have it. We believe that this assumption does not affect the analysis.

Under the same conditions for the monopulse-conical scan, the output signals of the gates on both the Σ and Δ channels may become

---

†Appendix K.

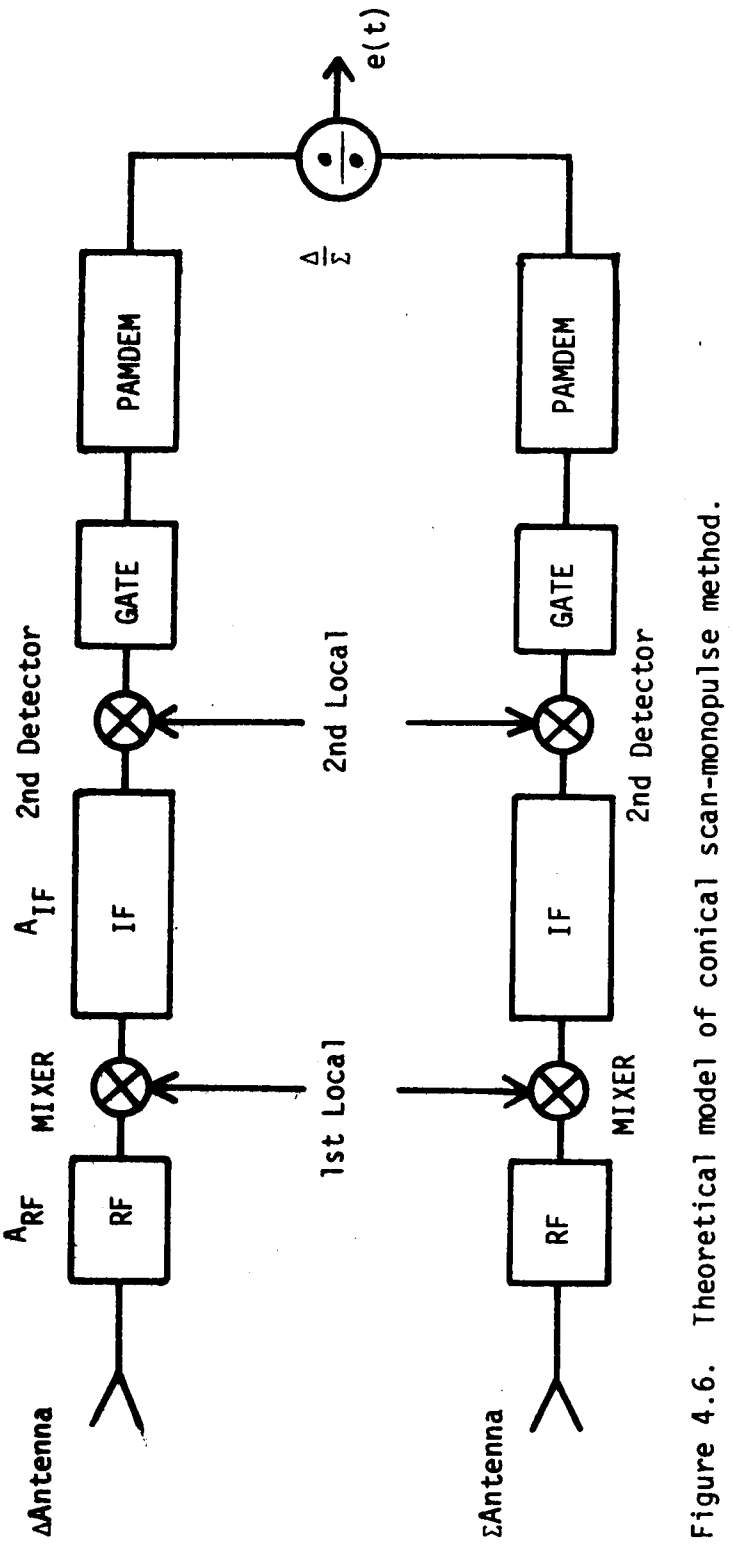


Figure 4.6. Theoretical model of conical scan-monopulse method.

$$\Sigma(t) = RA_{RF}A_{IF}\Sigma_a^2(t)F_k(t) + A_{RF}A_{IF}n_s(t)G_k(t), \tag{4.71}$$

and

$$\Delta(t) = RA_{RF}A_{IF}\Sigma_a(t)\Delta_a(t)F_k(t) + A_{RF}A_{IF}n_D(t)G_k(t). \tag{4.72}$$

Since the PAM-demodulator consists of the LPF having the cut-off frequency $1/2\tau$, the output signals become

$$\Sigma(t) = RA_{RF}A_{IF}\Sigma_a^2(t)C_o + A_{RF}A_{IF}n_s'(t), \tag{4.73}$$

and

$$\Delta(t) = RA_{RF}A_{IF}\Sigma_a(t)\Delta_a(t)C_o + A_{RF}A_{IF}n_D'(t), \tag{4.74}$$

where C_o is the coefficient of the complex Fourier series for $F_k(t)$, and $n_s'(t)$ and $n_D'(t)$ are the noise signals after $n_s(t)G_k(t)$ and $n_D(t)G_k(t)$ passed through the LPF.

The time dependent error signal by the divider circuit becomes, for large SNR,

$$e(t) = \frac{\Delta(t)}{\Sigma(t)} \simeq \frac{C_oRA_{RF}A_{IF}\Sigma_a(t)\Delta_a(t) + A_{RF}A_{IF}n_D'(t)}{C_oRA_{RF}A_{IF}\Sigma_a^2(t)}$$

$$= \frac{\Delta_a(t)}{\Sigma_a(t)} + \frac{1}{C_oRM}n_D'(t), \tag{4.75}$$

where $M = \Sigma_a^2(t)$ from Eq. (4.17).

The next problem is finding the noise power spectral density in Eq. (4.75).

The relation of the noises $n_D(t)G_k(t)$ and $n_D'(t)$ is shown in Figure 4.7. The noise power of $n_D(t)G_k(t)$ is given by

$$E\{[n_D(t)G_k(t)]^2\} = \sigma^2 \frac{\tau_p}{\tau}. \tag{4.76}$$

If the half bandwidth of the IF amplifier is represented by

$$B_{IF} = k' \frac{1}{\tau_p}, \tag{4.77}$$

where k' is constant, the noise power of $n_D'(t)$ becomes

$$E\{[n_D'(t)]^2\} = \sigma^2 \frac{\tau_p^2}{2k'\tau^2}. \tag{4.78}$$

Since Eq. (4.75) includes the constant C_o defined by the pulse shape, it can be expressed in terms of the pulse width τ_p and some constant.

Assuming that the pulse shape of $F_k(t)$ is positive and continuous in its pulse width ($|t| \leq \tau_p/2$), the first mean value theorem (11, p. 125) gives such a relation as

$$\int_{-\tau_p/2}^{\tau_p/2} F_k(t)dt = F_k(n)\tau_p, \text{ for } |n| \leq \tau_p/2, \tag{4.79}$$

where

$$0 \leq F_k(n) \leq 1.$$

This relation is shown in Figure 4.8.

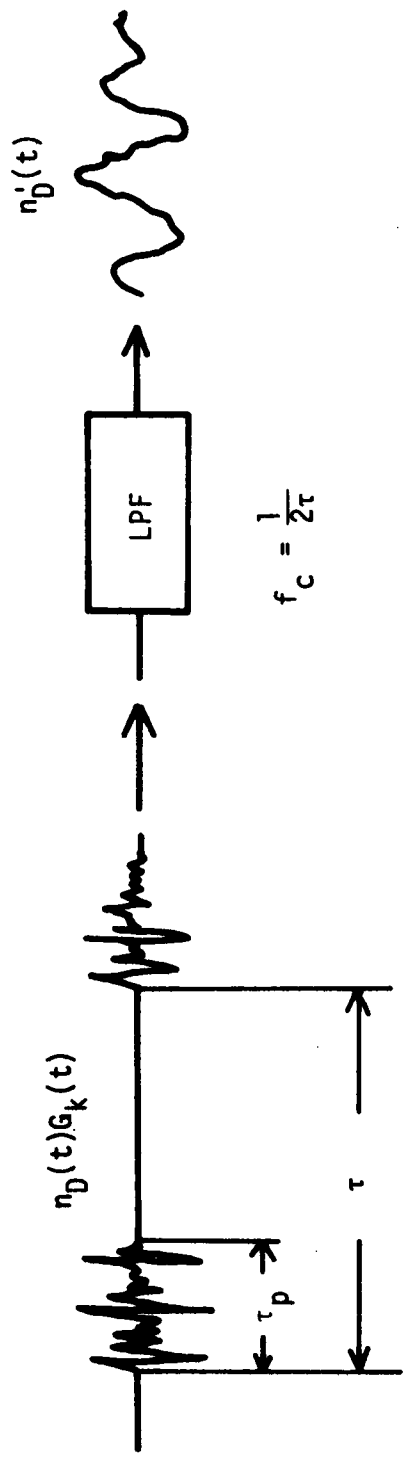


Figure 4.7. Relation of noises $n_D(t)G_k(t)$ and $n_D'(t)$.

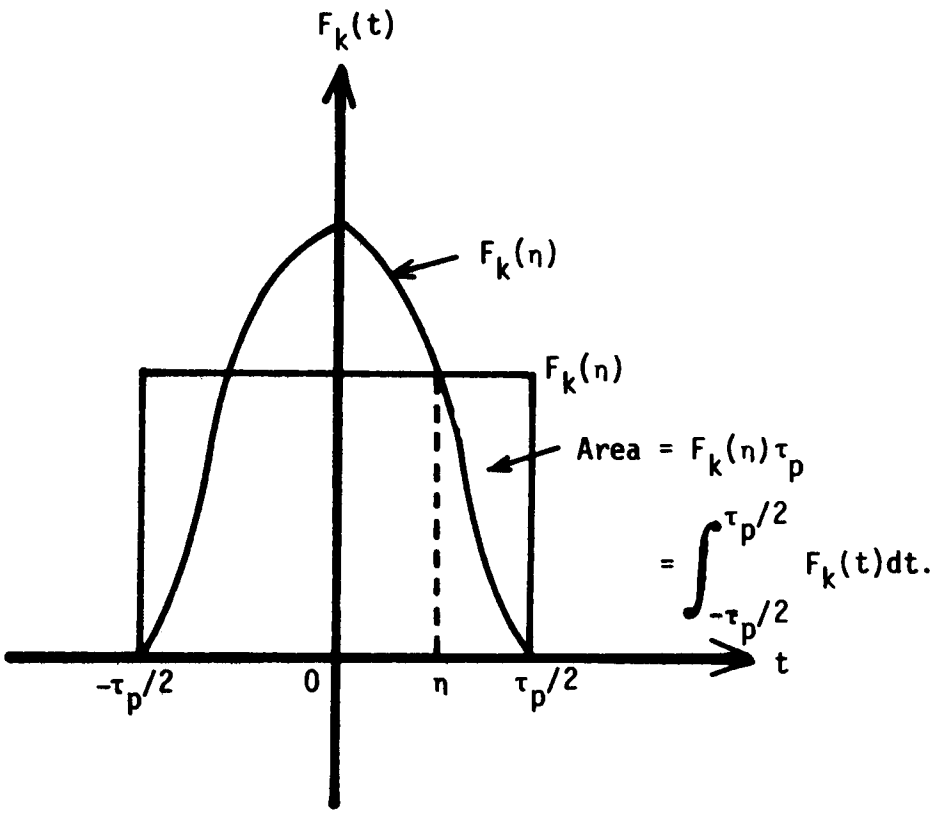


Figure 4.8. Relation of pulse shape $F_k(t)$ and its first mean value.

Upon using Eq. (4.79) and the relation of the Fourier coefficient in complex series form, the constant C_o is written as

$$C_o = \frac{1}{\tau}\int_{-\tau_p/2}^{\tau_p/2} F_k(t)dt = \frac{F_k(n)\tau_p}{\tau} . \tag{4.80}$$

Substituting Eq. (4.80) into Eq. (4.75), the time dependent error signal becomes

$$e(t) = \frac{\Delta_a(t)}{\Sigma_a(t)} + \frac{\tau}{F_k(n)\tau_p RM} n_D'(t). \tag{4.81}$$

Hence, the noise power in Eq. (4.81) becomes

$$\sigma^2_{noise} = E\left\{\left[\frac{\tau}{F_k(n)\tau_p RM} n_D'(t)\right]^2\right\}$$

$$= \frac{\sigma^2}{2F_k^2(n)k'R^2M^2} , \tag{4.82}$$

using Eq. (4.78).

Since this noise power expression has the terms of $F_k^2(n)$ and k', we will have to find the relation of them and k in the noise power of the monopulse-conical scan method to compare the accuracy in both methods.

Assuming that the IF bandwidth in both methods is the same, we have from Eqs. (4.65) and (4.77),

$$k' = k\frac{\tau_p}{\tau_{pe}} . \tag{4.83}$$

Upon using Eqs. (4.58), (4.79), and (4.83), the term $F_k^2(n)k'$ in Eq. (4.82) is represented by

$$F_k^2(n)k' = K\,k, \tag{4.84}$$

where

$$K = \frac{F_k(n)\int_{-\tau_p/2}^{\tau_p/2} F_k(t)dt}{\int_{-\tau_p/2}^{\tau_p/2} F_k^2(t)dt}. \tag{4.85}$$

Substituting Eq. (4.84) into Eq. (4.82) and dividing it by the one-sided band $1/2\tau$, the one-sided noise power spectral density becomes

$$\psi = \frac{\sigma^2\tau}{KkR^2M^2} \tag{4.86}$$

We shall now discuss the value of K. Under the conditions of the first mean value theorem and its wave form, they have such relations that

$$\begin{cases} 0 \le F_k(n) \le 1, \text{ for } |n| \le \tau_p/2 \\ F_k(t) \ge F_k^2(t), \text{ and} \\ \int_{-\tau_p/2}^{\tau_p/2} F_k(t)dt \ge \int_{-\tau_p/2}^{\tau_p/2} F_k^2(t)dt. \end{cases}$$

Therefore, there is no way to define in general whether or not the value of K is greater than one, i.e.,

$$F_k(n)\int_{-\tau_p/2}^{\tau_p/2} F_k(t)dt \overset{?}{\gtrless} \int_{-\tau_p/2}^{\tau_p/2} F_k^2(t)dt.$$

However, the value of K for a particular pulse shape can be obtained. So, the value of K for the several wave forms expected to be used in the actual radar system are shown in Table 4.1.

Table 4.1

The Value of K for Several Wave Forms

Wave Form	Value of K
Rectangular	1.0
Triangular	3/4
Squared cosine	1/2

From these results, it could be true that the value of K is less than or equal to one.

Finally, the variance and covariance matrix for the monopulse conical scan method becomes

$$[B]^{-1} = \begin{bmatrix} \dfrac{1}{\dfrac{2TkKM^2R^2}{\sigma^2\tau}\left(\dfrac{c_2d_1^2\theta_q}{\theta_B^2}\right)^2} & , & 0 \\ 0 & , & \dfrac{1}{\dfrac{2TKkM^2R^2}{\sigma^2\tau}\left(\dfrac{c_2d_1^2\theta_q}{\theta_B^2}\right)^2} \end{bmatrix}. \quad (4.87)$$

III. COMPARISON OF ACCURACIES

In the previous sections, we have obtained the accuracies for the raw data and the real systems. We will be interested in comparing the results and how the accuracy in the real system approaches to the theoretical limit, i.e., the accuracy of the raw data.

The accuracies for the real systems and the raw data have the factor which is a function of the squint angle. It appears from the transmitter antenna pattern for the raw data. On the other hand, both the transmitter and receiver antenna affect the factor in the real systems.

In order to compare the accuracies under the condition without the factor of M, it may be assumed that the M is unity, that is, the pattern squint angle is half of each antenna beamwidth where this angle is expected to be used in the actual pattern.

For the sake of convenience, letting the accuracy of the raw data, the monopulse-conical scan method, and the conical scan-monopulse method, be σ^2_{raw}, σ^2_{MC}, and σ^2_{CM}, respectively, where they are matrices, the relation among these accuracies become

$$\sigma^2_{raw} \leq \sigma^2_{MC} \leq \sigma^2_{CM}, \tag{4.88}$$

since

$$\sigma^2_{MC} = \frac{1}{k}\sigma^2_{raw}, \tag{4.89}$$

and

$$\sigma^2_{CM} = \frac{1}{Kk}\sigma^2_{raw}, \tag{4.90}$$

where K and k are less than or equal to unity, from Eqs. (4.38), (4.70), and (4.87).

From the result of Eq. (4.88), it is recognized that the monopulse-conical scan method has better accuracy than in the conical scan-monopulse method and the theoretical limit is realizable in the monopulse-conical scan method if the valud of k is unity which may be attained in the matched filter. On the other hand, it would be difficult for the values of K and k to be unity at the same time in the conical scan-monopulse method. Therefore, the theoretical limit would not be attained in the conical scan-monopulse method.

CHAPTER V

DISCUSSION, CONCLUSION, AND POSSIBLE FUTURE WORK

I. DISCUSSION AND CONCLUSION

In this dissertation we have attempted to analyze the concepts of the conopulse radar system.

The explanation for the two methods, the monopulse-conical scan method and the conical scan-monopulse method, in the conopulse radar system was carried out in Chapters I and II.

The error signal extractions for these two methods were described in Chapter II. We first started to extract the error signals for small pattern squint and target angles in case of general antenna pattern. The antenna pattern was expanded into the Maclaurin's series. The alternative analyses for the same conditions which used the suitable series expansions for the particular antenna patterns, the Bessel function antenna pattern and the Gaussian function antenna pattern, had been done, and these results were compared. Those results from the two different approaches coincided for the two particular antenna pattern representations. The general analyses for comparatively large pattern squint and target angles were developed by using the Maclaurin's series expansion method. The Fourier series method as the alternative approach which is suitable for the numerical computation was applied to the error signal extractions of the particular antenna patterns. The results from the two approaches also were compared and the error signals from the different approaches coincided

well above the pattern squint and target angles expected for the Bessel antenna pattern in the two methods. The error signal representation for the small pattern squint and target angles from the Maclaurin's series method may be adopted to the case of the target angles less than half of each antenna beamwidth without a large error.

The practical designs of the two methods were described in Chapter III.

The existence of noise was not taken into account in Chapters II and III. The noise causes an inaccurate determination in the system. Therefore, the accuracy was analyzed in Chapter IV. The Cramer-Rao lower bounds and the maximum-likelihood method were applied to the analyses for the raw data and the real system implementation, respectively. The closed form of the Cramer-Rao lower bounds for the multiple beams was developed for the analysis of raw data. The accuracies were obtained for the raw data and the real systems, and their relations were described. The accuracy in the monopulse-conical scan method is better than in the conical scan-monopulse method.

Finally, it could be concluded that the error signal extraction results by the Maclaurin's series method are very useful for the analysis of the system, and the monopulse-conical scan method is a better system than the conical scan-monopulse method.

II. POSSIBLE FUTURE WORK

We have developed the representations for the error signals, the practical system designs, and the accuracies in the conopulse radar system.

The results are fundamentally important factors for the analysis of the system. They, however, will not cover all the system analysis.

From the viewpoint of only the system analysis, the following two subjects as future work may be suggested:

1. Investigate the effect of the presence of a second (interference) target or multipath effect on the optimum system.
2. Develop a computer simulator of the optimum system to verify the theoretical performance of the optimum system with noise.

There may be many subjects for future work reflected from the practical design of the system. We think they should be considered case by case.

BIBLIOGRAPHY

BIBLIOGRAPHY

1. Abramowitz, M., and J. A. Stegun. Handbook of Mathematical Functions with Formulas, Graphs, Mathematical Tables. Dover Edition. New York: Dover Publications, Inc., 1972.

2. Arens, Richard. Complex Processes for Envelopes of Normal Noise. IEEE Trans., Vol. PGIT-3, pp. 204-207, September, 1957.

3. Ayres, Frank, Jr. Theory and Problems of Matrices. Schaum's outline series. New York: McGraw-Hill Book Co., 1962.

4. Barankin, E. W. Locally Best Unbiased Estimates. Ann. Math. Statist., Vol. 20, pp. 477-501, 1949.

5. Barton, David K. Radar System Analysis. New Jersey: Prentice-Hall, Inc., 1964.

6. Berkowitz, Raymond S. Modern Radar Analysis, Evaluation, and System Design. New York: John Wiley and Sons, Inc., 1965.

7. Cook, J. S., and R. Lowell. The Autotrack System. Bell System Technical Journal, Vol. 42, pp. 1283-1307, July, 1963.

8. Cramer, Harald. Mathematical Methods of Statistics. New Jersey: Princeton University Press, 1954.

9. Dettman, John W. Mathematical Methods in Physics and Engineering. Second Edition. New York: McGraw-Hill Book Co., 1969.

10. Dunn, John H., and Dean D. Howard. Precision Tracking with Monopulse Radar. Electronics, Vol. 33, No. 17, pp. 51-56, April 22, 1960.

11. Fulks, Watson. Advanced Calculus, An Introduction to Analysis. Second Edition. New York: John Wiley and Sons, Inc., 1969.

12. Gradshteyn, I. S., and J. M. Ryzhik. Table of Integrals, Series, and Products. (Translated from the Russian by Scripta Technica, Inc.), Translation edited by Alan Jeffrey, Fourth Edition. New York: Academic Press, Inc., 1965.

13. Hoel, Paul G. Introduction to Mathematical Statistics. Fourth Edition. New York: John Wiley and Sons, Inc., 1971.

14. Kailath, Thomas. Some Integral Equations with "Nonrational" Kernels. IEEE Trans., Vol. IT-12, No. 4, pp. 442-447, October, 1966.

15. Keely, E. J., I. S. Reed, and W. L. Root. The Detection of Radar Echoes in Noise.I. J. Soc. Indust. Appl. Math., Vol. 8, No. 2, pp. 309-341, June, 1960.

16. Keely, E. J., I. S. Reed, and W. L. Root. The Detection of Radar Echoes in Noise.II. J. Soc. Indust. Appl. Math., Vol. 8, No. 3, pp. 481-507, September, 1960.

17. Kharkevich, A. A. Spectra and Analysis. (Translated from Russian), New York: Consultant Bureau, 1960.

18. Lathi, B. P. Communications Systems. New York: John Wiley and Sons, Inc., 1968.

19. Levin, M. Joseph. Power Spectrum Parameter Estimation. IEEE Trans., Vol. IT-11, pp. 100-107, January, 1965.

20. Middleton, David. An Introduction to Statistical Communication Theory. New York: McGraw-Hill Book Co., 1960.

21. Noble, Ben. Applied Linear Algebra. New Jersey: Prentice-Hall, Inc., 1969.

22. Page, R. M. Monopulse Radar. IRE Conv. Rec., 8, pp. 132-134, 1955.

23. Peebles, Peyton Z., Jr. Signal Processors and Accuracy of Three-Beams Monopulse Tracking Radar. IEEE Trans., Vol. AES-5, pp. 52-57, January, 1969.

24. Peebles, Peyton Z., Jr. Communication System Principles and Method. Class notes of EE4100, to be published.

25. Peebles, Peyton Z., Jr. Processing Method and Basic Limitation of Multiple Target Monopulse Radar. Ph.D. Dissertation, The University of Pennsylvania, 1967.

26. Rao, C. Radhakrishna. Minimum Variance and the Estimation of Several Parameters. Proceeding of Cambridge Philosophical Society, Vol. 43, pp. 280-283, 1947.

27. Rhode, Donald R. Introduction to Monopulse. New York: McGraw-Hill Book Co., 1959.

28. Rubin, W. L., and S. K. Kamen. SCAMP--A Single-Channel Monopulse Radar Signal Processing Technique. IRE Trans. Vol. MIL-6, pp. 146-152, April, 1962.

29. Sharenson, S. Angle Estimation Accuracy with a Monopulse Radar in the Search Mode. IRE Trans., Vol. ANE-9, No. 3, pp. 175-179, September, 1962.

30. Silver, S. Microwave Antenna Theory and Design. MIT Radiation Laboratory Series. Vol. 12, New York: McGraw-Hill Book Co., 1949.

31. Skolnik, Merril I. Radar Handbook. New York: McGraw-Hill Book Co., 1970.

32. Skolnik, Merril I. Introduction to Radar Systems. New York: McGraw-Hill Book Co., 1962.

33. Slepian, David. Estimation of Signal Parameters in the Presence of Noise. IRE Trans., Vol. PGIT-3, pp. 64-89, March, 1954.

34. Spiegel, Murray R. Theory and Problems of Advanced Calculus. Schaum's outline series. New York: McGraw-Hill Book Co., 1963.

35. Swerling, Peter. Maximum Angular Accuracy of a Pulsed Search Radar. Proc. IRE, Vol. 44, pp. 1146-1155, September, 1956.

36. Swerling, Peter. Parameter Estimation for Waveforms in Additive Gaussian Noise. J. Soc. Indust. Appl. Math., Vol. 7, No. 2, pp. 152-166, June, 1959.

37. Swerling, Peter. Parameter Estimation Accuracy Formulas. IEEE Trans., Vol. IT-10, pp. 302-314, October, 1964.

38. Swerling, Peter. Detection of Radar Echoes Noise Revisited. IEEE Trans., Vol. IT-12, No. 3, pp. 348-361, July, 1966.

39. Taub, Herbert, and Donald L. Schilling. Principles of Communication Systems. New York: McGraw-Hill Book Co., 1971.

40. Thomas, John B. An Introduction to Statistical Communication Theory. New York: John Wiley and Sons, Inc., 1969.

41. Whittaker, E. T., and G. N. Watson. A Course of Modern Analysis. American Edition. New York: The Macmillan Co., 1946.

42. Wilks, S. S. Mathematical Statistics. New York: John Wiley and Sons, Inc., 1963.

43. Woodward, P. M. Probability and Information Theory, with Application to Radar. London, England: Pergamon Press, 1964.

APPENDICES

APPENDIX A

The output of the product device in Figure 2.3(A), p. 28, is defined in the frequency domain as

$$\Delta_{out}(\omega) = \frac{1}{2\pi} \Delta(\omega) * F_r(\omega), \tag{A-1}$$

where

$$F_r(\omega) = \mathfrak{F}[f_r(t)], \tag{A-2}$$

and the askerisk expresses convolution integral.

In case that

$$f_r(t) = V_r \cos\omega_s t, \tag{A-3}$$

the output for this reference signal $\Delta_{out(cos)}(\omega)$ becomes

$$\Delta_{out(cos)}(\omega) = \frac{V_r}{2} \int_{-\infty}^{\infty} \Delta(Y)[\delta(\omega-Y-\omega_s) + \delta(\omega-Y+\omega_s)]dY$$

$$= \frac{V_r}{2} [\Delta(\omega-\omega_s) + \Delta(\omega+\omega_s)], \tag{A-4}$$

since

$$F_r(\omega) = \pi V_r[\delta(\omega-\omega_s) + \delta(\omega+\omega_s)]. \tag{A-5}$$

From Eq. (2.62), we have

$$\Delta_{out(cos)}(\omega) = \frac{V_r}{2}[D_1 C_0 K'(\omega) \cos\phi_0$$

$$+ \text{other higher frequency components}]. \qquad \text{(A-6)}$$

Similarly, for the reference signal, $V_r \sin\omega_s t$, we have

$$\Delta_{out(sin)}(\omega) = \frac{V_r}{2}[D_1 C_0 K'(\omega) \cos\phi_0$$

$$+ \text{other higher frequency components}]. \qquad \text{(A-7)}$$

The, the outputs of the LPF's are

$$\Delta_{d(cos)}(\omega) = \frac{V_r}{2} D_1 C_0 K'(\omega) \cos\phi_0, \qquad \text{(A-8)}$$

and

$$\Delta_{d(sin)}(\omega) = \frac{V_r}{2} D_1 C_0 K'(\omega) \sin\phi_0. \qquad \text{(A-9)}$$

The output of the LPF on the Σ channel can be easily obtained from Eq. (2.60) as

$$\Sigma_d(\omega) = D_0 C_0 K'(\omega). \qquad \text{(A-10)}$$

APPENDIX B

The following relationship is derived from the expression for the modified Bessel function (41, p. 372)

$$I_n(x) = \sum_{r=0}^{\infty} \frac{(\frac{1}{2}x)^{n+2r}}{r!(n+r)!} . \tag{B-1}$$

Letting

$$x = 2a\theta_q\theta_T,$$

and assuming

$$x^2 \text{ or higher order} \simeq 0,$$

we have

$$I_0(x) = \sum_{r=0}^{\infty} \frac{(\frac{1}{2}x)^{2r}}{(r!)^2} \simeq 1, \tag{B-2}$$

$$\sum_{n=1}^{\infty} 2I_{2n}(x) \cos(4n\pi f_s t - 2n\phi_0) \simeq 0, \tag{B-3}$$

and

$$\sum_{n=1}^{\infty} 2I_{2n-1}(x) \cos[2(2n-1)\pi f_s t - (2n-1)\phi_0]$$

$$\simeq x \cos(2\pi f_s t - \phi_0). \tag{B-4}$$

Substituting these relations into Eq. (2.133), e(t) becomes

$$e(t) \simeq (2a^2\theta_q\theta_T)\cos(2\pi f_s t - \phi_o). \qquad \text{(B-5)}$$

APPENDIX C

From Eq. (2.124), we have

$$\sum_{n=1}^{\infty} [1 + (-1)^n]K_n \cos(2n\pi f_s t - n\phi_o)$$

$$= 2K_3 \cos(6\pi f_s t - 3\phi_o) + 2K_5 \cos(10\pi f_s t - 5\phi_o) + \cdots$$

$$= 2 \frac{2I_3(2a^2\theta_q\theta_T)}{I_o(2a^2\theta_q\theta_T)} \cos(6\pi f_s t - 3\phi_o)$$

$$+ 2 \frac{2I_3(2a^2\theta_q\theta_T)}{I_o(2a^2\theta_q\theta_T)} \cos(10\pi f_s t - 5\phi_o) + \cdots$$

$$\simeq 0, \qquad \text{(C-1)}$$

and

$$\sum_{n=1}^{\infty} [1 - (-1)^n]K_n \cos(2n\pi f_s t - n\phi_o)$$

$$= 2K_1 \cos(2\pi f_s t - \phi_o) + 2K_3 \cos(6\pi f_s t - 3\phi_o) + \cdots$$

$$= 2 \cdot \frac{2I_1(2a^2\theta_q\theta_T)}{I_o(2a^2\theta_q\theta_T)} \cos(2\pi f_s t - \phi_o)$$

$$+ 2 \frac{2I_1(2a^2\theta_q\theta_T)}{I_o(2a^2\theta_q\theta_T)} \cos(6\pi f_s t - 3\phi_o) + \cdots$$

$$\simeq 4(a^2\theta_q\theta_T) \cos(2\pi f_s t - \phi_o), \qquad \text{(C-2)}$$

since from Eq. (B-1) we have

$$I_0(2a^2\theta_q\theta_T) \simeq 1,$$

$$I_1(2a^2\theta_q\theta_T) \simeq a^2\theta_q\theta_T,$$

and

$$I_n(2a^2\theta_q\theta_T) \simeq 0 \quad \text{for } n \geq 2.$$

Then, substituting Eqs. (C-1) and (C-2) into Eqs. (2.138) and (2.139), the two signals become

$$\Sigma(t) \simeq 2K'(t)K''F_k(t), \tag{C-3}$$

and

$$\Delta(t) \simeq 4K'(t)K''F_k(t)(a^2\theta_q\theta_T)\cos(2\pi f_s t-\phi_o). \tag{C-4}$$

APPENDIX D

From Eq. (2.165), we have

$$f(x) = \frac{1}{A_o} = (a_o + a_1 x + a_2 x^2 + a_3 x^3 + a_4 x^4)^{-1}. \qquad \text{(D-1)}$$

If f(x) is infinitely differentiable in the region considered, we can apply the Maclaurin series to f(x).

Thus, the first derivatives of f(x) are

$$f(x) = -(a_0 + a_1 x + a_2 x^2 + a_3 x^3 + a_4 x^4)^{-2}$$

$$x\ (a_1 + 2a_2 x + 3a_3 x^2 + 4a_4 x^3). \qquad \text{(D-2)}$$

Then, we have

$$f'(0) = \frac{a_1}{a_o^2}. \qquad \text{(D-3)}$$

Similarly, we have

$$f''(x) = 2(a_o + a_1 x + a_2 x^2 + a_3 x^3 + a_4 x^4)^{-3}$$

$$x\ (a_1 + 2a_2 x + 3a_3 x^2 + 4a_4 x^3)^2$$

$$-\ (a_o + a_1 x + a_2 x^2 + a_3 x^3 + a_4 x^4)^{-2}$$

$$x\ (2a_2 + 6a_3 x + 12a_4 x^2), \qquad \text{(D-4)}$$

$$f''(0) = 2\left(\frac{a_1^2}{a_0^3} - \frac{a_2}{a_0^2}\right), \tag{D-5}$$

$$f'''(x) = -6(a_0 + a_1x + a_2x^2 + a_3x^3 + a_2x^4)^{-4}(a_1 + 2a_2x + 3a_3x^2$$

$$+ 4a_4x^3)^3 + 4(a_0 + a_1x + a_2x^2 + a_3x^3 + a_4x^4)^{-3}$$

$$x\ (a_1 + 2a_2x + 3a_3x^2 + 4a_4x^3)(2a_2 + 6a_3x + 12a_4x^2)$$

$$+ 2(a_0 + a_1x + a_2x^2 + a_3x^3 + a_4x^4)^{-3}$$

$$x\ (a_1 + 2a_2x + 3a_3x^2 + 4a_4x^3)(2a_2 + 6a_3x + 12a_4x^2)$$

$$- (a_0 + a_1x + a_2x^2 + a_3x^3 + a_4x^4)^{-2}(6a_3 + 24a_4x), \tag{D-6}$$

and

$$f'''(0) = -\frac{6a_1^3}{a_0^4} + \frac{12a_1a_2}{a_0^3} - \frac{6a_3}{a_0^2}. \tag{D-7}$$

Hence, the Maclaurin series becomes

$$f(x) = \frac{1}{a_0} - \frac{a_1}{a_0^2}x + \left(\frac{a_1^2}{a_0^3} - \frac{a_2}{a_0^2}\right)x^2 - \left(\frac{a_1^3}{a_0^4} - \frac{2a_1a_2}{a_0^3} + \frac{a_3}{a_0^2}\right)x^3$$

$$+ R_4, \tag{D-8}$$

where

$$R_4 = \frac{f^{(4)}(\beta)}{4!} x^4 , \qquad \text{(D-9)}$$

and β lies between o and x.

It should be recognized that Eq. (D-8) coincides the with the result from the direct division of $1/A_o$.

Upon using Eqs. (D-8) and (2.167), we have

$$\frac{A_1}{A_o} = \left[\frac{1}{a_o} - \frac{a_1}{a_o^2} x + \left(\frac{a_1^2}{a_o^3} - \frac{a_2}{a_o^2} \right) x^2 - \left(\frac{a_1^3}{a_o^4} - \frac{2a_1 a_2}{a_o^3} + \frac{a_3}{a_o^2} \right) x^3 \right.$$

$$\left. + R_4 \right] (a_1 + 2a_2 x + 3a_3 x^2 + 4a_4 x^3)$$

$$= \frac{a_1}{a_o} - \left(\frac{a_1^2}{a_o^2} - \frac{2a_2}{a_o} \right) x + \left(\frac{a_1^3}{a_o^3} - \frac{3a_1 a_2}{a_o^2} + \frac{3a_3}{a_o} \right) x^2$$

$$- \left(\frac{a_1^4}{a_o^4} - \frac{4a_1^2 a_2}{a_o^3} + \frac{4a_1 a_3}{a_o^2} + \frac{2a_2^2}{a_o^2} - \frac{4a_4}{a_o} \right) x^3$$

$$+ \text{higher order terms} \qquad \text{(D-10)}$$

Also from Eq. (2.166), $1/A_o^2$ becomes

$$\frac{1}{A_o^2} = \frac{1}{(a_o + a_1 x + a_2 x^2 + a_3 x^3 + a_4 x^4)^2}$$

$$= \frac{1}{\{a_0^2 + 2a_0a_1x + (a_1^2 + 2a_0a_1)x^2 + 2(a_0a_3 + a_1a_2)x^3}$$

$$+ (2a_0a_4 + 2a_1a_3 + a_2^2)x^4 + 2(a_1a_4 + a_2a_3)x^5$$

$$+ (2a_2a_4 + a_3^2)x^6 + 2a_3a_4x^7 + a_4^2x^8\} . \qquad \text{(D-11)}$$

By the same procedure for f(x), Eq. (D-11) becomes

$$\frac{1}{A_0^2} = \frac{1}{a_0^2} - \frac{2a_1}{a_0^3}x + \frac{1}{a_0^2}\left(\frac{3a_1^2}{a_0^2} - \frac{2a_2}{a_0}\right)x^2$$

$$+ \text{higher order terms.} \qquad \text{(D-12)}$$

From Eqs. (2.166) and (2.167), we have

$$A_1A_2 = (a_1 + 2a_2x + 3a_3x^2 + 4a_4x^3)(a_2 + 3a_3x + 6a_4x^2)$$

$$= a_1a_2 + (2a_2^2 + 3a_1a_3)x + (9a_2a_3 + 6a_1a_4)x^2$$

$$+ (16a_2a_4 + 9a_3^2)x^3 + 30a_3a_4x^4 + 24a_4^2x^5. \qquad \text{(D-13)}$$

Upon using Eqs. (D-12) and (D-13), we have

$$\frac{A_1A_2}{A_0^2} = \frac{a_1a_2}{a_0^2} - \left(\frac{2a_1^2a_2}{a_0^2} - \frac{3a_1a_3}{a_0^2} - \frac{2a_2^2}{a_0^2}\right)x$$

$$+ \text{higher order terms.} \qquad \text{(D-14)}$$

Similarly, upon using Eqs. (2.169) and (D-8), we have

$$\frac{A_3}{A_o} = (a_3 + 4a_4x)$$

$$x \left[\left(\frac{1}{a_o} - \frac{a_1}{a_2} \right) x + \left(\frac{a_1^2}{a_o^3} - \frac{a_2}{a_o^2} \right) x^2 - \left(\frac{a_1^3}{a_o^4} - \frac{2a_1a_2}{a_o^3} + \frac{a_3}{a_o^2} \right) x^3 + R_4 \right]$$

$$= \frac{a_3}{a_o} - \left(\frac{a_1a_3}{a_o^2} - \frac{4a_4}{a_o} \right) x + \text{higher order terms.} \qquad \text{(D-15)}$$

APPENDIX E

Taking the Fourier transform of Eqs. (2.184) and (2.185), we have

$$\Sigma(\omega) = \mathcal{F}[\Sigma(t)] = \frac{D_0}{2\pi} K'(\omega) * F_k(\omega) + \frac{D_2}{2\pi} F_2(\omega) * F_k(\omega) + \frac{D_4}{2\pi} F_4(\omega) * F_k(\omega), \tag{E-1}$$

and

$$\Delta(\omega) = \mathcal{F}[\Delta(t)] = \frac{D_1}{2\pi} F_1(\omega) * F_k(\omega) + \frac{D_3}{2\pi} F_4(\omega) * F_k(\omega), \tag{E-2}$$

where

$$\left.\begin{aligned} F_k(\omega) &= \mathcal{F}[F_k(t)], \\ \text{and} \\ F_\ell(\omega) &= \mathcal{F}[f_\ell(t)], \ \ell = 1 \sim 4. \end{aligned}\right\} \tag{E-3}$$

The Fourier transforms of $f_\ell(t)$ in terms of the Fourier transform of $K'(t)$ become

$$F_\ell(\omega) = \mathcal{F}[f_\ell(t)] = \frac{e^{-j\ell\phi_0}}{2} K'(\omega - \ell\omega_s) + \frac{e^{j\ell\phi_0}}{2} K'(\omega + \ell\omega_s), \quad \text{for } \ell = 1 \sim 4, \tag{E-4}$$

where

$$K'(\omega) = \mathcal{F}[K'(t)]. \tag{E-5}$$

Rewriting Eq. (2.58) gives

$$F_k(\omega) = \mathcal{F}[F_k(t)] = 2\pi \sum_{n=-\infty}^{\infty} C_n \delta(\omega - n\omega_p).$$

The terms of the convolution in Eqs. (E-1) and (E-2) become

$$K'(\omega) * F_k(\omega) = 2\pi C_n \int_{-\infty}^{\infty} K'(Y)\delta(\omega - Y - n\omega_p)dY$$

$$= 2\pi \sum_{n=-\infty}^{\infty} C_n K'(\omega - n\omega_p), \qquad \text{(E-6)}$$

and

$$F_\ell(\omega) * F_k(\omega) = 2\pi \sum_{n=-\infty}^{\infty} C_n F_\ell(\omega - n\omega_p), \text{ for } \ell = 1 \sim 4. \qquad \text{(E-7)}$$

Upon using Eqs. (E-5), (E-6), and (E-7), $\Sigma(\omega)$ and $\Delta(\omega)$ are written as

$$\Sigma(\omega) = \sum_{n=-\infty}^{\infty} D_o C_n K'(\omega - n\omega_p)$$

$$+ \sum_{n=-\infty}^{\infty} D_2 C_n \left\{ \frac{e^{-j2\phi_o}}{2} K'(\omega - n\omega_p - 2\omega_s) + \frac{e^{j2\phi_o}}{2} K'(\omega - n\omega_p + 2\omega_s) \right\}$$

$$+ \sum_{n=-\infty}^{\infty} D_4 C_n \left\{ \frac{e^{-j4\phi_o}}{2} K'(\omega - n\omega_p - 4\omega_s) + \frac{e^{j4\phi_o}}{2} K'(\omega - n\omega_p + 4\omega_s) \right\}, \qquad \text{(E-8)}$$

and

$$\Delta(\omega) = \sum_{n=-\infty}^{\infty} D_1 C_n \left\{ \frac{e^{-j\phi_o}}{2} K'(\omega - n\omega_p - \omega_s) \right.$$

$$\left. + \frac{e^{j\phi_o}}{2} K'(\omega - n\omega_p + \omega_s) \right\}$$

$$+ \sum_{n=-\infty}^{\infty} D_3 C_n \left\{ \frac{e^{-j3\phi_o}}{2} K'(\omega - n\omega_p - 3\omega_s) \right.$$

$$\left. + \frac{e^{j3\phi_o}}{2} K'(\omega - n\omega_p + 3\omega_s) \right\} . \qquad \text{(E-9)}$$

APPENDIX F

Replacing the variables in Eq. (2.190) as follows

$$A_o \longleftrightarrow A_o'$$

$$A_1 \longleftrightarrow A_1'$$

$$\frac{A_2}{2} \longleftrightarrow A_2'$$

$$\frac{3A_3}{4} \longleftrightarrow A_3' \qquad \text{(F-1)}$$

$$\frac{3A_4}{8} \longleftrightarrow A_4'$$

$$\frac{2\theta_q\theta_T}{\theta_B^2} \longleftrightarrow y$$

We have

$$\frac{D_o}{D_1} = -\frac{A_1'y + A_3'y^3}{A_o' + A_2'y^2 + A_4'y^4} . \qquad \text{(F-2)}$$

Eq. (F-2) has completely the same form as Eq. (2.160) but it is not a function of time and A_rs(r=1~4) and y are functions of θ_q and θ_T. If Eq. (F-2) is continuous and the inverse of the denominator is infinitely differentiable with respect to θ_T for any values of θ_q within their region defined, the results for Eq. (2.160) can be applied to Eq. (F-2).

From Eq. (2.162), Eq. (F-2) is approximated as

$$\frac{D_0}{D_1} \simeq \frac{A_1'}{A_0'} y - \left(\frac{A_1' A_2'}{A_0'^2} - \frac{A_3'}{A_0'} \right) y^3. \tag{F-3}$$

Upon using Eqs. (D-10), (D-14), and (D-15) in Appendix D, we have

$$\frac{A_1'}{A_0} = \frac{A_1}{A_0} \simeq \frac{a_1}{a_0} - \left(\frac{a_1^2}{a_0^2} - \frac{2a_2}{a_0} \right) x + \left(\frac{a_1^3}{a_0^3} - \frac{3a_1 a_2}{a_0^2} + \frac{3a_3}{a_0} \right) x^2$$

$$- \left(\frac{a_1^4}{a_0^4} - \frac{4a_1^2 a_2}{a_0^3} + \frac{4a_1 a_3}{a_0^2} + \frac{2a_2^2}{a_0^2} - \frac{4a_4}{a_0} \right) x^3, \tag{F-4}$$

$$\frac{A_1' A_2'}{A_0'^2} = \frac{1}{2} \frac{A_1 A_2}{A_0^2}$$

$$\simeq \frac{1}{2} \left[\frac{a_1 a_2}{a_0^2} - \left(\frac{2a_1^2 a_2}{a_0^3} - \frac{3a_1 a_3}{a_0^2} - \frac{2a_2^2}{a_0^2} \right) x \right], \tag{F-5}$$

and

$$\frac{A_3'}{A_0'} = \frac{3}{4} \frac{A_3}{A_0}$$

$$\simeq \frac{3}{4} \left[\frac{a_3}{a_0} \left(\frac{a_1 a_3}{a_0^2} - \frac{4a_4}{a_0} \right) x \right]. \tag{F-6}$$

Substituting Eqs. (F-4), (F-5), (F-6), and the relation for y given by Eq. (F-1) into Eq. (F-3), we have

$$\frac{D_o}{D_1} = \left\{ \frac{a_1}{a_o} - \left(\frac{a_1^2}{a_o^2} - \frac{2a_2}{a_o} \right) x + \left(\frac{a_1^3}{a_o^3} - \frac{3a_1 a_2}{a_o^2} + \frac{3a_3}{a_o} \right) x^2 \right.$$

$$- \left(\frac{a_1^4}{a_o^4} - \frac{4a_1^2 a_2}{a_o^3} + \frac{4a_1 a_3}{a_o^2} + \frac{2a_2^2}{a_o^2} - \frac{4a_4}{a_o} \right) x^3$$

$$+ \left(\frac{2\theta_q \theta_T}{\theta_B^2} \right)^2 \left[\frac{1}{2} \frac{a_1 a_2}{a_o^2} - \frac{3a_3}{4a_o} - \frac{1}{2} \left(\frac{2a_1^2 a_2}{a_o^3} - \frac{9}{2} \frac{a_1 a_3}{2a_o^2} \right. \right.$$

$$\left. \left. \left. - \frac{2a_2^2}{a_o^2} + \frac{6a_4}{a_o} \right) x \right] \right\} \left(\frac{2\theta_q \theta_T}{\theta_B^2} \right) . \qquad \text{(F-7)}$$

APPENDIX G

From Eq. (2.199), we have

$$K'(\omega-n\omega_p-\omega_s)\,\frac{e}{2}^{-j\phi_o} = \frac{R_o D_o e^{-j\phi_o}}{2} S(\omega-n\omega_p-\omega_s)$$

$$+ \frac{R_o D_2 e^{-j3\phi_o}}{4} S(\omega-n\omega_p-3\omega_s) + \frac{R_o D_2 e^{j\phi_o}}{4} S(\omega-n\omega_p+\omega_s)$$

$$+ \frac{R_o D_4 e^{-j5\phi_o}}{4} S(\omega-n\omega_p-5\omega_s) + \frac{R_o D_4 e^{j3\phi_o}}{4} S(\omega-n\omega_p+3\omega_s), \qquad \text{(G-1)}$$

$$K'(\omega-n\omega_p+\omega_s)\,\frac{e}{2}^{j\phi_o} = \frac{R_o D_o e^{j\phi_o}}{2} S(\omega-n\omega_p+\omega_s)$$

$$+ \frac{R_o D_2 e^{-j\phi_o}}{4} S(\omega-n\omega_p-\omega_s) + \frac{R_o D_2 e^{j3\phi_o}}{4} S(\omega-n\omega_p+3\omega_s)$$

$$+ \frac{R_o D_4 e^{-j3\phi_o}}{4} S(\omega-n\omega_p-3\omega_s) + \frac{R_o D_4 e^{j5\phi_o}}{4} S(\omega-n\omega_p+5\omega_s), \qquad \text{(G-2)}$$

$$K'(\omega-n\omega_p-3\omega_s)\,\frac{e}{2}^{-j3\phi_o} = \frac{R_o D_o e^{-j3\phi_o}}{2} S(\omega-n\omega_p-3\omega_s)$$

$$+ \frac{R_o D_2 e^{-j5\phi_o}}{4} S(\omega-n\omega_p-5\omega_s) + \frac{R_o D_2 e^{-j\phi_o}}{4} S(\omega-n\omega_p-\omega_s)$$

$$+ \frac{R_o D_4 e^{-j7\phi_o}}{4} S(\omega-n\omega_p-7\omega_s) + \frac{R_o D_4 e^{-j\phi_o}}{4} S(\omega-n\omega_p+\omega_s), \qquad \text{(G-3)}$$

$$K'(\omega-n\omega_p+3\omega_s)\,\frac{e^{j3\phi_o}}{2} = \frac{R_1D_o e^{j3\phi_o}}{2}\,S(\omega-n\omega_p+3\omega_s)$$

$$+\frac{R_oD_2e^{j\phi_o}}{4}\,S(\omega-n\omega_p+\omega_s)+\frac{R_oD_2e^{j5\phi_o}}{4}\,S(\omega-n\omega_p+5\omega_s)$$

$$+\frac{R_oD_4e^{-j\phi_o}}{4}\,S(\omega-n\omega_p-\omega_s)+\frac{R_oD_4e^{j7\phi_o}}{4}\,S(\omega-n\omega_p+7\omega_s), \qquad \text{(G-4)}$$

$$K'(\omega-n\omega_p) = R_oD_oS(\omega-n\omega_p)$$

$$+\frac{R_oD_2e^{-j2\phi_o}}{2}\,S(\omega-n\omega_p-2\omega_s)+\frac{R_oD_2e^{j2\phi_o}}{2}\,S(\omega-n\omega_p+2\omega_s)$$

$$+\frac{R_oD_4e^{-j4\phi_o}}{2}\,S(\omega-n\omega_p-4\omega_s)+\frac{R_oD_4e^{j4\phi_o}}{2}\,S(\omega-n\omega_p+4\omega_s), \qquad \text{(G-5)}$$

$$K'(\omega-n\omega_p-2\omega_s)\,\frac{e^{-j2\phi_o}}{2} = \frac{e^{-j2\phi_o}}{2}\Big\{R_oD_oS(\omega-n\omega_p-2\omega_s)$$

$$+\frac{R_oD_2e^{-j2\phi_o}}{2}\,S(\omega-n\omega_p-4\omega_s)+\frac{R_oD_2e^{j2\phi_o}}{2}\,S(\omega-n\omega_p)$$

$$+\frac{R_oD_4e^{-j4\phi_o}}{2}\,S(\omega-n\omega_p-6\omega_s)+\frac{R_oD_4e^{j4\phi_o}}{2}\,S(\omega-n\omega_p+2\omega_s)\Big\}, \qquad \text{(G-6)}$$

$$K'(\omega-n\omega_p+2\omega_s)\,\frac{e^{j2\phi_o}}{2} = \frac{e^{j2\phi_o}}{2}\Big\{R_oD_oS(\omega-n\omega_p+2\omega_s)$$

$$+\frac{R_oD_2e^{-j2\phi_o}}{2}\,S(\omega-n\omega_p)+\frac{R_oD_2e^{j2\phi_o}}{2}\,S(\omega-n\omega_p+4\omega_s)$$

$$+\frac{R_oD_4e^{-j4\phi_o}}{2}\,S(\omega-n\omega_p-2\omega_s)+\frac{R_oD_4e^{j4\phi_o}}{2}\,S(\omega-n\omega_p+6\omega_s)\Big\}, \qquad \text{(G-7)}$$

$$K'(\omega-n\omega_p-4\omega_s)\,\frac{e}{2}^{-j4\phi_o} = \frac{e}{2}^{-j4\phi_o}\Big\{ R_oD_oS(\omega-n\omega_p-4\omega_s)$$

$$+ \frac{R_oD_2e^{-j2\phi_o}}{2} S(\omega-n\omega_p-6\omega_s) + \frac{R_oD_2e^{j2\phi_o}}{2} S(\omega-n\omega_p-2\omega_s)$$

$$+ \frac{R_oD_4e^{-j4\phi_o}}{2} S(\omega-n\omega_p-8\omega_s) + \frac{R_oD_4e^{j4\phi_o}}{2} S(\omega-n\omega_p)\Big\}\ , \qquad \text{(G-8)}$$

and

$$K'(\omega-n\omega_p+4\omega_s)\,\frac{e}{2}^{j4\phi_o} = \frac{e}{2}^{j4\phi_o}\Big\{ R_oD_oS(\omega-n\omega_p+4\omega_s)$$

$$+ \frac{R_oD_2e^{-j2\phi_o}}{2} S(\omega-n\omega_p+2\omega_s) + \frac{R_oD_2e^{j2\phi_o}}{2} S(\omega-n\omega_p+6\omega_s)$$

$$+ \frac{R_oD_4e^{-j4\phi_o}}{2} S(\omega-n\omega_p) + \frac{R_oD_4e^{j4\phi_o}}{2} S(\omega-n\omega_p+8\omega_s)\Big\}. \qquad \text{(G-9)}$$

Substituting the results above into the $\Sigma(\omega)$ and $\Delta(\omega)$ given by Eqs. (2.186) and (2.187), respectively, the $\Sigma(\omega)$ and $\Delta(\omega)$ in terms of $S(\omega)$ are determined by

$$\Sigma(\omega) = \sum_{n=-\infty}^{\infty} R_oC_n\Big\{\Big[D_o^2 + \frac{D_2^2}{2} + \frac{D_4^2}{2}\Big]S(\omega-n\omega_p)$$

$$+ [2D_1D_2 + D_2D_4]\,\frac{e}{2}^{-j2\phi_o}S(\omega-n\omega_p-2\omega_s)$$

$$+ [2D_oD_2 + D_2D_4]\,\frac{e}{2}^{j2\phi_o}S(\omega-n\omega_p+2\omega_s)$$

$$+ \left[2D_oD_4 + \frac{D_2^2}{2}\right] \frac{e^{-j4\phi_o}}{2} S(\omega - n\omega_p - 4\omega_s)$$

$$+ \left[2D_oD_4 + \frac{D_2^2}{2}\right] \frac{e^{j4\phi_o}}{2} S(\omega - n\omega_p + 4\omega_s)$$

$$+ [D_2D_4] \frac{e^{-j6\phi_o}}{2} S(\omega - n\omega_p - 6\omega_s)$$

$$+ [D_2D_4] \frac{e^{j6\phi_o}}{2} S(\omega - n\omega_p + 6\omega_s)$$

$$+ \left[\frac{D_4^2}{2}\right] \frac{e^{-j8\phi_o}}{2} S(\omega - n\omega_p - 8\omega_s)$$

$$+ \left[\frac{D_4^2}{2}\right] \frac{e^{j8\phi_o}}{2} S(\omega - n\omega_p + 8\omega_s) \Bigg\} , \qquad \text{(G-10)}$$

and

$$\Delta(\omega) = \sum_{n=-\infty}^{\infty} R_o C_n \left\{ \left[D_oD_1 + \frac{D_1D_2}{2} + \frac{D_2D_3}{2} + \frac{D_3D_4}{2} \right] \frac{e^{-j\phi_o}}{2} S(\omega - n\omega_p - \omega_s) \right.$$

$$+ \left[D_oD_1 + \frac{D_1D_2}{2} + \frac{D_2D_3}{2} + \frac{D_3D_4}{2} \right] \frac{e^{+j\phi_o}}{2} S(\omega - n\omega_p + \omega_s)$$

$$+ \left[D_oD_3 + \frac{D_1D_2}{2} + \frac{D_1D_4}{2} \right] \frac{e^{-j3\phi_o}}{2} S(\omega - n\omega_p - 3\omega_s)$$

$$+ \left[D_oD_3 + \frac{D_1D_2}{2} + \frac{D_1D_4}{2} \right] \frac{e^{j3\phi_o}}{2} S(\omega - n\omega_p + 3\omega_s)$$

$$+ \left[\frac{D_1D_4}{2} + \frac{D_2D_3}{2} \right] \frac{e^{-j5\phi_o}}{2} S(\omega - n\omega_p - 5\omega_s)$$

$$+\left[\frac{D_1D_4}{2}+\frac{D_2D_3}{2}\right]\frac{e}{2}^{j5\phi_o}S(\omega-n\omega_p+5\omega_s)$$

$$+\left[\frac{D_3D_4}{2}\right]\frac{e}{2}^{-j7\phi_o}S(\omega-n\omega_p-7\omega_s)$$

$$+\left[\frac{D_3D_4}{2}\right]\frac{e}{2}^{j7\phi_o}S(\omega-n\omega_p+7\omega_s)\Bigg\}. \qquad \text{(G-11)}$$

Substituting the relations of Eq. (2.202) into Eqs. (G-10) and (G-11), we can obtain the results of Eqs. (2.200) and (2.201).

APPENDIX H

Rewriting Eq. (2.208), we have

$$\frac{B_1}{B_o} = \frac{A_1A_1y + \frac{3}{4}(A_1A_2 + A_oA_3)y^3}{A_o{}^2 + A_oA_2y^2 + \left(\frac{3A_oA_4}{8} + \frac{3A_2{}^2}{8} + \frac{3A_2A_4}{16}\right)y^4} \tag{H-1}$$

If Eq. (H-1) is continuous and the inverse of the denominator is differentiable with respect to θ_T for any value of θ_q in the region defined for θ_q and θ_T, we can apply the results of Eq. (2.162) onto Eq. (H-1) the same as in Appendix F.

Replacing the terms in Eq. (H-1) as follows

$$\left.\begin{aligned} A_o{}^2 &\longleftrightarrow A_o' \\ A_oA_1 &\longleftrightarrow A_1' \\ A_oA_2 &\longleftrightarrow A_2' \\ \tfrac{3}{4}(A_1A_2 + A_oA_3) &\longleftrightarrow A_3' \\ \frac{3A_oA_4}{8} + \frac{3A_2{}^2}{8} + \frac{3A_2A_4}{16} &\longleftrightarrow A_4' \end{aligned}\right\}, \tag{H-2}$$

we have

$$\frac{B_1}{B_o} = \frac{A_1'y + A_3'y^3}{A_o' + A_2'y^2 + A_4'y^4} \tag{H-3}$$

and then Eq. (H-3) is approximate as

$$\frac{B_1}{B_0} \simeq \frac{A_1'}{A_0'} y - \left(\frac{A_1'A_2'}{A_0'^2} - \frac{A_3'}{A_0'} \right) y^3. \tag{H-4}$$

By the same procedure as in Appendix F, we have

$$\frac{A_1'}{A_0'} = \frac{A_0 A_1}{A_0^2} = \frac{A_1}{A_0}$$

$$\simeq \frac{a_1}{a_0} - \left(\frac{a_1^2}{a_0^2} - \frac{2a_2}{a_0} \right) x + \left(\frac{a_1^3}{a_0^3} - \frac{3a_1 a_2}{a_0^2} + \frac{3a_3}{a_0} \right) x^2$$

$$- \left(\frac{a_1^4}{a_0^4} - \frac{4a_1^2 a_2}{a_0^3} + \frac{4a_1 a_3}{a_0^2} + \frac{2a_2^2}{a_0^2} - \frac{4a_4}{a_0} \right) x^3 \tag{H-5}$$

$$\frac{A_1'A_2'}{A_0'^2} = \frac{A_1 A_2}{A_0^2}$$

$$\simeq \frac{a_1 a_2}{a_0^2} - \left(\frac{2a_1^2 a_2}{a_0^3} - \frac{3a_1 a_3}{a_0^2} - \frac{2a_2^2}{a_0^2} \right) x, \tag{H-6}$$

$$\frac{A_3'}{A_0'} = \frac{3}{4} \frac{A_1 A_2}{A_0^2} + \frac{3}{4} \frac{A_3}{A_0}, \tag{H-7}$$

and then

$$\frac{A_1'A_2'}{A_0'^2} - \frac{A_3'}{A_0'} = \frac{1}{4}\frac{A_1A_2}{A_0^2} - \frac{3}{4}\frac{A_3}{A}$$

$$\simeq \frac{1}{4}\frac{a_1a_2}{a_0^2} - \frac{3}{4}\frac{a_3}{a_0} - \left(\frac{1}{2}\frac{a_1^2a_2}{a_0^3} - \frac{3}{2}\frac{a_1a_3}{a_0^3} - \frac{1}{2}\frac{a_2^2}{a_0^2} + \frac{3a_4}{a_0^2}\right)x. \quad \text{(H-8)}$$

Substituting Eqs. (H-5), (H-6), (H-7), and (H-8) into (H-4), we have

$$\frac{B_1}{B_0} = \left\{ \frac{a_1}{a_0} - \left(\frac{a_1^2}{a_0^2} - \frac{2a_2}{a_0}\right)x + \left(\frac{a_1^3}{a_0^3} - \frac{3a_1a_2}{a_0^2} + \frac{3a_2}{a_0}\right)x^2 \right.$$

$$- \left(\frac{a_1^4}{a_0^4} - \frac{4a_1^2a^2}{a_0^3} + \frac{4a_1a_3}{a_0^2} + \frac{2a_2^2}{a_0^2} - \frac{4a_4}{a_0}\right)x^3$$

$$- y^2\left[\frac{1}{4}\frac{a_1a_2}{a_0^2} - \frac{3}{4}\frac{a_3}{a_0} - \left(\frac{1}{2}\frac{a_1^2a_2}{a_0^3} - \frac{3}{2}\frac{a_1a_2}{a_0^2} - \frac{1}{2}\frac{a_2^2}{a_0^2}\right.\right.$$

$$\left.\left. + \frac{3a_4}{a_0}\right)x\right]\Bigg\} y. \quad \text{(H-9)}$$

APPENDIX I

Each derivative in Eqs. (4.28), (4.29), and (4.30) is given by

$$\frac{\partial G_1(x,y,t)}{\partial x} = \frac{c_2 d_1^2}{\theta_B^2} x$$

$$- \frac{(-1)^{\ell} c_2 d_1^2 \theta_q}{\theta_B^2} \frac{1}{\sqrt{x^2+y^2}} [x \cos(\omega_s t - \tan^{-1} \frac{y}{x}) \qquad \text{(I-1)}$$

$$-y \sin(\omega_s t - \tan^{-1} \frac{y}{x})], \qquad \text{(I-2)}$$

$$\frac{\partial G_2(x,y,t)}{\partial y} = \frac{c_2 d_1^2}{\theta_B^2} x$$

$$+ \frac{(-1)^{\ell} c_2 d_1^2 \theta_q}{\theta_B^2} \frac{1}{\sqrt{x^2+y^2}} [x \cos(\omega_s t - \tan^{-1} \frac{y}{x})$$

$$-y \sin(\omega_s t - \tan^{-1} \frac{y}{x})], \qquad \text{(I-2)}$$

$$\frac{\partial G_1(x,y,t)}{\partial y} = \frac{c_2 d_1^2}{\theta_B^2} y$$

$$- \frac{(-1)^{\ell} c_2 d_1^2 \theta_q}{\theta_B^2} \frac{1}{\sqrt{x^2+y^2}} [y \cos(\omega_s t - \tan^{-1} \frac{y}{x})$$

$$+ x \sin(\omega_s t - \tan^{-1} \frac{y}{x})], \qquad \text{(I-3)}$$

and

$$\frac{\partial G_2(x,y,t)}{\partial y} = \frac{c_2 d_1^2}{\theta_B^2} y$$

$$- \frac{(-1)^{\ell} c_2 d_1^2 \theta_q}{\theta_B^2} \frac{1}{\sqrt{x^2+y^2}} [y \cos(\omega_s t - \tan^{-1} \frac{y}{x})$$

$$+ x \sin(\omega_s t - \tan^{-1} \frac{y}{x})]. \qquad \text{(I-4)}$$

Then, we have

$$\left(\frac{\partial G_1(x,y,t)}{\partial x}\right)^2 = \left(\frac{c_2 d_1^2}{\theta_B^2}\right)^2 x^2$$

$$- (-1)^{\ell} 2 \left(\frac{c_2 d_1^2}{\theta_B^2}\right)^2 \theta_q \frac{x}{\sqrt{x^2+y^2}} [x \cos(\omega_s t - \tan^{-1} \frac{y}{x})$$

$$- y \sin(\omega_s t - \tan^{-1} \frac{y}{x})]$$

$$+ \left(\frac{c_2 d_1^2 \theta_q}{\theta_B^2}\right)^2 \frac{1}{x^2+y^2} [x \cos(\omega_s t - \tan^{-1} \frac{y}{x}$$

$$- y \sin(\omega_s t - \tan^{-1} \frac{y}{x})]^2, \qquad \text{(I-5)}$$

$$\left(\frac{\partial G_2(x,y,t)}{\partial x}\right)^2 = \left(\frac{c_2 d_1^2}{\theta_B^2}\right)^2 x^2$$

$$+ (-1)^{\ell} 2 \left(\frac{c_2 d_1}{\theta_B^2}\right)^2 \theta_q \frac{1}{\sqrt{x^2+y^2}} [x \cos(\omega_s t - \tan^{-1} \frac{y}{x})$$

$$-y \sin(\omega_s t - \tan^{-1} \frac{y}{x})]^2,$$

$$+ \left(\frac{c_2 d_1}{\theta_B^2}\right)^2 \frac{1}{x^2+y^2} [x \cos(\omega_s t - \tan^{-1} \frac{y}{x})]^2, \qquad \text{(I-6)}$$

$$\left(\frac{\partial G_1(x,y,t)}{\partial y}\right)^2 = \left(\frac{c_2 d_1}{\theta_B^2}\right)^2 y^2$$

$$- (-1)^{\ell} 2 \left(\frac{c_2 d_1}{\theta_B^2}\right)^2 \theta_q \frac{1}{\sqrt{x^2+y^2}} [y \cos(\omega_s t - \tan^{-1} \frac{y}{x})$$

$$+ x \sin(\omega_s t - \tan^{-1} \frac{y}{x})]$$

$$+ \left(\frac{c_2 d_1}{\theta_B^2}\right)^2 \frac{1}{x^2+y^2} [y \cos(\omega_s t - \tan^{-1} \frac{y}{x})$$

$$+ x \sin(\omega_s t - \tan^{-1} \frac{y}{x})]^2, \qquad \text{(I-7)}$$

$$\left(\frac{\partial G_2(x,y,t)}{\partial y}\right)^2 = \left(\frac{c_2 d_1}{\theta_B^2}\right)^2 y^2$$

$$+ (-1)^{\ell} 2 \left(\frac{c_2 d_1}{\theta_B^2}\right)^2 \theta_q \frac{1}{\sqrt{x^2+y^2}} [y \cos(\omega_s t - \tan^{-1} \frac{y}{x})$$

$$- x \sin(\omega_s t - \tan^{-1} \frac{y}{x})$$

$$+\left(\frac{c_2 d_1^{\,2}}{\theta_B^2}\right)^2 \frac{1}{x^2+y^2}\ [y\cos(\omega_s t-\tan^{-1}\frac{y}{x})$$

$$+ x\sin(\omega_s t-\tan^{-1}\frac{y}{x})]^2, \qquad \text{(I-8)}$$

$$\left(\frac{\partial G_1(x,y,t)}{\partial x}\right)\left(\frac{\partial G_1(x,y,t)}{\partial y}\right)$$

$$= \left\{\frac{c_2 d_1^{\,2}}{\theta_B^2} x - \frac{(-1)^{\ell} c_2 d_1^{\,2}\theta_q}{\theta_B^2}\frac{1}{\sqrt{x^2+y^2}}[x\cos(\omega_s t-\tan^{-1}\frac{y}{x})\right.$$

$$\left. - y\sin(\omega_s t-\tan^{-1}\frac{y}{x})]\right.$$

$$x\left\{\frac{c_2 d_1^{\,2}}{\theta_B^2} y - \frac{(-1)^{\ell} c_2 d_1^{\,2}\theta_q}{\theta_B^2}\frac{1}{\sqrt{x^2+y^2}}[y\cos(\omega_s t-\tan^{-1}\frac{y}{x})\right.$$

$$\left. + x\sin(\omega_s t-\tan^{-1}\frac{y}{x})]\right\}$$

$$= \left(\frac{c_2 d_1^{\,2}}{\theta_B^2}\right)^2 xy - (-1)^{\ell}\left(\frac{c_2 d_1^{\,2}}{\theta_B^2}\right)\theta_q \frac{1}{\sqrt{x^2+y^2}}[2xy\cos(\omega_s t-\tan^{-1}\frac{y}{x})$$

$$+ (x^2-y^2)\sin(\omega_s t-\tan^{-1}\frac{y}{x})]$$

$$+\left(\frac{c_2 d_1^{\,2}\theta_q}{\theta_B^2}\right)^2 \frac{1}{x^2+y^2}\left\{xy[\cos^2(\omega_s t-\tan^{-1}\frac{y}{x}) - \sin^2(\omega_s t-\tan^{-1}\frac{y}{x})\right.$$

$$+ (x^2-y^2)\cos(\omega_s t-\tan^{-1}\frac{y}{x})$$

$$\left.\sin(\omega_s t-\tan^{-1}\frac{y}{x})\right\}, \qquad \text{(I-9)}$$

and

$$\left(\frac{\partial G_2(x,y,t)}{\partial x}\right)\left(\frac{\partial G_2(x,y,t)}{\partial y}\right)$$

$$= \left\{\frac{c_2 d_1^{\,2}}{\theta_B^2}\, x + \frac{(-1)^{\ell} c_2 d_1^{\,2}\theta_q}{\theta_B^2}\,\frac{1}{\sqrt{x^2+y^2}}\,[x\cos(\omega_s t-\tan^{-1}\tfrac{y}{x}) - y\sin(\omega_s t-\tan^{-1}\tfrac{y}{x})]\right\}$$

$$\times\left\{\frac{c_2 d_1^{\,2}}{\theta_B^2}\, y + \frac{(-1)^{\ell} c_2 d_1^{\,2}\theta_q}{\theta_B^2}\,\frac{1}{\sqrt{x^2+y^2}}\,[y\cos(\omega_s t-\tan^{-1}\tfrac{y}{x}) + x\sin(\omega_s t-\tan^{-1}\tfrac{y}{x})]\right\}$$

$$= \left(\frac{c_2 d_1^{\,2}}{\theta_B^2}\right)^2 xy + (-1)\left(\frac{c_2 d_1^{\,2}}{\theta_B^2}\right)^2\theta_q\,\frac{1}{\sqrt{x^2+y^2}}\,[2xy\cos(\omega_s t-\tan^{-1}\tfrac{y}{x}) + (x^2-y^2)\sin(\omega_s t-\tan^{-1}\tfrac{y}{x})]$$

$$+\left(\frac{c_2 d_1^{\,2}\theta_q}{\theta_B^2}\right)^2\frac{1}{x^2+y^2}\left\{xy[\cos^2(\omega_s t-\tan^{-1}\tfrac{y}{x}) - \sin^2(\omega_s t-\tan^{-1}\tfrac{y}{x})] + (x^2-y^2)\cos(\omega_s t-\tan^{-1}\tfrac{y}{x})\sin(\omega_s t-\tan^{-1}\tfrac{y}{x})\right\}. \quad \text{(I-10)}$$

Hence, the integrands of Eqs. (4.28), (4.29), and (4.30) become

$$\left(\frac{\partial G_1(x,y,t)}{\partial x}\right)^2 + \left(\frac{\partial G_2(x,y,t)}{\partial y}\right)^2$$

$$= 2\left(\frac{c_2 d_1^2}{\theta_B^2}\right)^2 x^2 + \left(\frac{c_2 d_1^2 \theta_q}{\theta_B^2}\right)^2 \frac{2}{x^2+y^2}\left[x\cos(\omega_s t - \tan^{-1}\frac{y}{x})\right.$$

$$\left. - y\sin(\omega_s t - \tan^{-1}\frac{y}{x})\right]^2, \qquad \text{(I-11)}$$

$$\left(\frac{\partial G_1(x,y,t)}{\partial y}\right)^2 + \left(\frac{\partial G_2(x,y,t)}{\partial y}\right)^2$$

$$= 2\left(\frac{c_2 d_1^2}{\theta_B^2}\right) y^2 + \left(\frac{c_2 d_1^2 \theta_q}{\theta_B^2}\right)^2 \frac{2}{x^2+y^2}\left[y\cos(\omega_s t - \tan^{-1}\frac{y}{x})\right.$$

$$\left. + x\sin(\omega_s t - \tan^{-1}\frac{y}{x})\right]^2, \qquad \text{(I-12)}$$

and

$$\left(\frac{\partial G_1(x,y,t)}{\partial x}\right)\left(\frac{\partial G_1(x,y,t)}{\partial y}\right) + \left(\frac{\partial G_2(x,y,t)}{\partial x}\right)\left(\frac{\partial G_2(x,y,t)}{\partial y}\right)$$

$$= 2\left(\frac{c_2 d_1^2}{\theta_B^2}\right)^2 xy + \left(\frac{c_2 d_1 \theta_q}{\theta_B^2}\right)^2 \frac{2}{x_2+y_2}\left\{xy\left[\cos^2(\omega_s t - \tan^{-1}\frac{y}{x})\right.\right.$$

$$\left. - \sin^2(\omega_s t - \tan^{-1}\frac{y}{x})\right]$$

$$\left. + (x^2-y^2)\cos(\omega_s t - \tan^{-1}\frac{y}{x})\sin(\omega_s t - \tan^{-1}\frac{y}{x})\right\}. \qquad \text{(I-13)}$$

We will be able to obtain easily such relations that

$$\left.\begin{aligned} &\int_{-T}^{T} \cos^2(\omega_s t - \tan^{-1}\frac{y}{x}) = T, \\ &\int_{-T}^{T} \sin(\omega_s t - \tan^{-1}\frac{y}{x}) = T, \end{aligned}\right\} \quad \text{(I-14)}$$

and

$$\int_{-T}^{T} \cos(\omega_s t - \tan^{-1}\frac{y}{x}) \sin(\omega_s t - \tan^{-1}\frac{y}{x}) dt = 0,$$

where $T = n\pi/2\omega s$.

Using the relations of Eq. (I-14), the elements become

$$I_{xx} = \frac{R^2}{\sigma^2\tau}\left\{4Tx^2\left(\frac{c_2 d_1^2}{\theta_B^2}\right)^2 + 2T\left(\frac{c_2 d_1^2}{\theta_B^2}\right)^2\right\}, \quad \text{(I-15)}$$

$$I_{xy} = I_{yx} = \frac{4R^2 xyT}{\sigma^2\tau}\left(\frac{c_2 d_1^2}{\theta_B^2}\right)^2, \quad \text{(I-16)}$$

and

$$I_{yy} = \frac{R^2}{\sigma^2\tau}\left\{4Ty^2\left(\frac{c_2 d_1^2}{\theta_B^2}\right)^2 + 2T\left(\frac{c_2 d_1^2}{\theta_B^2}\right)^2\right\}. \quad \text{(I-17)}$$

APPENDIX J

From Eq. (4.44), the partial derivatives of the terms are

$$\frac{\partial F(t,x,y)}{\partial x} = \frac{(-1)^{\ell} A\theta_q}{\theta_B^2} \frac{1}{\sqrt{x^2+y^2}} [x \cos(\omega_s t - \tan^{-1} \frac{y}{x}) - y \sin(\omega_s t - \tan^{-1} \frac{y}{x})], \quad \text{(J-1)}$$

and

$$\frac{\partial F(t,x,y)}{\partial y} = \frac{(-1)^{\ell} A\theta_q}{\theta_B^2} \frac{1}{\sqrt{x^2+y^2}} [x \cos(\omega_s t - \tan^{-1} \frac{y}{x} - y \sin(\omega_s t - \tan^{-1} \frac{x}{y})], \quad \text{(J-2)}$$

Using the relations given by Eq. (I-14), the elements of the inverse variance and covariance matrix become

$$B_{11} = \frac{2}{\psi} \int_{-T}^{T} \left(\frac{\partial F(t,x,y)}{\partial x} \right)^2 dt$$

$$= \frac{2}{\psi} \left(\frac{A\theta_q}{\theta_B^2} \right)^2 \frac{1}{x^2+y^2} \int_{-T}^{T} [x \cos(\omega_s t - \tan^{-1} \frac{y}{x}) - y \sin(\omega_s t - \tan^{-1} \frac{y}{x})]^2 dt$$

$$= \frac{2T}{\psi} \left(\frac{A\theta_q}{\theta_B^2} \right)^2, \quad \text{(J-3)}$$

$$B_{12} = B_{21} = \frac{2}{\psi}\int_{-T}^{T} \frac{\partial F(t,x,y)}{\partial x}\,\frac{\partial F(t,x,y)}{\partial y}\,dt$$

$$= \frac{2}{\psi}\left(\frac{A\theta_q}{\theta_B^2}\right)^2 \frac{1}{x^2+y^2}\int_{-T}^{T} [x\cos(\omega_s t-\tan^{-1}\frac{y}{x})$$

$$- y\sin(\omega_s t-\tan^{-1}\frac{y}{x})]\,[y\cos(\omega_s t-\tan^{-1}\frac{y}{x})$$

$$+ x\sin(\omega_s t-\tan^{-1}\frac{y}{x})]dt$$

$$= 0, \qquad \text{(J-4)}$$

and similarly,

$$B_{22} = \frac{2}{\psi}\int_{-T}^{T}\left(\frac{\partial F(t,x,y)}{\partial y}\right)^2 dt$$

$$= \frac{2}{\psi}\left(\frac{A\theta_q}{\theta_B^2}\right)^2 \frac{1}{x^2+y^2}\int_{-T}^{T} [y\cos(\omega_s t-\tan^{-1}\frac{y}{x})$$

$$+ x\sin(\omega_s t-\tan^{-1}\frac{y}{x})]^2 dt$$

$$= \frac{2T}{\psi}\left(\frac{A\theta_q}{\theta_B^2}\right)^2 . \qquad \text{(J-5)}$$

APPENDIX K

The value of k is defined by

$$k = \tau_{pe} B, \tag{K-1}$$

from Eq. (4.64), where τ_{pe} is given by

$$\tau_{pe} = \frac{\int_{-\tau_p/2}^{\tau_p/2} F_k^2(t)dt}{F_k^2(0)}, \tag{K-2}$$

where the pulse of $F_k(t)$ is the output of the filter having the bandwidth B.

There is no way to find the upper limit of Eq. (K-1) due to uncertainty principle.

However, it will be found case by case. As an example, we will find the value of k for the matched filter to a rectangular pulse.

Suppose that the input rectangular pulse is expressed by

$$s(t) = u(t+\tau) - u(t), \tag{K-3}$$

the matched filter impulse response (40, p. 190) becomes

$$h^{\dagger}(t) = s(t_1-t) = u(t_1-t+\tau) - u(t_1-t). \tag{K-4}$$

The filter output can be easily obtained as

$$s_o(t) = \int_{-\infty}^{t} s(x)s(x-t+t_1)dx$$

$$= \begin{cases} 0 & , \text{for } t \leq t_1 - \tau \\ t - t_1 + \tau & , \text{for } t_1 - \tau \leq t \leq t_1 \\ -t + t_1 + \tau & , \text{for } t_1 \leq t \leq t_1 + \tau \\ 0 & , \text{for } t_1 + \tau \leq t \end{cases} . \qquad \text{(K-5)}$$

For the sake of convenience, letting $t_1 = 0$, the output pulse shape well-known is shown in Figure K-1.

Replacing τ by $\tau_{p/2}$ in the output signal, $s_o(t)$ becomes pulse signal $F_k(t)$ in our discussion.

Then, the pulse width τ_{pe} in terms of the input puise width τ_p becomes

$$\tau_{pe} = \frac{\int_{-\tau_p/2}^{\tau_p/2} F_k^2(t)dt}{F_k^2(0)} = \frac{8}{\tau_p^2} \int_{-\tau_p/2}^{0} (t + \tfrac{\tau_p}{2})^2 dt$$

$$= \frac{\tau_p}{3} . \qquad \text{(K-6)}$$

The Fourier transform of $h^{\dagger}(t)$ is given by

$$H^{\dagger}(\omega) = \mathcal{F}[h^{\dagger}(t)] = \mathcal{F}[u(t+\tau_p/2) - u(t)]$$

$$= \frac{\tau_p}{2} \frac{\sin(\omega\tau_p/4)}{\omega\tau_p/4} e^{j\omega\tau_p/4} . \qquad \text{(K-7)}$$

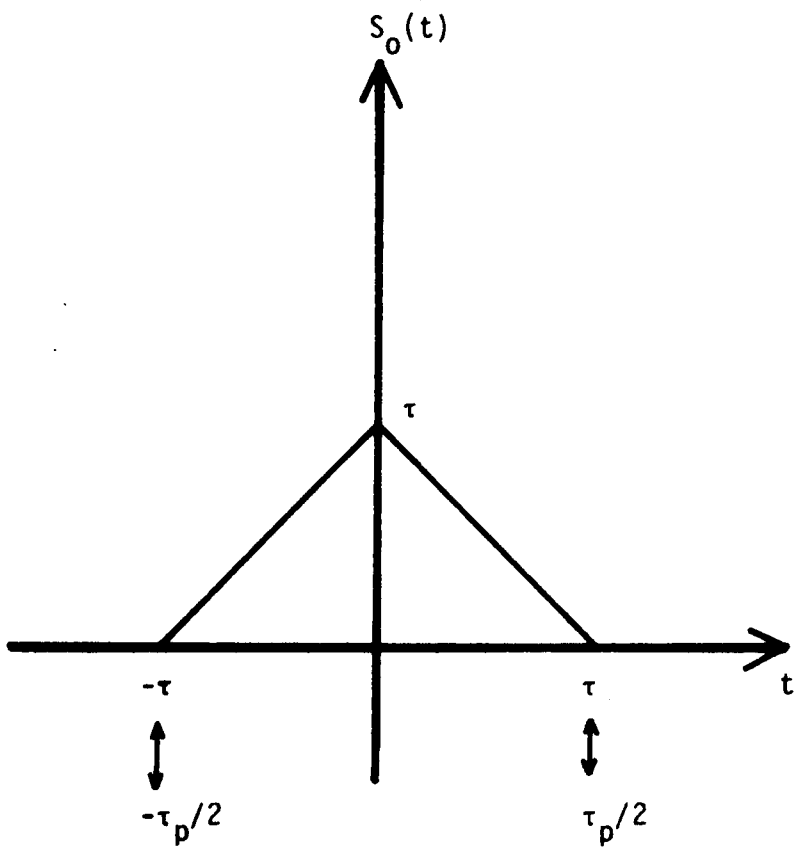


Figure K-1. Output pulse of matched filter for rectangular pulse.

If the bandwidth is defined by its noise bandwidth, it is given as

$$W_n = \frac{\int_{-\infty}^{\infty} \left|H^{\dagger}(\omega)\right|^2 d\omega}{2\left|H^{\dagger}(0)\right|^2} = \frac{2\pi}{\tau_p}, \qquad \text{(K-8)}$$

since the parseval's theorem gives

$$\int_{-\infty}^{\infty} \left|H^{+}(\omega)\right|^2 d\omega = 2\pi \int_{-\infty}^{\infty} s^2(t)dt$$

$$= 2\pi \int_{-\tau_p/2}^{0} dt = \pi\tau_p. \qquad \text{(K-9)}$$

Then, the value of k is

$$k = B\tau_{pe} = \frac{\pi}{\tau_p} \cdot \frac{\tau p}{3} \simeq 1, \qquad \text{(K-10)}$$

since

$$B = W_n/2.$$

In this case, the k is slightly greater than unity. It may come up from the noise bandwidth. If we use the other definition for bandwidth, it may become to unity.

In this appendix, we have examined only one case of k. However, it could be assumed that the value of k may be unity in matched filter case.

VITA

Hajime Sakamoto was born in Yokohama, Japan on January 23, 1938. His educational background includes the B.S. degree in 1963 and the M.S. degree in 1965 from Waseda University, Tokyo, Japan; all are in electrical engineering.

In 1965, he entered the Japan Defense Agency and has served for seven years as a Research Engineer. In the fall of 1972, he was sent to study at the University of Tennessee Space Institute toward the doctoral degree in Electrical Engineering and accepted a research assistantship. He transferred to the University of Tennessee, Knoxville, and accepted a graduate teaching assistantship in September 1973. He received the Doctor of Philosophy degree with a major in Electrical Engineering in December 1975.

He is a member of Eta Kappa Nu, Phi Kappa Phi, the Institute of Electronics and Communication Engineers, Japan, and IEEE.